1-1-1983

Satellite Image Interpretation and Laboratory Spectral Reflectance Measurements of Saline and Gypsiferous Soils of West Baghdad, Iraq

S. M. H. Al-Mahawili

M. F. Baumgardner

R. A. Weismiller

W. N. Melhorn

Al-Mahawili, S. M. H.; Baumgardner, M. F.; Weismiller, R. A.; and Melhorn, W. N., "Satellite Image Interpretation and Laboratory Spectral Reflectance Measurements of Saline and Gypsiferous Soils of West Baghdad, Iraq" (1983). *LARS Technical Reports.* Paper 104.
http://docs.lib.purdue.edu/larstech/104

SATELLITE IMAGE INTERPRETATION AND LABORATORY SPECTRAL

REFLECTANCE MEASUREMENTS OF SALINE AND GYPSIFEROUS

SOILS OF WEST BAGHDAD, IRAQ

S. M. H. Al-Mahawili
M. F. Baumgardner
R. A. Weismiller
W. N. Melhorn

What is page iii?

TABLE OF CONTENTS

LIST OF TABLES

LIST OF FIGURES

ABSTRACT

Salinization is a major factor in the deterioration of irrigated-alluvial soils. To establish early detection measures to prevent soil salinity, panchromatic black and white aerial photographs, standard soil surveys and laboratory measures have been used to achieve such a goal since the 1930's.

Not until the 1960's was spectral reflectance, in multiband photography, used in an indirect detection of the effect of soil salinity upon crop leaves.

To study the specific spectral reflectance characteristics of different soil salinity levels, an area located to the west of Baghdad, Iraq was selected.

The applied research methodology was accomplished in three phases: (1) field data acquisition and analysis, (2) laboratory measurements of spectral reflectance characteristics of saline and gypsiferous soils under different water content levels, before and after leaching, and (3) computer-digital-analysis of Landsat satellite MSS data and production of a final digitized map of the research area.

Laboratory measurements have indicated that saline soils have lower reflectance characteristics than do nonsaline and gypsiferous soils. The near and middle infrared bands were superior to the visible bands in detecting different soil salinity levels. Low reflectance was directly related to the type(s) of existing salts and their degree of solubility.

The digital analysis of Landsat multispectral scanner data demonstrated that spectral separation of different soil salinity levels and various land cover types is an efficient, reliable and dependable tool. The near infrared bands of Landsat were superior to the visible bands in characterizing different soil salinity levels.

INTRODUCTION

The salinization of the irrigated-alluvial soils in the arid
and semi-arid zones of the world is considered, among many other
associated factors, to be the most influential direct factor in
decreasing agricultural production, hence, creating a continuous
food shortage and socio-economic crisis.

Many countries which are affected by soil salinity have taken
preventive measures to decrease the level of land degradation caused
by this problem. Such measures, in the forms of land reclamation,
effective irrigation and drainage systems and controlled irrigation
practices, too often have been applied only after soil salinity has
become a serious threat to production.

During the past decade reflectance characteristics of field
crops under salinity stress have been used as an indirect procedure
of an early detection and determination of the salinity level in the
soil. This application of reflectance to study plant stress caused
by salinity was more easily accomplished than the direct character-
ization of the quantity and quality of salts in soils.

If early detection of salinity hazards can be obtained by reflec-
tance measurements, a valuable tool will become available for charac-
terizing the saline, nonsaline and gypsiferous conditions of soils.

Since Earth observation satellites are equipped with sensors which
systematically measure reflectance from the Earth surface, it is
possible to study repetitively the spectral characteristics of Earth
surface features. Both visible and infrared reflectance measurements
are made.

The objectives of this research are to (1) study the reflectance
characteristics of the nonsaline, saline and gypsiferous soil samples
of different salt concentrations and salt types, (2) study the

influence of the salt-water interaction upon reflectance under different saturation conditions, (3) study the effect of the water content, organic matter and gypsum contents as individual factors influencing the soils' reflection-absorption characteristics, (4) analyze satellite sensor data to produce a digital map of the research area through computer-aided digital analysis and processing, (5) classify the different land cover types in the research area into spectrally separable groups of water-vegetation-soil, (6) develop a spectral classification of the non-saline, saline and gypsiferous soils, and (7) determine, if possible, the reflectance characteristics of surface soils ranging from nonsaline, slightly saline, saline, extremely saline alluvial soils to gypsiferous "desert" soils in four wavelength bands of Landsat multispectral scanner (MSS) data.

As a major part of the research, experimental work was involved in the determination of the reflectance characteristics of the saline and gypsiferous soils under different saturation conditions. Such measures were considered in an effort to simulate important conditions under which saline soils are often observed.

The most effective treatment against salinization is the leaching out of excess dissolved salts from the soil profile. Leaching is considered the "bridge" between unproductive "saline" soil conditions and productive "nonsaline" soil conditions within the same field and/or area. Thus, it is important to observe the changes of the reflectance characteristics of the soil under two stages as an essential fulfillment of dealing with the dynamic soil system.

The physical basis for remote sensing is that different materials at the Earth surface reflect or adsorb solar energy in differing qualities and quantities. Thus, it is possible to differentiate between various land cover types because of their different spectral characteristics. The same principle has been considered within this research.

The results of this work are entirely related and applicable to an area to the west of Baghdad, Iraq from which the soil samples were collected. The results may or may not be related or applied to other soil salinity conditions other than the research area.

LITERATURE REVIEW

Soil Salinity

In areas of low rainfall, salts formed in the weathering of soil minerals are not fully leached. During periods of higher than average precipitation the more soluble salts are frequently leached from the more permeable and high-lying soils. These salt-charged waters find their way to low-lying soils and there, if drainage is impeded, the ground waters gradually accumulate high concentrations of salts. Upon evaporation of these waters, salt deposits are left in the soil. A repetition of this leaching-deposition process results in a complex pattern of soils high in salts and intermixed with nonsaline soils. The soluble salts that accumulate in these soils consist principally of the cations of calcium, magnesium and sodium and the chloride and sulfate anions (19,45,55).

In arid and semi-arid regions leaching is usually local in nature, and the soluble salts may not be transported far. This is due to the fact that there is less rainfall to leach them away, and the high rates of evaporation in the arid climates tend to concentrate the salt in the soil profiles, especially on the surfaces, as well as in the normally shallow ground water (19,45,55).

A saline soil is defined as one in which the electrical conductivity (EC) of the saturation extract is greater than 4 mmhos/cm at 25°C and the exchangeable sodium percentage (ESP) less than 15, while the pH value is usually less than 8.5 (55). Saline soils are often recognized by the presence of white salt crusts, dark brown-oily looking surfaces devoid of vegetation, by stunted growth of crop plants with considerable variability in size and deep blue-green foliage, and sometimes by tipburn and firing of the margins of leaves (6,19,55).

The amount of soluble salts present controls the osmotic pressure of the soil solution. Sodium seldom comprises more than half of the soluble cations and, hence, is not adsorbed to any significant extent. The major anions are chlorides, sulfates and sometimes nitrates. In addition to the readily soluble salts, saline soils may contain salts of low solubility such as calcium sulfate (gypsum), calcium and magnesium carbonate (lime)(4,44,55). In soils salinity should be expressed to take into account the moisture holding characteristics as an index of texture of the soil in addition to the salt content. A given amount of salt is more injurious in a sandy soil than in a clay soil because the coarse texture holds less water and, therefore, produces a more concentrated salt solution (13,14,19,55). Under arid and semi-arid climatic conditions, accumulation of salts on the soil surface is a direct result of high rates of evapotranspiration, very active capillary movement, high-saline ground water and medium-fine soil textures (6,11,19,22,24,30,38,53,55).

More recently, multiband photography has been used for indirect detection of soil salinity (33,34). Exposures were taken with a 9-lens camera to isolate specific wavelengths where reflectance contrasts could be detected (37,44). The longer visible and near infrared wavelengths which were used have exhibited the best tonal contrasts for detecting the extent of salinity as registered by plants. If dissolved salts are present in the soil solution, the thermodynamic activity of the water is reduced. Consequently, the soil water is rendered less available to plants. A reduction in the rate of water uptake by roots and a decrease in the water content of the stalks are among the first detectable plant responses to salinity. Thus, the transpiration rate is reduced and the accompanying temperature increases (37). The same reference has indicated the superiority of the wavelengths of 0.49-0.58, 0.53-0.63, 0.58-0.66 and 0.63-0.70 μm in detecting tonal contrasts in soils (37). Landsat multispectral scanner (MSS) data were used recently and reported to be successful in delineating salt affected soils (49).

Soil Water Content

The amount of water stored in the surface soil, or near the surface, has a distinct influence on the variation of reflectance characteristics in the visible and near infrared regions of the electromagnetic spectrum (32). It was reported by Blanchard et al. (9) that reflectance decreased as soil water content increased for wavelengths from 0.4-1.3 μm. While this observation is valid for any soil, it can only be applied for a given soil at any one time because of the effects produced in the soil by different grain sizes, texture, and mineralogy (9). Hoffer and Johannsen concluded that there was a significant influence of moisture content of soils on their reflectance characteristics (15). In the same study, the authors also concluded that spectral curves for both sandy and clayey soils showed a large decrease in spectral reflectance with an increase in soil moisture content (0.5-2.6 μm).

Reflectance curves for the clayey soils have maintained the same spectral shape. The sandy soils exhibited a marked change in the shape of the spectral curve with the change of moisture (15). The study also reported that the water absorption bands at approximately 1.4 μm and 1.9 μm became more pronounced for sandy soils with a moisture content in excess of 4 percent (Figures 1 and 2).

Surface moisture content, organic matter and particle size strongly influence reflectance. Reflectance was found to decrease as moisture increased. Reflectance measurement could be used, as concluded from the study, to determine the surface soil moisture especially in the 1.95 μm region of the spectrum (9,46).

Most soils appear darker when wet than when dry (9,13,14,23,36, 40,46,51). This results from decreased reflectance of incident radiation in the visible region of the spectrum. Angstrom attributed this darkening effect of moisture in soils to the internal total reflections with the thin water film covering the soil particles (2).

The reflectance difference of a soil between its dry and wet states can be determined if the following factors are taken into account; (a) variation in index of refraction of the water due to dissolved soil constituents, (b) change in the physical nature of soil
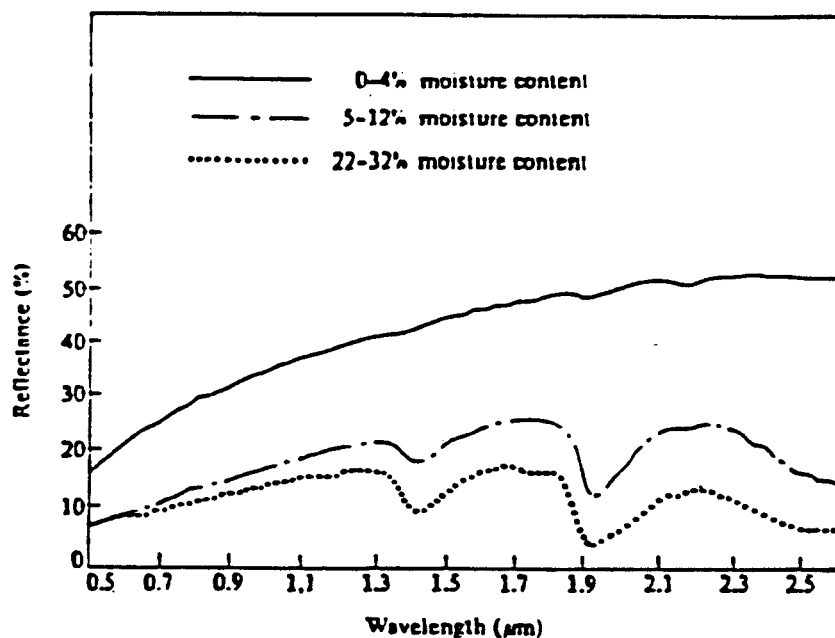
Figure 1.   Spectral reflectance curves for Chelsea sand
in 3-moisture content grouping (15).
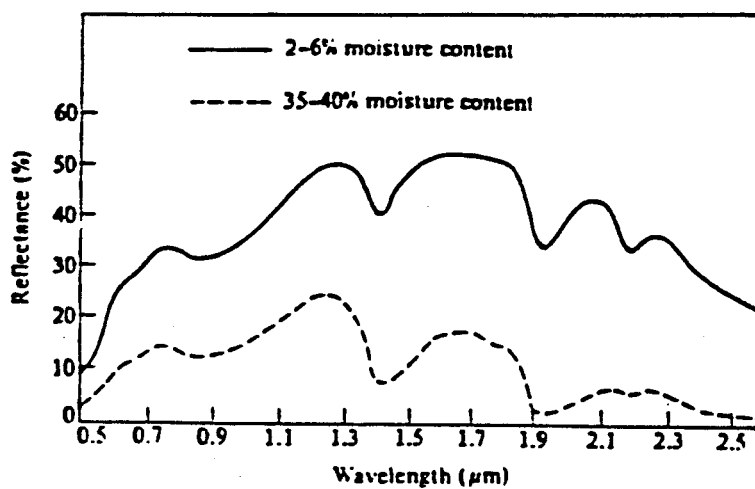
Figure 2.   Spectral reflectance curves for a typical clayey
soil at 2-moisture levels (15).

particles by the presence of water, and (c) similarities in the indices of refraction of the soil and water leading to the Christiansen effect (39,46).

Soil reflectance curves are affected by the presence of strong water absorption bands at 1.45 µm and 1.95 µm. The band at 1.95 µm, a combination of the "$V_2 + V_3$" fundamental frequencies, is the most sensitive to water and has been found best for relating reflectance measurements to soil moisture content (9,46). An absorption band at 2.2 µm was identified by Hunt et al. as a vibrational mode of the hydroxyl ion (17,18). Absorption due to the hydroxyl ion also gives rise to band 1.45 µm, the same as that of liquid water. The appearance of the 1.45 µm band without the 1.95 µm band indicates that the hydroxyl group and not free water are present in the material. Sharp bands at 1.45 µm and 1.95 µm indicate that the water molecules are located in well defined ordered sites while broad bands at these wavelengths indicate that they are relatively unordered as is often the case in naturally occurring soils (17,18).

Organic Matter

In arid and semi-arid regions, soil organic matter content is usually low, and decreases with the increase of depth in the soil profile (55). This fact is directly related to the depth and shape of the root zone. Soil organic matter and the composition of organic constituents are known to have a strong influence on soil reflectance. Many studies have reported that soil reflectance decreases as organic matter increases (3,5). This interrelationship between organic matter and reflectance was observed in the range of wavelengths from 0.4-2.5 µm of the spectrum.

Baumgardner et al. found that organic matter played a major and dominant part in bestowing spectral properties to soils when the organic matter content exceeded 2.0 percent (3). As the organic matter dropped below the 2.0 percent level, it became less effective in masking out the effects on reflectance of other soil constituents (3). Soil reflectance in the 0.6-1.1 µm was reported to have the highest correlation with certain organic constituents (3).

Irrigation waters are considered a good source of increasing the organic matter content in the soil in most of the irrigated alluvial soils in addition to the normal agricultural practices (55). High organic matter contents are also found to be dominant in highly saline soil conditions due to the long periods of land utilization (55). The presence of both organic matter and different salts usually complicates the development of soil color. For instance, organic matter and magnesium chloride add a dark brown-gray color to the surface soil. Since reflectance decreases with the increase of organic matter, it is not really known under the conditions stated above if such a decrease of reflectance is only related to one or more constituents. A better technique for determining the interrelationships between reflectance characteristics of irrigated-salt affected alluvial soils is required to differentiate between the effects of organic matter and salts on soil color.

Gypsum

Gypsum is usually colorless or white, but is sometimes gray, brown or pale shades of red, yellow or blue. Colored varieties typically contain traces of iron (16). Gypsum ($CaSO_4 \cdot 2H_2O$) is found in many soils of arid origins in amounts ranging from trace to several percent. In some soils, gypsum is present in the sedimentary deposits from which soil was originally derived. In other soils, gypsum is formed by the precipitation of calcium and sulfate during salinization. Owing to the leaching process, gypsum occurs at some depth in the former instance, while in the latter, its content is usually greater in the surface layers (sometimes immediately exposed on the soil surface) of the soil (1,11,16,55).

Hunt et al. (16) extensively studied the variations of spectral reflectance characteristics of different types of pure gypsum. They concluded that most of the features which the gypsum samples displayed were explained in terms of overtone and combination tones of the molecular water which is essential to the gypsum structure (16). Different gypsum types were spectrally analyzed by the same authors (16). In their conclusions, the "hydrite gypsum
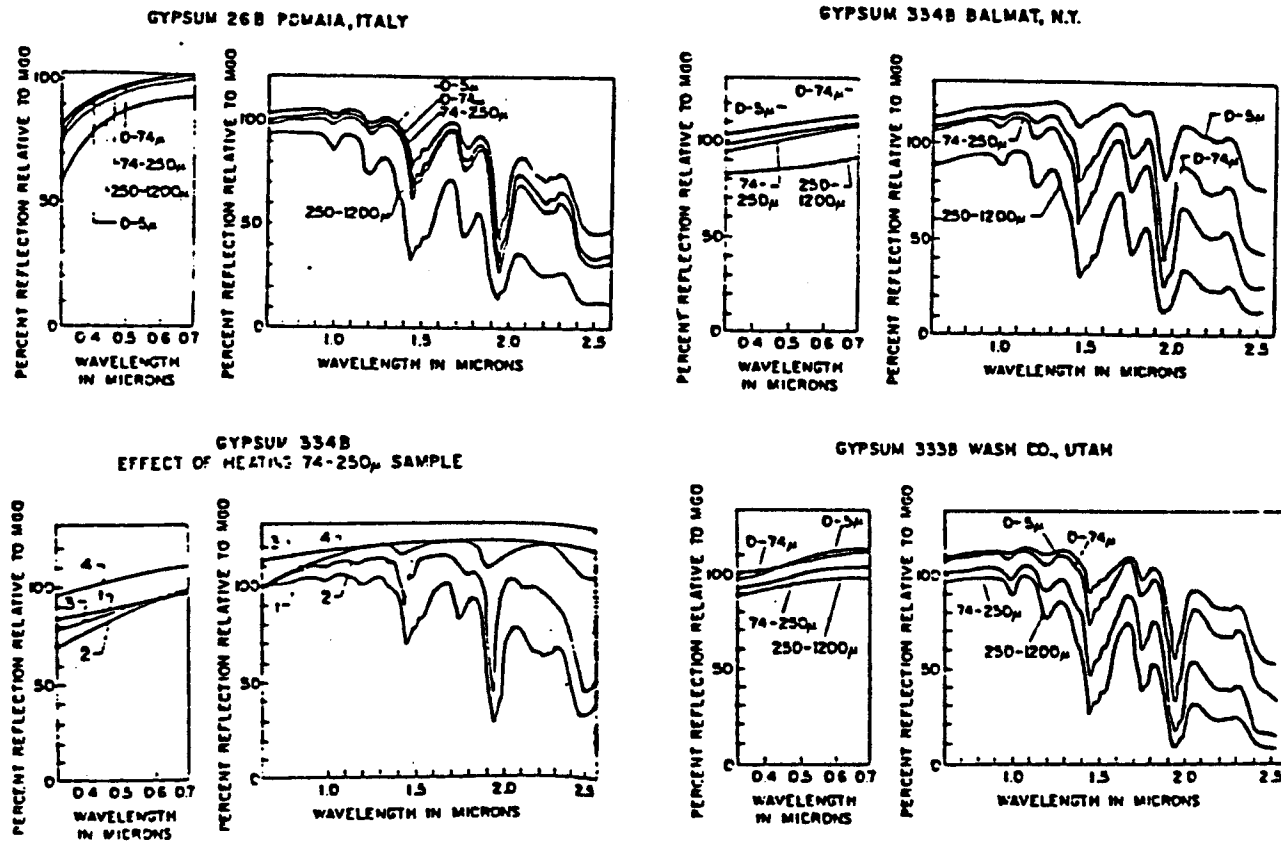
Figure 3. Reflectance characteristics of gypsum from different origins (16).

$CaSO_4 \cdot 2H_2O$" showed a prominent water absorption band in the near infrared spectral bands beginning from 1.0 μm and continuing to 2.5 μm, while the "hemihydrate gypsum, $CaSO_4 \cdot \frac{1}{2}H_2O$" showed the same water bands, but they were narrower and less structured. On the other hand, the "anhydrite gypsum, $CaSO_4$" also showed a strong water absorption band, and lost water upon heating (Figure 3).

Hunt et al. concluded that the presence of the molecular water which made the group of bands near the 1.9 μm wavelength diagnostic because they required the presence of the "H-O-H" bending mode for their appearance. Also, the strong band at 1.75 μm was quite unusual in that they have not previously seen a band in that region in hydrated materials, i.e., clay minerals (16,17).

Leaching

Leaching, in its application to the salt affected soils of the arid and semi-arid regions, is the artificial substitute of the natural leaching process which is carried out by rainfall in the humid zones. Leaching is the only way possible to create a salt-free seed bed and root zone in soil profiles whose salt concentration is more than 4 mmhos/cm (19,55).

Vaious physical and chemical changes normally occur after leaching has been accomplished. Among such changes in the soil are (a) an increasing water content due to the increasing pore spaces between the soil particles as a result of decreasing the total concentration of salts, (b) better aeration is established for the same reason, (c) loss of nutrients from the soil profile, and (d) a change of the soil color to higher values and chroma "lighter" due to the immediate loss of salts of high concentration in the profile which have had their effect on the soil color, i.e., white, dark brown for the sodium and magnesium chlorides, respectively (12,13,19,55).

Leaching is normally a time consuming process as far as saline-fine textured soils are concerned. It usually takes about 25 days to leach the first 50 cm of the soil profile. Less time is required to leach medium-coarse textured soils. The leaching time required

depends on the total concentration of salts (EC), infiltration rate and the soil stratification system, especially if an alluvial soil is involved (19,55).

Bidirectional Reflectance Factor

Variation in reflectance, defined as the ratio of the reflected flux to the incident irradiation as a function of wavelength, provides the basis for characterization of target scenes, as is the case in spectroradiometric measurements of soil reflectance. The directional characteristics of the reflectance process are crucial to remote sensing studies. For example, aside from the effect that the sun angle can have on image classification results, the presence of clouds may lead to diffuse, rather than collimated irradiation of the target of interest. Also, many early studies of soil reflectance properties utilized a laboratory integrating sphere reflectometer whose directional characteristics differ from bidirectional reflectance factor (BRF) measurements. The technical basis for BRF measurements allow for direct comparison of field-collected data with laboratory-collected data when a standard calibration procedure is closely followed (28,47,48,52,54,56).

The fundamental property describing the geometrical reflectance distribution characteristics of a surface is the bidirectional reflectance function (BDRF). Immeasurable amounts of radiant flux through infinitesimal elements of solid angle render this function useful only as an underlying concept with a more practical measure being bidirectional reflectance factor. Hence, BRF can be described as the ratio of the flux reflected by an object under specified conditions of irradiation and viewing to that reflected by the ideal, completely reflecting, perfectly diffusing surface, identically irradiated and viewed with the restriction that measurements are made through negligibly small solid angles of illumination and viewing (47,54).

A bidirectional reflectance factor reflectometer developed as an accessory to a field spectroradiometer permits conditions of

variable incident irradiance of a horizontally placed 3.2 cm diameter soil sample area. In this manner, specially prepared soil samples can be irradiated and viewed from above, thus, simulating the remote sensing situation as closely as possible. Quantitative measurements of soil reflectance using this instrument setup have been helpful in relating BRF to important soil properties (35,47,54).

Landsat Imagery

The availability of the visible and near infrared multispectral scanner (MSS) data from 0.45 ha resolution elements within a 34,000 square kilometer image frame presented new possibilities in soil mapping in the 1970's. The Landsat series of satellites obtain spectral data in four bands ranging from 0.5 to 1.1 micrometers in a 18-day repetitive cycles. These data are processed to provide imagery in the form of various photographic products as well as numerical format magnetic tapes for digital analysis (37,39,41,42, 43). (See Figures 4 and 5.)

Computer-aided analysis of Landsat multispectral scanner data was used to produce a spectral map based on drainage characteristics at a scale of 1:20,000 (59). Weismiller et al. successfully presented a procedure of partitioning an area in Jasper County, Indiana into different parent material sub-areas based on photointerpretation of Landsat false color imagery (59). They then used computer-aided spectral classification within parent material groupings to prepare 1:15,840 scale spectral maps for use in the soil survey of the county (20,58,59).

The use of data from an air- or spaceborne multispectral scanner allows the analyst to obtain a quantitative radiation response value for each resolution element at ground level. This approach has been successfully used with computer-implemented pattern recognition techniques to produce maps which delineate spectrally separable classes of surface features. These techniques for mapping spectral classes were applied by Kristof to produce a computer classification of green vegetation, bare soil and water (25)(Figure 6). The results of several other studies have reported the use of computer-implemented
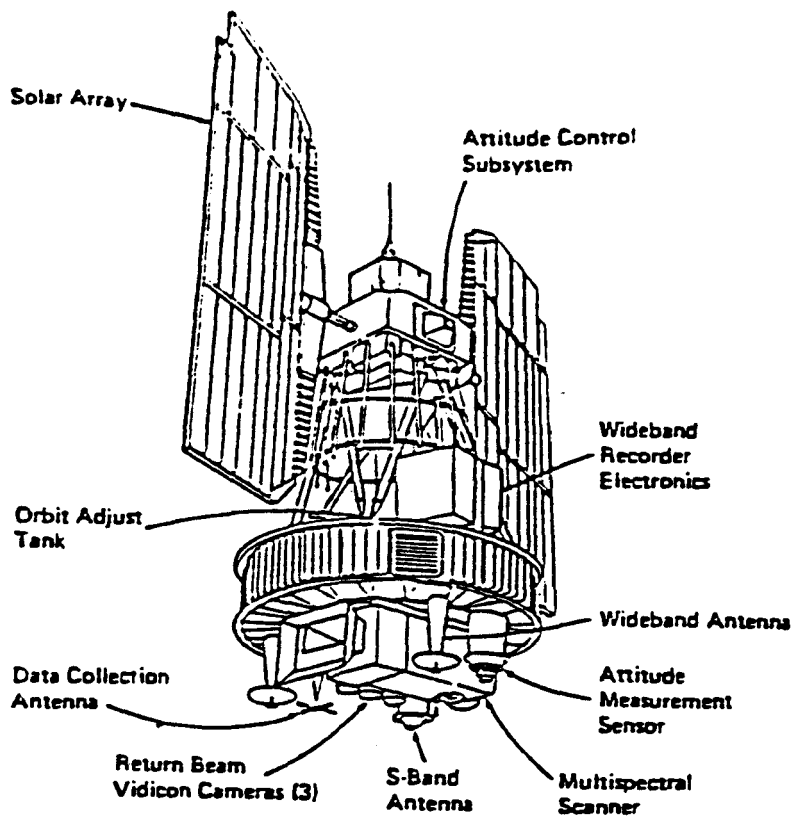
Figure 4.   The Landsat satellite.
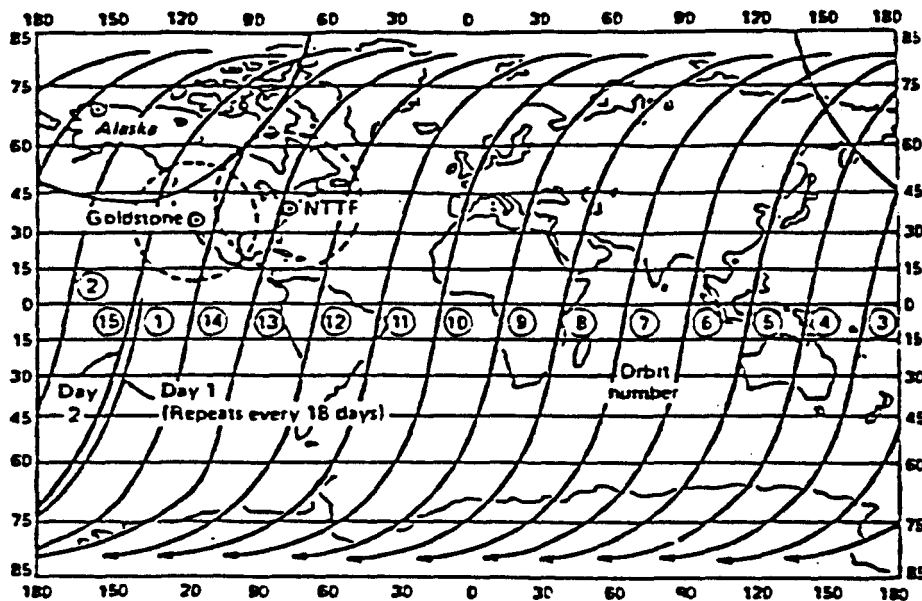
Figure 5.   The Landsat space orbit diagram.

(a)   (b)
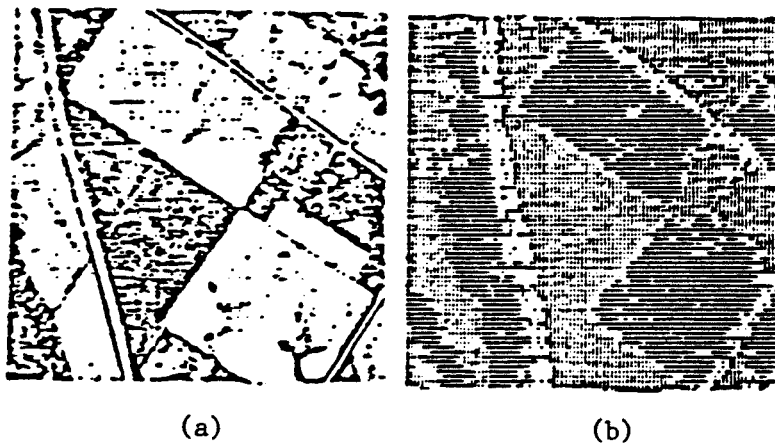
Figure 6. A comparison between (a) an aerial photograph and
     (b) a computer classification of green vegetation, soil
     and water of the same area (25).

analysis of multispectral data to produce spectral maps of surface
soils which compare favorably with soil maps prepared by the conven-
tional soil survey techniques (21,25,26,27).

Most agricultural areas in the world do not consist of soils as
the major land cover type; instead, green vegetation or vegetation
cover usually exist. Spectral reflectance variation from both covers
is easily separated according to the specific spectral reflectance
characteristics of each land cover type.
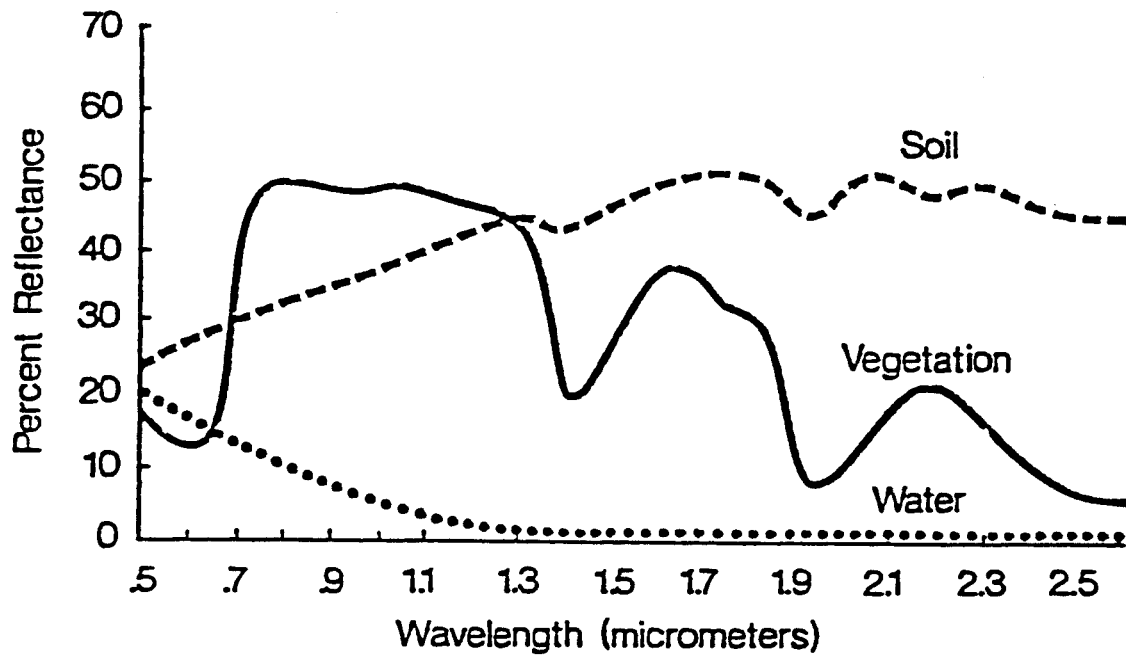
Figure 7. Generalized spectral response patterns for three
    basic land cover types (54).

METHODS AND MATERIALS

The Research Area

Location

The research area is located within the central portion of the
Abu-Ghraib project, west of Baghdad, Iraq. It covers an area of
about 3,750 km^2 in the Mesopotamian plain between the Tigris and
Euphrates Rivers (Figure 8).

Geology

The geological history of the area starts at the end of lower
Miocene time with recession of the Tethys Sea, which until then
covered most of present Iraq. In the shallow sea, clay/shell breccia/
gypsum-anhydrite layers formed during the middle Miocene (Lower Fars).
Reddish brown clays, always very rich in gypsum, alternated with sand-
stone and siltstone, rich in mica and dark-colored minerals; a remark-
ably high percentage of lime also was deposited during the upper
Miocene (Upper Fars) when alternating marine and terrestrial condi-
tions resulted in a great variety of lithological character (11,38).

The Lower Fars formations grade into the Bakhtiari formation
(Pliocene-Pleistocene), consisting of gravel conglomerate and gravel
interbedded with lenses of sand and marly clays. The gravels are
partly of sedimentary character and partly crystalline (11,38).
Gypsum cementation occurs mostly in the upper layers of the forma-
tion (38).

It is thought that the Bakhtiari sediments were deposited by the
Tigris and its tributaries. In areas under influence of the ancient
Euphrates River, the Upper Fars formation is overlaid by remnants of

LEGEND

•••••••• project boundary

——————— main road

—•——•——• railway

——————— irrigation canal

---------- drainage canal

[hatched box] high desert

[symbol] town

A   study area
B   sampling area
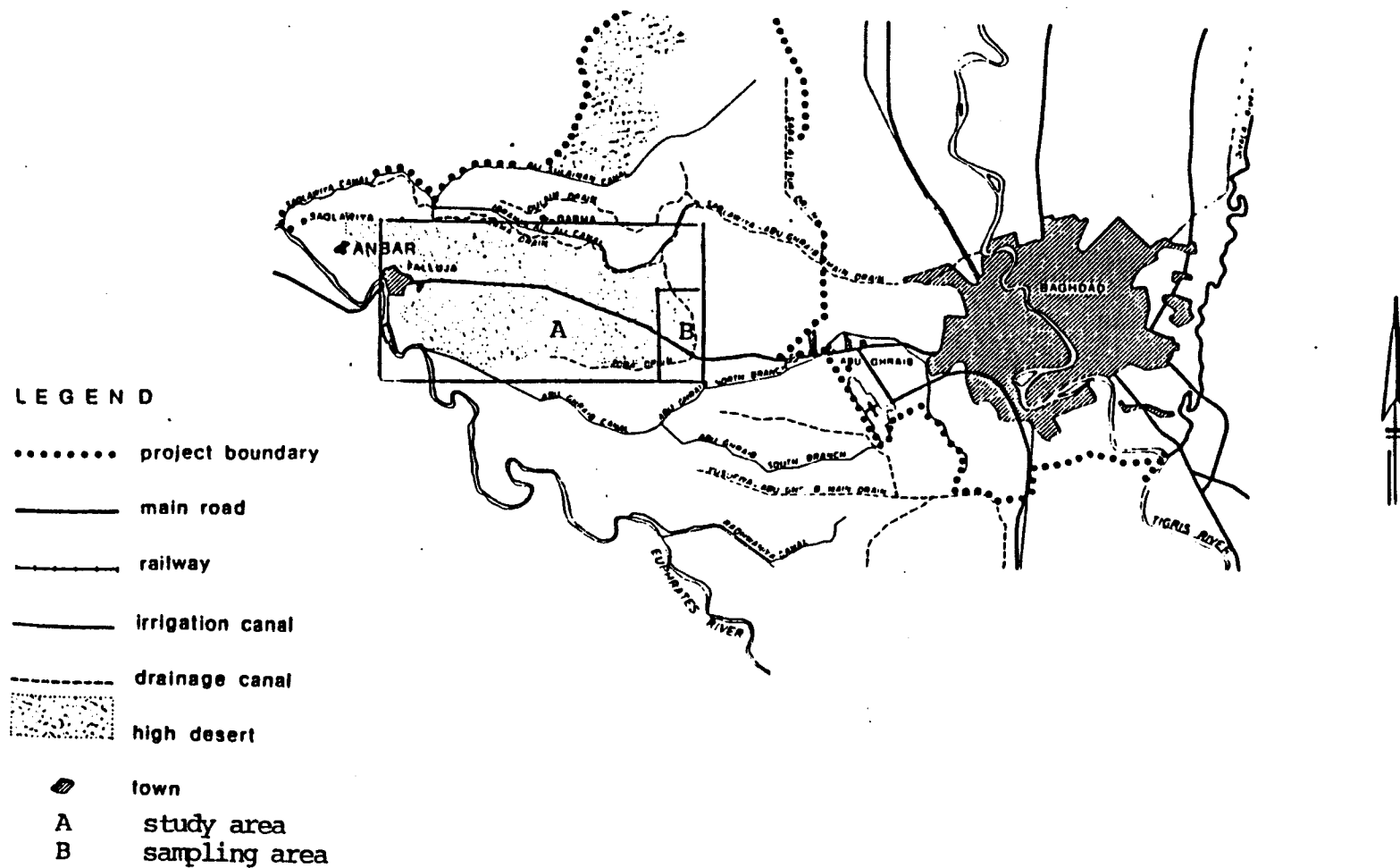
Figure 8. Location map of the study and sampling areas
(approximate scale 1:600,000)(38).

Old Terraces of the same age as the Bakhtiari Formation. These deposits are of clayey sand, soft sandstone and silt that is rich in scattered gravel (11,38).

There are few remains of the old alluvial terrace in the Abu-Ghraib area because of dissection of the Bakhtiari formation and its Coeval terrace deposits. Moreover, secondary gypsum and limestone cementations are thought to have formed also in these sediments during pluvial periods. The sedimentation of the older alluvium materials occurred mainly south of the research area in the Lower Mesopotamian plain (11,38).

At present, the streams deposit clay, silt and sand, rarely interbedded with gravels. These Holocene deposits vary greatly in thickness in the Abu-Ghraib area, ranging from 0-20 meters (38).

Geomorphology

Most Holocene deposts in the Abu-Ghraib area belong the the flood plain of the Euphrates River, with only a narrow strip in the east containing sediments from the Tigris River. For the greater part, this flood plain is underlaid by the Bakhtiari Formations, but these coarse-grained deposits disappear east of the Baghdad-Hilla highway, southeast of Baghdad.

In the western and northern parts of the area, the Bakhtiari Formations emerge from the flood plain and form remnants of old terraces, commonly called "High Desert" deposits (Figure 9).

The mostly medium and fine textured Euphrates-Tigris flood plain is of the meander-belt type (38). This flood plain is characterized by river levees, back swamps, and sandy point-bar deposits in the inner bends of the river, and sandy crevasse splay deposits overlying medium and fine textured deposits.

The first irrigation systems in the world were in the Mesopotamian plain about 5000 years ago (mid-Holocene time). These ancient engineering works reflect the great influence of sedimentation on the flood plain. This randomized irrigation system occasioned winding
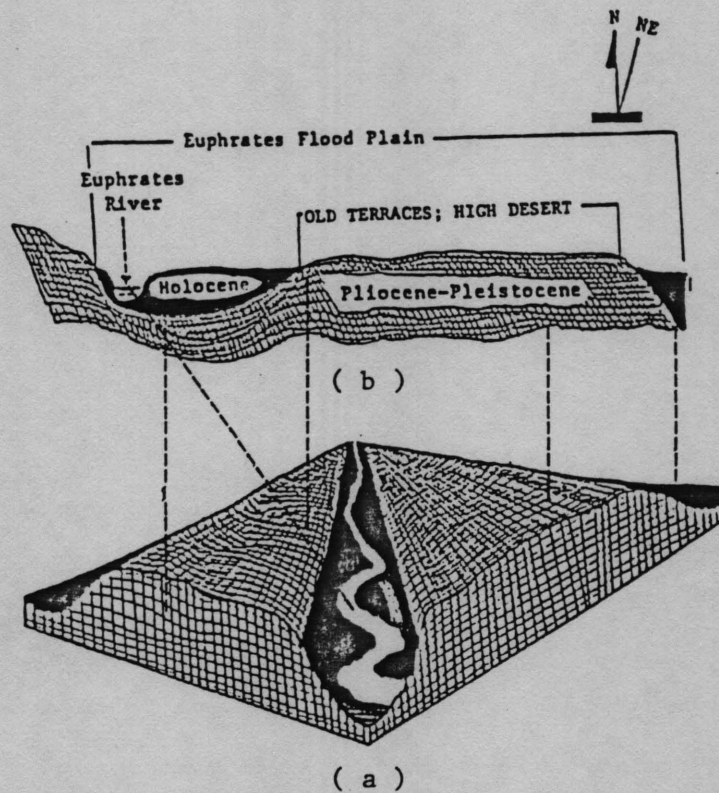
Figure 9. An approximation of the research area's (a) three-dimensional, and (b) cross sectional diagrams of the geological and physiographical features.

streams that behaved as small rivers which built small levees on both sides. The profile of these levees reveals mostly sandy layers, most of which can be traced from aerial photographs and borings (11,38).

Gradually, these small rivers (fishbone types) were used to carry and transport water to other areas. This controlled irrigation system has produced, in the interval from the Neo-Babylonian to the early Islamic civilizations, very wide levees between which lay depressional soils (11,38). These irrigation levees consist of medium- and moderately fine-grained, thick irrigation deposits.

Variation in topographic features is gradually distinguished in the "High Desert" terraces to the west. Such variation ranges from light-undulating to undulating while the alluvial portions are commonly semi-flat to flat in topography. The calculated difference between the first and the latter is approximately 4 meters and both are approximately 46 meters from Mean Sea Level (MSL).

Climate

The Abu-Ghraib area, as a part of the Mesopotamian plain, has the same climate which characterizes the flood plain: subtropical; hot and dry.

The climate is characterized by two well-marked seasons with short transitional periods: (a) a long, hot, rainless summer from May-October and (b) a comparatively short, cool winter from December-February.

Average rainfall is about 150 mm, but it varies considerably from one year to another and in seasonal distribution. There are also great differences in rainfall over short distances laterally. Rainfall usually falls in showers in the months of November through April (Table 1.).

There are wide diurnal and annual ranges of temperatures. The absolute maximum temperature recorded was 51°C and -8.5°C for the minimum. Diurnal difference in temperature is often 15°C and may be more than 20°C. Air humidity is usually low during summer and averages

Table 1. The climatic data of the research area .*

	Jan	Feb.	March	April	May	June	July	Aug.	Sep.	Oct.	Nov.	Dec.	year	Period of observation
Temperature absolute max.	25.0	30.0	36.1	43.3	44.6	48.3	50.0	50.2	47.2	42.0	36.7	26.7	50.2	1923-1974
mean max.	16.0	18.7	22.7	28.7	35.8	41.0	43.4	43.3	39.8	33.4	24.6	17.6	30.4	1941-1970
(°C) mean	10.0	12.3	16.3	22.0	28.4	33.0	34.8	34.4	30.6	24.6	17.1	11.0	22.9	1941-1970
mean min.	4.3	5.9	9.6	14.6	20.0	23.4	25.3	24.6	21.0	16.2	10.3	5.2	15.0	1941-1970
absolute min.	-8.5	-6.0	-3.3	1.2	10.0	13.5	16.6	17.8	10.7	3.5	-3.0	-6.7	-8.5	1923-1974
Soil temperature 5 cm, 06 GMT	7.3	9.2	14.8	20.6	27.0	31.3	33.3	33.3	29.9	23.4	15.1	8.8		
12 GMT	12.9	15.6	22.4	28.3	34.9	39.8	41.1	40.7	37.5	30.7	21.0	13.7		
(°C) 50 cm, 06 GMT	13.3	13.9	18.4	22.6	28.0	32.3	34.1	35.0	33.3	28.7	22.3	15.9		1970-1975
12 GMT	13.3	13.8	18.4	22.6	27.0	32.2	34.1	34.9	33.2	28.6	22.2	15.9		
Relative humidity 03 GMT	84	77	70	63	48	34	32	35	40	50	71	83	57	1941-1970
06 GMT	79	70	60	43	34	25	26	27	30	38	59	78	47	1937-1952
(%) 12 GMT	50	39	34	29	19	13	13	13	15	22	38	51	28	1941-1970
average	71	63	56	47	33	24	23	24	28	36	56	71	44	1937-1952
Rainfall monthly mean	25.3	24.4	22.7	22.3	8.1	0.1	0	0	0.3	3.7	17.1	22.9	146.9	1941-1970
(mm) max. in 24 hrs	35	64	56	44	20	1	0	12	1	16	53	39	64	1937-1952
Sunshine hours	6.5	7.3	8.1	9.0	10.6	12.7	12.9	12.2	11.4	9.4	7.7	6.0		1971-1975
Total incoming radiation (cal/cm²/day)	343	439	576	672	779	864	844	785	669	524	386	315	7195	1967-1975
Mean low cloudiness (oktas)	1.3	1.4	1.1	1.1	0.6	0.2	0.2	0.1	0.1	0.4	0.9	1.1	0.7	1941-1970
Windspeed (15 m level) (m/sec)	3.1	3.6	3.9	3.8	3.8	4.2	4.5	4.0	3.3	2.8	2.6	2.7	3.5	1941-1970
Evaporation Class A Pan (mm)	73.9	99.3	184.5	261.3	403.8	522.8	600.5	533.0	370.5	247.0	134.6	61.4	3492.6	1967-1974
Evaporation from a free water surface (mm)	50	84	146	198	260	309	332	298	213	133	69	43	2135	-

* Baghdad Meteorological Station, 1977 (38).

about 13% at 3:00 p.m. in July. The potential evapotranspiration of
the free water surface is estimated as in the high range (by the
Penman method) but no figure is yet published and considered final
(Table 1).

Salinization

In the Mesopotamian plain natural salts in the marine Pliocene-
Miocene deposits could be a cause of salinization. However, in this
case, poor/lack of natural drainage may be the major reason that these
deposits are still saline because they are situated under higher
slopes north of the Abu-Ghraib area and have a lower salt content.
It is reasonable to assume that changes in natural drainage have
greatly contributed to the increase of salinity as the climate may
be considered a constant factor. Changes in natural drainage con-
ditions in Holocene time are explicable only by tectonic movements,
changes in sedimentation and flood patterns, or by some combination
of these factors (11,38).

These two factors are, therefore, most probably the main causes
of the increased salinity in the flood plain. In addition, very high
evaporation rates, lack of natural drainage because of flat topography,
high-saline ground water, and the effect of thousands of years of
uncontrolled irrigation practices may be added to past and present
factors which have contributed to salinization of the flood plain.

Vegetation

The Lower Mesopotamian plain belongs climatically to the vegeta-
tion zone of the sub-desert region of Iraq. However, throughout the
Mesopotamian plain, hardly a vestige of natural vegetation remains
today, whereas most of this important agricultural region formerly
was under intensive irrigation-cultivation practices which replaced
the original vegetation (11,38).

The present vegetative cover is a mixture of natural weeds,
scattered field crops and isolated date palm and citrus gardens.
Weeds are the most common and dense vegetation cover in the saline

alluvial soils (mostly irrigated). These deep leguminous species are as follows:

    a. <u>Alhagi maurorum</u> (local name: Agool)

    b. <u>Prosopis farcta</u> (local name: Showk)

    c. <u>Suaeda baccata</u> (local name: Terta'e)

    d. <u>Cressa cretica</u> (alkali weeds)

Soils

The most common soils in the Abu-Ghraib research area are the Typic Torrifluvents. These are mostly brownish soils formed in recent water-deposited sediments of flood plains. They have a torric (hot and dry) moisture regime, are calcareous and locally saline, and are not flooded frequently or for a long time (10,38,50).

In very saline sites, Typic Salorthids occur, especially in areas where the topsoil or the subsoil includes a salic horizon within the upper 25 cm. These soils are usually associated with saline-high ground water table, which in turn saturates them at some time of the year. Such soils have severe salt accumulations on the immediate surfaces owing to high concentration of salts, high ground water table, high evaporation rates, and very active capillary movement. Such salt accumulations have a dark brown (10YR4/4-4/3) color owing to the presence of magnesium chloride. Sodium chloride is the most common (white-colored) salt in the area (11).

The predominant clay is montmorillonite (more than 47%) with some illite, kaolinite and calcite (11,38).

Typic Torrerts also occur in the neighborhood of the high desert plateau. These soils are clayey and develop deep, wide desiccation cracks during most of the year. The bulk-density between these cracks is high, and gypsum content also is relatively high, ranging from 4% on the surface to 11% in the substrata (38,50).

The "high desert" soils all are Gypsiorthids. The commonest type is the Petrogypsic Gypsiorthids. These soils formed in a climate wetter than at present, and are characterized by an undulating topography, sandy, loamy and silty materials mixed with gravel, with a

desert pavement and commonly a dune-crust (11,38). Wind erosion is very active and at times severe. This is especially noticeable at gravel and gypsum mining sites where human activities increase the effectiveness of wind.

Chemical and Physical Analysis

Exchangeable Base

Five gm of soil were weighed and placed in a centrifuge tube. Thirty-three ml of Ammonium Acetate solution (1.0N) were added. After being shaken for five minutes, the mixture was centrifuged at RCF 1000 for five minutes until the supernatant liquid was clear. The supernatant liquid was decanted as completely as possible into a 100 ml volumetric flask. This extraction process was repeated twice after the initial extraction. The extract was diluted to volume, mixed and the amount of the extracted cations was determined by flame photometry (8,55).

Cation Exchange Capacity

Five gm of soil were weighed and placed in a centrifuge tube, then 33 ml of Sodium Acetate (1.0N) were added. After being shaken for five minutes, the mixture was centrifuged at RCF 1000 for five minutes or until the supernatant liquid was clear. The supernatant liquid was decanted and discarded. The sample was treated in this manner with 33 ml portions of the same solution four times. Thirty-three ml of Ethanol (95%) were added to the sample which was then shaken for five minutes and centrifuged for five minutes. The supernatant liquid was then decanted and discarded. Then the sample was washed in the same manner three times. The adsorbed sodium from the sample was replaced by extracting the sample with three 33 ml portions of Ammonium Acetate (1.0N). The mixture was then shaken for five minutes and centrifuged at RCF 1000 for five minutes. The supernatant liquid was collected in a 100 ml volumetric flask, diluted to volume and the sodium concentration was determined by flame photometry (8,55).

Chlorides

The chlorides were determined by the autoanalyzer. The process depends upon the reaction between chloride and mercuric thiocyanate which results in the formation of a soluble, but not ionized mercuric chloride. In the presence of ferric ions, the thiocyanate is librated from a red-colored compound which was colometrically measured.

Sulfate

The sulfate ($SO_4^=$) was determined by using the autoanalyzer where Barium Chloride solution was added and the precipitated Barium Sulfate was held in a homogeneous suspension by polyvinyl pyrrolidone. The reaction was carried out in an acid medium to prevent the precipitation of carbonate, chromates, phosphates and oxalates of barium.

Carbonate and Bicarbonate

The carbonate and bicarbonate were determined by using the auto-analyzer based on the standard method of acid-base titration in which the methyl orange was used as an indicator.

Electrical Conductivity, pH and Soluble Cations

Since these determinations are carried out from the preparation of the same saturated soil paste, distilled water was added to the soil samples while stirring with a spatula. After the soil samples reached the saturation stage (the soil paste glistens as it reflects light and flows slightly when the container is tipped), the paste then was mixed and let stand for an hour or more (8,55). Then:

Electrical Conductivity was determined using the conductivity bridge;

pH was determined by the pH-meter;

Soluble Sodium was determined by the Flame-Emission Spectro-photometer; and

Soluble Calcium and Magnesium were determined by the Atomic Absorption Spectrometry.

Lime

A 25 gm soil sample was placed in a 150 ml beaker, then (0.5N) hydrochloric acid was added, covered and gently boiled for five minutes. After cooling, the amount of unused acid was determined by adding two drops of phenolphthalein (1% in 60% ethanol) and back-titrating with sodium hydroxide (0.25N) (8,55).

Organic Matter Content

A soil sample was ground to pass through a 0.5 mm screen. Then the weighed sample was transferred (10 gm) to a 500 ml Erlenmeyer flask; 10 ml of potassium dichromate were added then immediately followed by 20 ml of sulfuric acid. The flask was swirled and gently heated to 150°C. The flask was removed after reaching the desired temperature and allowed to cool down. Then, 200 ml of water and five drops of Ferroin indicator were added, titrated with ferrous sulfate until the color changed from green to red (8,55).

Gypsum ($CaSO_4 \cdot 2H_2O$) Content

Gypsum content was determined (in percentage) by the increase of soluble calcium plus magnesium upon using the dilution method. Another water extract of soil was prepared using a moisture content sufficient to dissolve the gypsum present. The concentrations of calcium plus magnesium were determined for the two extracts by automatic adsorption spectrophotometry (8,55).

Soil Color

All soil colors were determined in the dry and moist states for the soil samples using the Munsell color charts.

Soil Texture

Due to the high gypsum in most of the soil samples (8%) which prevented the texture determination in the laboratory (gypsum percent greater than 8%), feeling by fingers was used instead.

Field Sampling

Field sampling was conducted after intensive investigation of the variations in surface features occurring in the soils of the Project Area. Among specific variations taken into account were: (a) soil color as related to the density and accumulation of salinity and salt(s), (b) apparent surface wetness caused by existence of a specific salt, (c) type and density of vegetative growth, (d) agricultural and irrigation practices, and (e) the percentage occurrence of the above factors in the whole area.

With the aid of a soil salinity map*, it was possible to divide the area into three sub-areas:

1. Sub-Area #1: Saline-extremely saline soils;
   (soil samples number: 3,4,5,6,7,8,9)

2. Sub-Area #2: Moderately saline-saline soils;
   (soil samples number: 11,12)

3. Sub-Area #3: Nonsaline Gypsiferous soils;
   (soil samples number: 1,10)

Each representative soil sample was obtained within an area of 4 x 4 meters to a maximum depth of 2.5 cm from the soil surface. After a careful mixing, each individual soil sample was equally divided into two parts**.

Sub-Area No. 1

Soil conditions in this area are considered a direct result of high evapotranspiration, saline ground water and, hence, very active capillary movement. Soil salinity is within the range of "very - extremely saline" in most of the area.

---

*Soil Salinity Map (Scale 1:50,000), Abu-Ghraib Project, NEDECO, 1978

**The first half was used for the chemical and physical analysis, while the second was shipped to the United States, Purdue University/LARS for laboratory measurements of spectral reflectance and the experimental work.

Magnesium and sodium chlorides are the predominant salts. This combination of two salts of different colors gives the soil surface a light-dark brown color.

Agricultural practices are greatly restricted and limited to scattered areas where soil salinity is below average*. Vegetation is restricted to xerophobic weeds, in growth percentages which vary according to the variation of salt types in the first 20 cm of the soil profile. Nevertheless, scattered date palms (salt resistant plants) also exist along with fruit shrubs in well-managed gardens. The most common weed is Alhagi maurorum (English: Camelthorne; Arabic: Agool)(Figure 11).
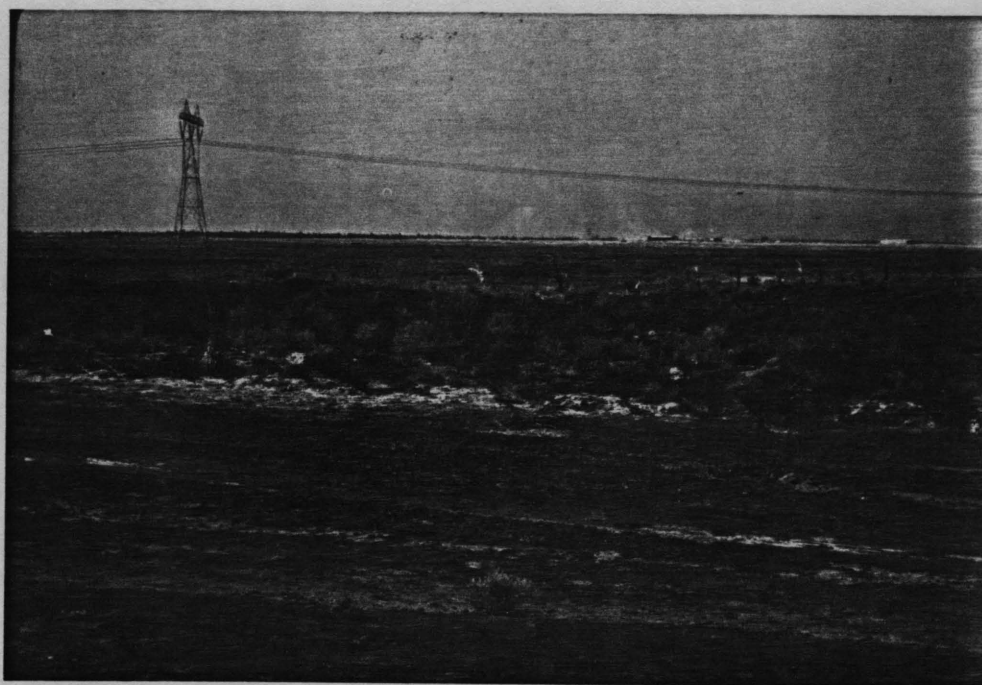
Figure 10. A general view of the area (Photograph: Al-Mahawili, 1981).

*In areas where controlled irrigation and drainage net works do not exist, farmers cultivate after heavy irrigation (flooding method). This method, being uncontrolled, is one of the many factors which contributed to salinity increase.

Figure 11. Existence of weeds (Camelthorne) is
associated with severe soil salinity levels
and generally considered the only vegetation
cover. (Photograph: Al-Mahawili, 1981)

Figure 12. Existence and predominance of $MgCl_2$ gives a brown color to the soil surface. This color scale varies with the existence of co-salts, i.e., NaCl, then light brown color becomes predominant. (Photograph: Al-Mahawili, 1981)

Figure 13. Continuous attraction of moisture from the atmosphere by the soil surface accumulated salts maintains a moist dark brown surface throughout the year. (Photograph: Al-Mahawili, 1981)
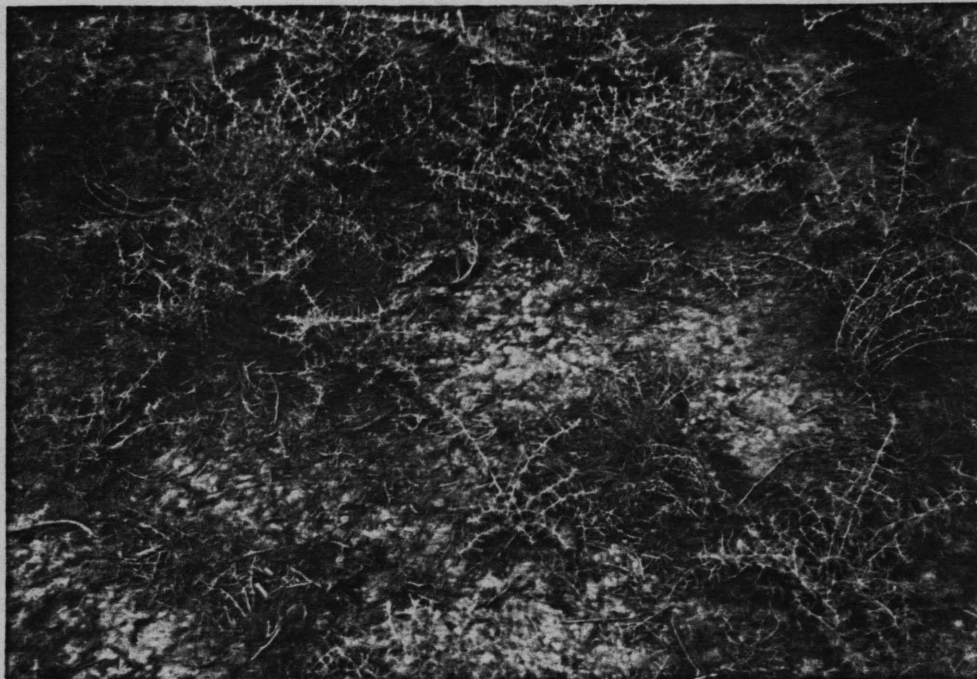
Figure 14. Effect of NaCl on soil surface is reflected by a white color and less moist soil compared with the $MgCl_2$ effect. (Photograph: Al-Mahawili, 1981)

Figure 15. Loose, puffy and white-needle shape features of soils affected by Na_2SO_4. (Photograph: Al-Mahawili, 1981)

Sub-Area No. 2

This area has a soil subject to continuous leaching as part of
land reclamation operations. Thus, the level of soil salinity has
decreased from extremely to slightly saline. As a direct effect of
the complete irrigation-drainage network, ground water (being saline
and unsuitable for irrigation) levels were decreased. Hence, capil-
lary action was greatly retarded.

This area is characterized by cracked soil surfaces owing to the
existence of montmorillonite (over 46%) when dry (shrinkage) (4,29,
31,55). This shrinkage is always associated with deep desiccation
cracks (Figure 16). Because leaching is a continuing process, organic
matter contents also have greatly decreased (4,55). Thus, agriculture
is restricted to such crops as Alfalfa (Medicago sativa) to enhance
soil fertility after in-place harvesting to be part of the future
fertile soil.
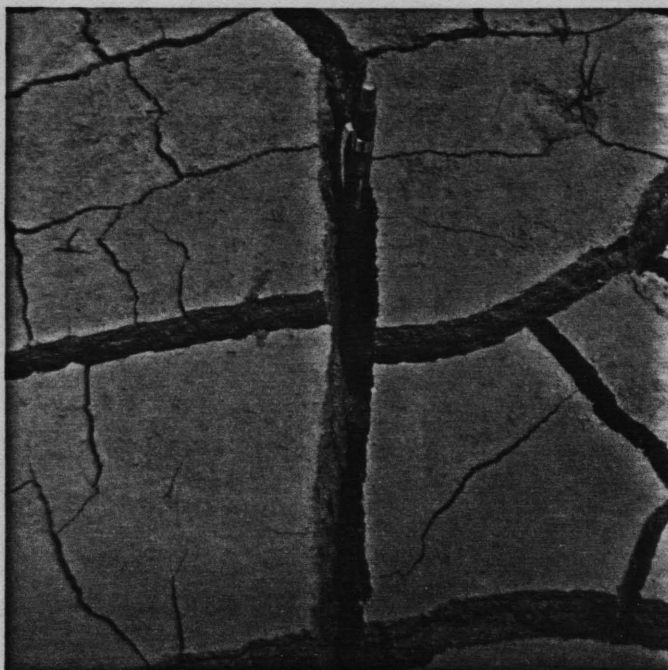
Figure 16. The cracked soil surface due to clay (montmorillonite)
shrinkage upon drying. (Photograph: Al-Mahawili, 1981)

Sub-Area No. 3

This area, also referred to as high-desert soil, is considered unsuitable for agriculture because of the shallow depth of the immature soil profile (top soil) overlying cemented layers. Layers of pure gypsum commonly occur within the first 60 cm from the surface.

Generally, the soil surface consists of sandy to sandy loam textures, is light brown, and usually is mixed with gravels and pebbles. Natural vegetation is rare, and where present, is limited to scattered weed species. Conversely, agricultural practices are limited in depressions where the thickness of the soil profile increases and frequent rainfall runoff is trapped.

Ground water is generally more than 7 meters below the surface and is affected greatly by the presence of gypsum, as far as taste is concerned. Thus, the main usage from wells is restricted to livestock.

For engineering purposes this area is considered valuable because of the presence of thick layers (below the first meter depth) of sand and gravel which are of commercial-engineering specifications and standards. Commonly, these layers are strongly cemented or have a high gypsum content which decreases the commercial value, and thus other mining sites must be located (38).

Having sand and gravel mining as the main commercial activity in this area is of great disadvantage inasmuch as extraction exposes fine-grained loamy sand which is very susceptible to deflation by the strong winds characteristic of this region (Figure 18).

Preparations of Soil Samples for Spectral
Reflectance Measurements

All the soil samples were air (room) dried, mildly crushed by a wooden rolling pin to break up the clods, and passed through a 10-mesh sieve to remove all particles and aggregates larger than 2 mm diameter. The use of the soil size fraction less than 2 mm for soil reflectance measurements was an attempt to standardize this procedure in line with the use of this same size fraction for most laboratory determination of soil properties (50).

Figure 17. Undulating topography and scattered growth of Prosopis are major land characteristics of the non-saline gypsiferous soils. (Photograph: Al-Mahawili, 1981)

Figure 18. Mining of sand and gravel contributes to severe wind erosion of gypsiferous soils. (Photograph: Al-Mahawili, 1981)

35

Figure 19. Typical crusted soil surface in gypsiferous soil mixed
with gravel and pebbles associated with loamy or sandy textures.
(Photograph: Al-Mahawili, 1981)

Figure 20. Prosopis (Lagonychium farctum) is considered the only
natural vegetation in this desert environment of gypsiferous
soils. (Photograph: Al-Mahawili, 1981)

Sieved soil samples were carefully divided and placed in cardboard containers which were identified by sample number and location (Figure 21).

Later, all the soil samples were placed in the sample holders which were basically designed to fit the specifications of the spectroradiometer field of view. A 10 cm inside diameter sample holder was selected to allow sample leeway in positioning the sample with the 3.2 cm diameter field of view of the instrument (36,51).

The depth of 2 cm provided sufficient soil bulk to obscure the bottom of the sample holder and assuring that only soil being viewed. The plastic sample rings were painted with a non-reflecting paint to reduce unwanted reflectance (36,51). Soil samples were transferred to the sample holders with extra care in order to avoid segregation of aggregate sizes. A leveled soil surface was maintained by striking off the excess soil with a straight edge.

Figure 21. The process of air drying of soil samples was followed by placing them in numbered cardboard containers. (Photograph: Al-Mahawili, 1981)

Measurement of Bidirectional Reflectance Factor (BRF)

An Exotech Model 20C spectroradiometer was used in an indoor
configuration with a bidirectional reflectometer in order to obtain
spectral readings in 0.01 micrometer increments in the 0.52-2.32 µm
wavelength range (Figure 22). The short wavelength head of the
spectroradiometer contains a silicon detector for measuring radiation
in the 0.37-0.74 µm wavelength range and a lead sulfide detector to
cover two wavelength ranges: 0.65-1.3 and 1.25-2.5 µm (48).

Each of these wavelength ranges corresponds to one segment of a
circular variable filter (CVF) through which spectral scans are made
by rotation through the optical path in front of the detectors.
Circular variable filters provide the instrument with the capability
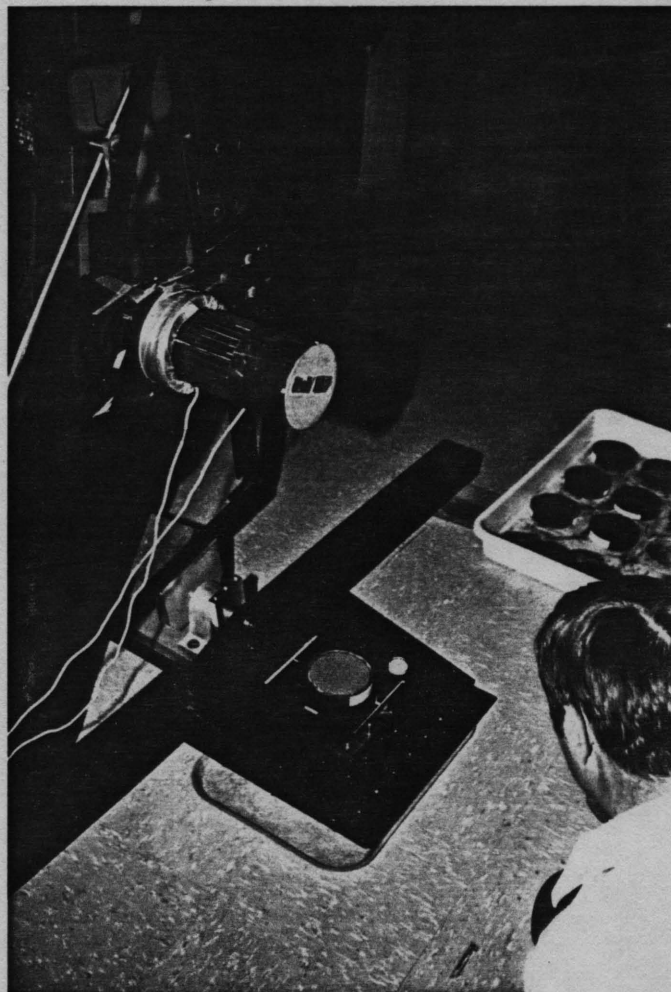
Figure 22. BRF reflectometer positioned for soil sample detection
by the Exotech Model 20C spectroradiometer. (Photograph: Al-
Mahawili, 1981)

to operate under natural conditions because of the rapid spectrum scan time of 2 complete scans per second (28).

Data recording is carried out on both a multichannel strip chart recorder and on magnetic tape for subsequent digitization and computer processing.

The sensing head of the spectroradiometer is mounted in a vertical fixed position approximately 2.4 meters above the sample stage. The illumination source is a 1000 watt tungsten iodine coiled filament lamp which transfers a highly collimated beam by means of a paraboloidal mirror to the sample-viewing plane. Incident irradiation is about 6° off vertical. The 3/4° field of view mode of the spectroradiometer is used to detect a sample area of about 3.2 cm diameter.

Pressed barium sulfate is used as a standard to calibrate the instrument (Figure 23). After every fifth soil sample, the pressed barium sulfate is measured to account for changes in intensity of the illumination source. The bidirectional reflectance factor data are corrected for dark-level instrument offset and less than unity reflectance of the barium sulfate standard. Six complete scans covering the entire wavelength range are made and later averaged when the magnetic tapes are digitized and processed (51).

Design of the Experiment:
Its Structure and Parameters Involved

The major concepts behind the experimental design were to (1) recreate the actual soil conditions in an arid/semi-arid environment related to soil-water relationships, salt accumulations on the surface soil due to capillary movement, and the changes of the saline surfaces after leaching has taken place and (2) relate each phase of such soil-water relationships to specific spectral reflectance characteristics for use in the digital analysis and interpretation of Landsat multispectral scanner data. Such an attempt will certainly have its interpretive influence in relating spectral classes within the same saline soils depending on the level of salt concentrations, salt-water-soil interactions and their impact on changing the spectral reflectance of the saline soils before and after leaching.
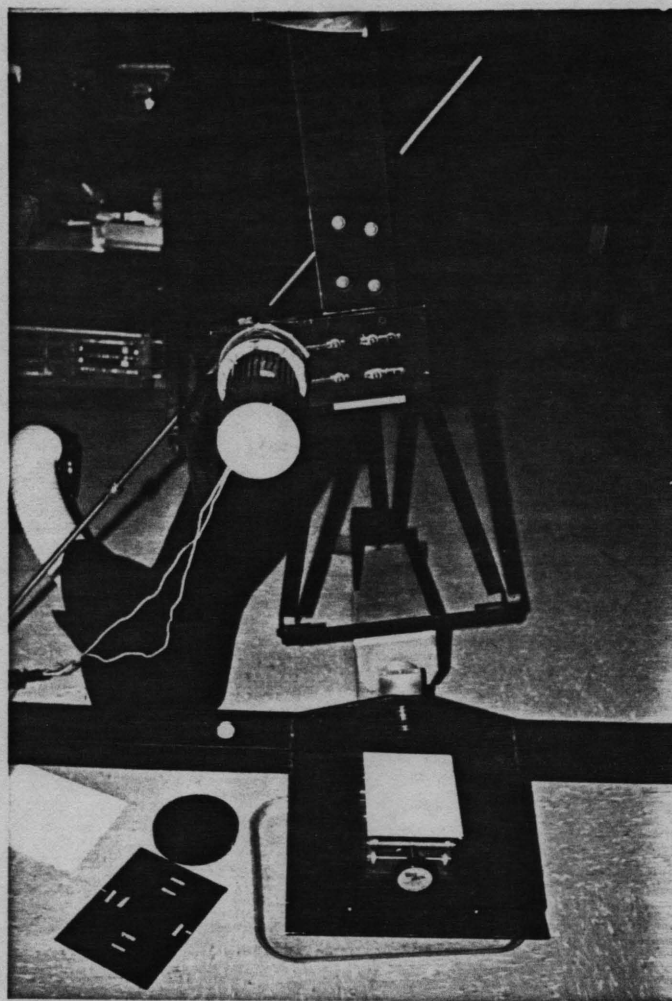
Figure 23. The pressed barium sulfate is used as
a standard of the Exotech Model 20C calibration.
(Photograph: Al-Mahawili, 1981)

Since the quantity and quality of salts affect the general soil
color, a quantitative measurement of reflectance characteristics
should be related to the differences in salts present. Soil color
then should be changed when leaching takes place and most salts are
dissolved and leached from the soil profile(s). Thus, the expected
high levels of value and chroma of soil colors, upon leaching, will
change the spectral reflectance characteristics of the same saline
soils, before leaching. This type of field observation is widely
observed in areas where water (irrigation water) is used for leaching
saline soils.

The experiment is divided into three stages: (a) before leaching where 3 soil sample groups A,B,C are put under 3 water content levels (24 hr saturation, 2-day and 6-day air drying) with spectral measurements taken after each level, (b) after leaching where the three soil sample groups are leached in the laboratory using the water suction, then air dried, and prepared again for the same sample preparation steps mentioned before, and treated with 2 saturation levels (48 hr saturation, and oven drying for 5 hr at 50°C)*, and (c) the non-treated "control" soil sample group D where no saturation treatment is applied. Instead, direct spectral reflectance measurements are taken when air dried, then oven dried for 5 hr at 50°C.

The sequence of different water content levels represents the actual soil-water relationships in the field where saturation for 24 hr is normally observed as a typical representation of the uncontrolled irrigation practice (flooding). Each decrease of water content is calculated to fit the soil condition after intensive irrigation, at field capacity and at approximately the wilting point or maximum salt accumulations on the soil surface.

Field experience in Iraq has shown that using a range of 25 to 50 cm static water head is effective for leaching salts from the profile over a period of several months. In this laboratory procedure an attempt was made to recreate field conditions of saturated surface soils after leaching of salts had been achieved by saturating for 48 hours (Figure 24).

---

*The 5 hr at 50°C time setting for the oven dry was selected from the climatic data in summer. It is an average-maximum sunshine (from 10:00 A.M. to 3:00 P.M.) in summer. The 50°C is an average temperature (maximum) in this 5 hr period calculated from actual data in June, July and August of the last 25 years.

GROUPS " A,B,C "   GROUP "D" (CONTROL)
_____   _____

```
                    ┌─────────────────────────────────────┐
                    │  AIR DRYING, MILD CRUSHING THEN SIEVING │
   ┌──────────────────┐│        THROUGH A 2mm SIEVE          │
   │ SATURATION FOR 24 hrs. │└─────────────────────────────────────┘   ┌──────────────────────┐
   └──────────────────┘                                        │ OVEN DRYING FOR 5 hrs. │
                                                               │      AT 50°C.          │
                                                               └──────────────────────┘
   ┌──────────────────────┐   ┌─────────────────────────┐
   │ AIR DRYING FOR 2 DAYS │   │  SPECTRAL REFLECTANCE   │
   └──────────────────────┘   │     MEASUREMENTS        │
                              └─────────────────────────┘
       ┌──────────────────────┐
       │ AIR DRYING FOR 6 DAYS │
       └──────────────────────┘

              ┌─────────────────┐
              │  L E A C H I N G │
              └─────────────────┘

                  ┌──────────────────────┐
                  │ SATURATION FOR 48 hrs. │
                  └──────────────────────┘

                        ┌──────────────────────┐
                        │ OVEN DRYING FOR 5 hrs. │
                        │      AT 50°C.          │
                        └──────────────────────┘
```
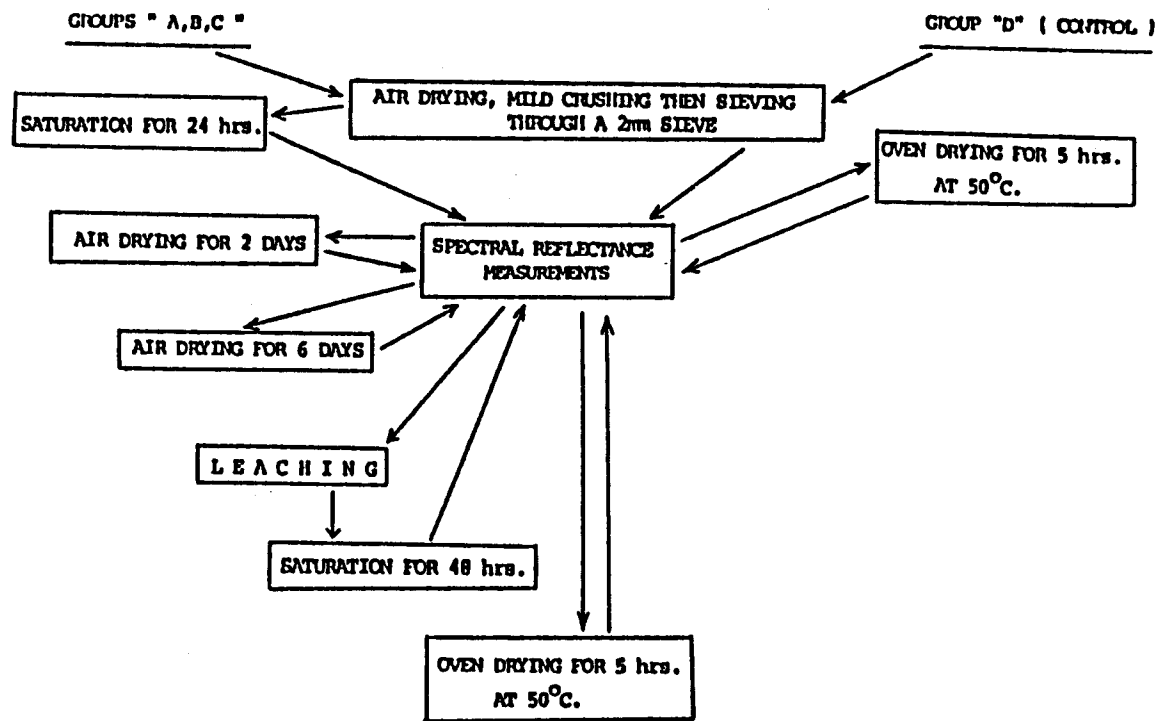
Figure 24. Structure of experimental design.

RESULTS AND DISCUSSION

Chemical and Physical Analyses of Samples

The chemical and physical analyses of the soil samples (Table 2) have indicated some important properties which influenced, directly and indirectly, the reflectance characteristics of soils.

Some of these indications or relationships were : (a) a linear relationship exists between electrical conductivity (EC) and the sodium adsorption ratio (SAR); (b) the exchangeable sodium percentage (ESP) has a clear influence on electrical conductivity in most of the soil samples whose ECs have exceeded the salinity limit of 4 mmhos/cm; (c) the sodium cation (Na^+) has a greater influence on electrical conductivity than the other cations (Mg^{++} and Ca^{++}) (Figures 25 and 26); and (d) water retention characteristics of all the soil samples were greatly affected by the sodium exchangeability. The co-existence of major and minor salts influences the light-dark brown color of all the saline soil samples (Table 2 and 3). Such predominance was shared between the magnesium, sodium and calcium chlorides. It was noticed that in all the saline soil samples, these salts were always present (Table 3). Although the sodium chloride, with its white color, was predominant in almost all the samples, its color effect on the soil surfaces was, in most of the examined field surfaces, decreased markedly by the presence of the magnesium chloride.

The relatively high organic matter percent in the saline soil samples (Sample #: 2,3,4,5,6,7,8) is not a characteristic of the saline soils, but a result of the intensive agricultural practices

Table 2. Chemical and physical analyses of soil samples.*

Sample No.	Tex-ture	pH	EC mmhos/cm	Ca	Mg	Na meq/1	Cl	SO_4	ESP %	CEC —value—	SAR	O.M. —%	Gypsum —
1	LS	8.6	2.4	15.3	3.9	3.5	1.7	17.0	3.0	10.5	1.1	0.4	4.6
2	SL	5.9	379.5	2733.8	948.5	1167.4	4397.9	0.5	95.5	8.2	27.2	2.3	11.3
3	SiCL	7.3	372.0	69.3	596.2	3734.8	4141.8	139.5	89.2	17.2	204.7	2.3	13.6
4	SiCL	7.5	326.0	22.2	1336.3	2542.2	2133.9	695.4	93.0	14.4	97.5	2.0	20.0
5	CL	7.1	428.0	12.4	1850.3	3633.8	4577.9	707.0	96.7	14.1	119.0	2.0	22.1
6	SiCL	7.3	269.0	84.5	1439.1	2196.6	3447.5	112.4	92.4	14.1	79.5	2.8	16.7
7	SiC	7.5	276.0	40.9	1038.2	2124.2	2511.2	454.9	96.4	15.0	91.4	2.2	19.9
8	CL	7.8	224.0	38.4	1145.4	1709.8	2200.4	400.0	98.0	11.6	70.2	1.1	10.5
9	CL	6.3	281.3	1343.7	1446.7	944.6	3310.6	0.6	98.4	11.1	25.8	3.2	10.5
10	LS	8.4	7.3	37.8	6.4	25.5	25.3	31.6	2.6	6.6	5.4	0.4	10.0
11	L	7.9	37.2	186.6	69.5	195.0	303.7	12.0	26.1	12.2	17.2	0.4	6.4
12	SiC	8.5	4.2	29.1	11.5	15.5	5.6	43.5	6.0	30.7	3.4	0.9	0.06

*Central Laboratories: The State Organization for Soils and Land Reclamation, 1981, Baghdad, Iraq.
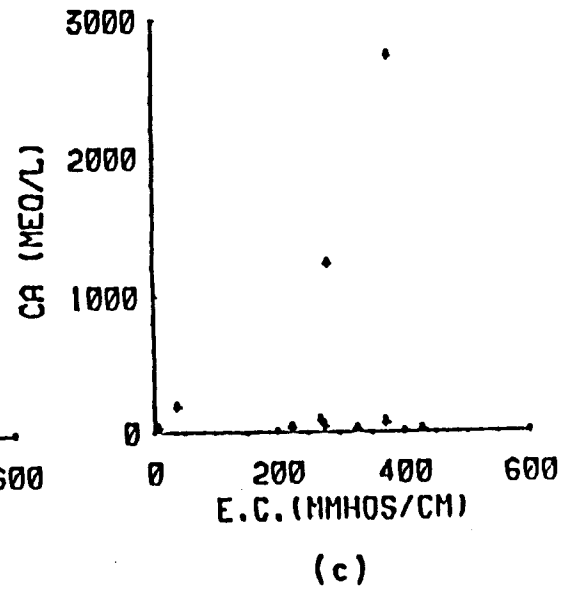
43
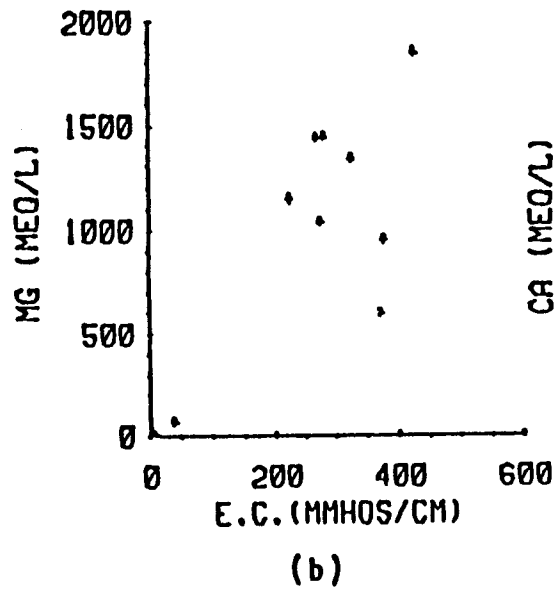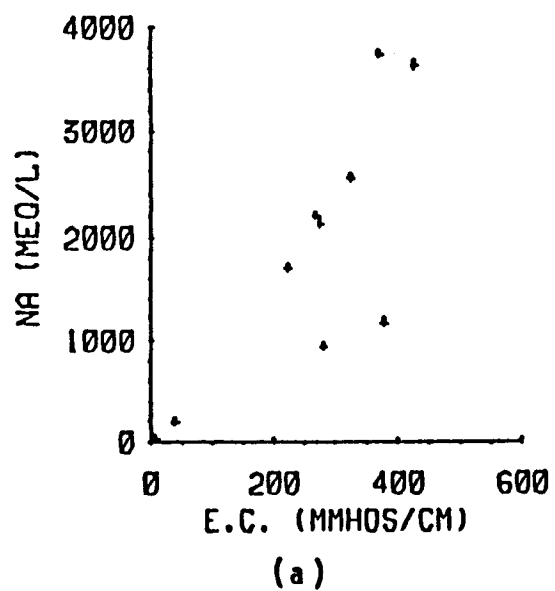
Figure 25. Relationships between electrical conductivity and concentration of the three major cations: (a) sodium, (b) magnesium, and (c) calcium.
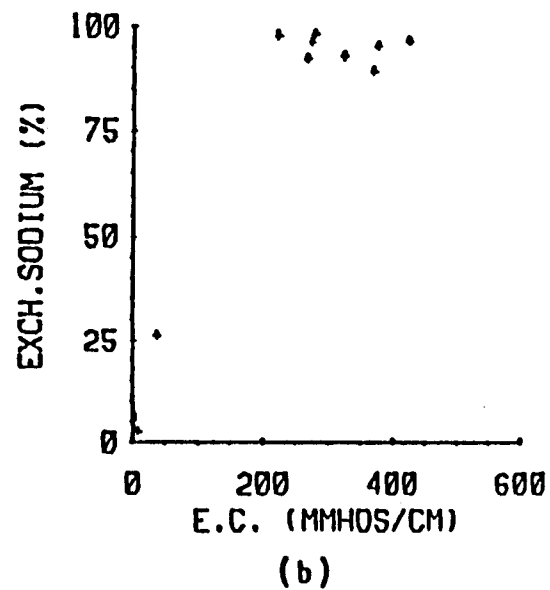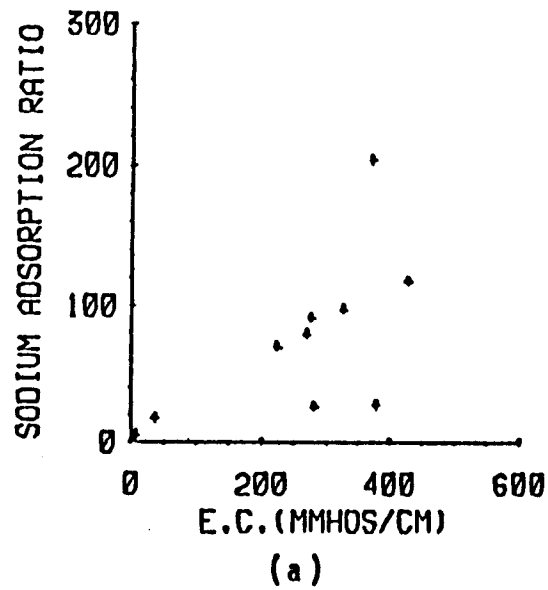
Figure 26. Relationship between electrical conductivity with (a) sodium adsorption ratio and (b) exchangeable sodium percentage.

Table 3. The major and associated salts of the soil samples.

Soil sample no.	Major salt*	Associated salts*
1	Gypsum	$MgSO_4$ – $NaCl$
2	$CaCl_2$	$NaCl$ – $MgCl_2$
3	$NaCl$	$MgCl_2$ – $CaSO_4 \cdot 2H_2O$
4	$NaCl$	$MgCl_2$ – $CaSO_4 \cdot 2H_2O$
5	$NaCl$	$MgCl_2$ – $MgSO_4$ – $CaSO_4 \cdot 2H_2O$
6	$NaCl$	$MgCl_2$ – $MgSO_4$ – $CaSO_4 \cdot 2H_2O$
7	$NaCl$	$MgSO_4$ – $MgCl_2$ – $CaSO_4 \cdot 2H_2O$
8	$NaCl$	$MgSO_4$ – $MgCl_2$ – $CaSO_4 \cdot 2H_2O$
9	$MgCl_2$	$CaCl_2$ – $NaCl$ – $CaSO_4 \cdot 2H_2O$
10	Gypsum	$NaCl$ – $MgSO_4$
11	$NaCl$	$CaCl_2$ – $MgSO_4$ – $CaSO_4 \cdot 2H_2O$
12	$CaSO_4$	$MgSO_4$ – $NaCl$

*Based on the salts' value of milliequivalent per liter.

of hundreds of years, even with the high electrical conductivity values. In addition, using irrigation water from the river is considered to be an additional source of organic matter in these soils.

Occurrence of gypsum ($CaSO_4 \cdot 2H_2O$) seemed to be as effective as the presence of other salts. Presence of gypsum may have a decreasing effect on the solubility of the total salts. Furthermore, gypsum may decrease reflectance as well as water retention (Table 4).

Table 4. Crystalline form properties, index of refraction and solubility of some selected salts (57).

Crystalline form properties and index of refraction	Solubility in cold water (g/100 cc)
NaCl: colorless, cubic, 1.5442	$(35.70)^0$
$MgCl_2$: white, lustrous, hexagonal crystalline, 1.59	$(54.25)^{20}$
$CaSO_4 \cdot 2H_2O$: colorless, monoclinic, 1.53	$(0.241)^0$
$CaCl_2$: colorless, cubic, deliquescent, 1.52	$(74.50)^0$

Since the salts usually tend to disolve then remain as crystals at saturation conditions depending on their solubility class and concentration as expressed in milliequivalents per liter, hence the surface physical properties of the soils are greatly influenced and related to the types of salts in the soil. In addition, such physical properties, i.e., water retention, color, infiltration, and aeration are directly related to the amount and type of crystals, type and amount of salts, type and percent clay, texture and organic matter.

Gypsum ($CaSO_4 \cdot 2H_2O$) which occurred in different percentages has been influenced by the anions ($SO_4^=$) rather than the cations (Ca^{++}).

Laboratory Measurements of Spectral Reflectance

Before Leaching

Bidirectional reflectance factor (BRF) measurements of the soil samples at saturation have indicated that with the presence of excess water content (multiple molecular water films on particle surfaces), specular reflection occurred and had a striking effect on the spectral characteristics of the soil samples by increasing the BRF values (Figures 27 and 28). Such an increase was primarily noticed in the 0.4-1.1 micrometer portion of the spectrum (Landsat bands range) due to the energy's absorption characteristics of the visible and near infrared bands.

The major reason behind the creation of such a specular reflection was the angle of view (0°) and the zenith viewing angle of the spectroradiometer (the Exotech Model 20C). In order to avoid such unrealistic spectral reflectance measurements and/or characteristics, another angle of view, i.e., 30°, may have presented better measurements of soils under excess water content conditions (Figure 28).

Upon drying the soil samples for two days, or at field capacity, there was no longer specular reflection which was directly related to the existence of extra water films on the soil surfaces. Instead, all of the samples especially the saline samples (Sample #: 2,3,4, 5,6,7,8,9,11) appeared darker due to the slow release of moisture which is basically related to the stronger water retention by the soil particles and the associated dissolved salts. Thin cracks started to occur as a result of the shrinkage characteristics of montmorillonite upon drying (Figure 29).

As a result of this condition, most of the samples showed lower BRF values than did the saturated samples, especially in the water absorption bands (Figure 30)(Tables 5,6,7 and 8).

Upon further drying for six days, maximum accumulation of salts in different colors and crystal forms was clearly noticed on the saline soil surfaces (Sample #: 2,3,4,5,6,7,8,9,11) due to capillary movement (Figures 31,32 and 33). The cracks due to shrinkage became even

(a)

(b)

Figure 27. Soil samples after 24 hours saturation (before leaching)
(a) top view; (b) side view. (Photograph: Al-Mahawili, 1981)

Order of samples in both photos (top to bottom; left to right):
Row 1: 9-10-11-12; Row 2: 5-6-7-8; Row 3: 1-2-3-4

Figure 28. Selected soil samples 1,2,3,9 at the first water content level (saturation) before leaching.

(a)
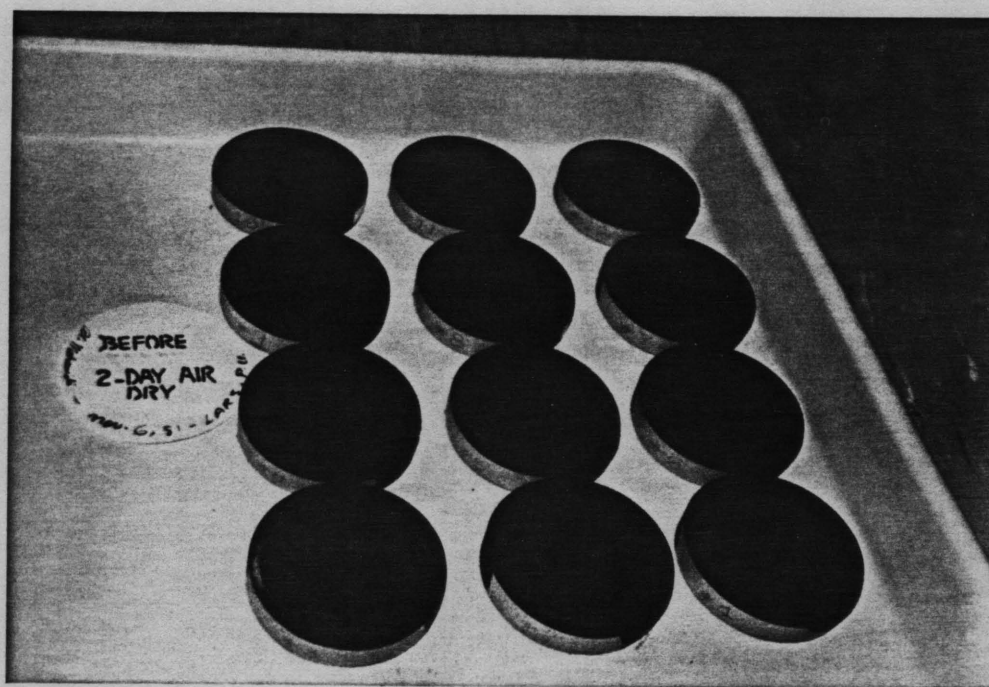
(b)

Figure 29. Soil samples after 2 days of air drying (before leaching).
    (a) top view; (b) side view (Photograph: Al-Mahawili, 1981)

Order of samples in both photos (top to bottom; left to right):
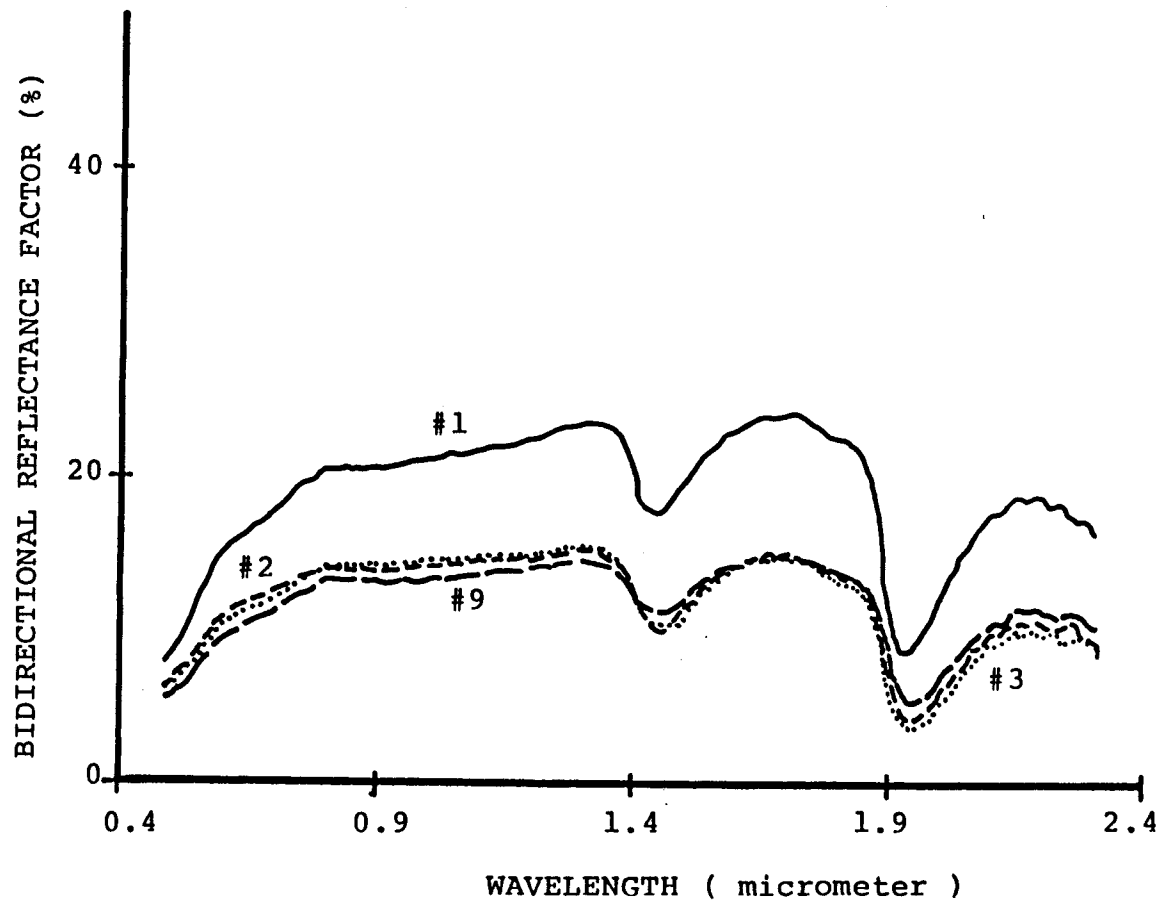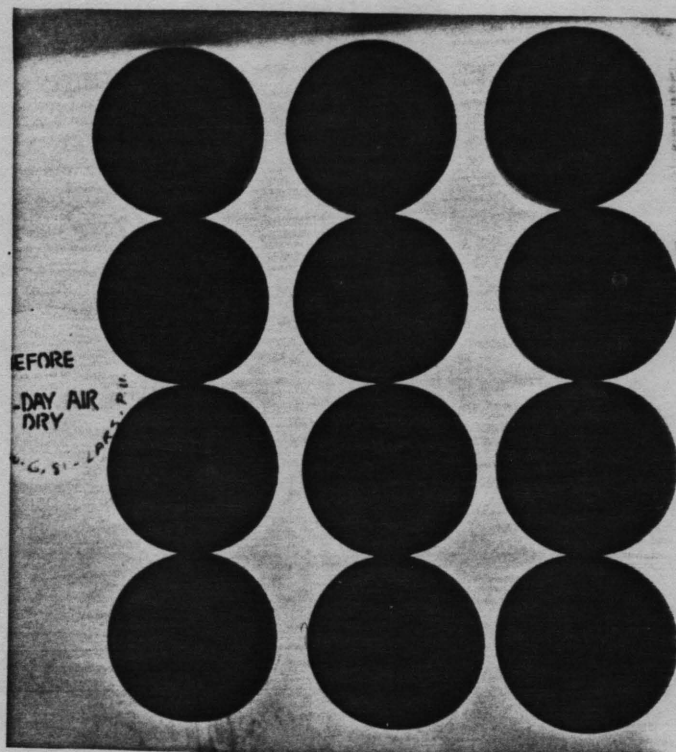Row 1: 10-11-12; Row 2: 9-8-7; Row 3: 4-5-6; Row 4: 3-2-1
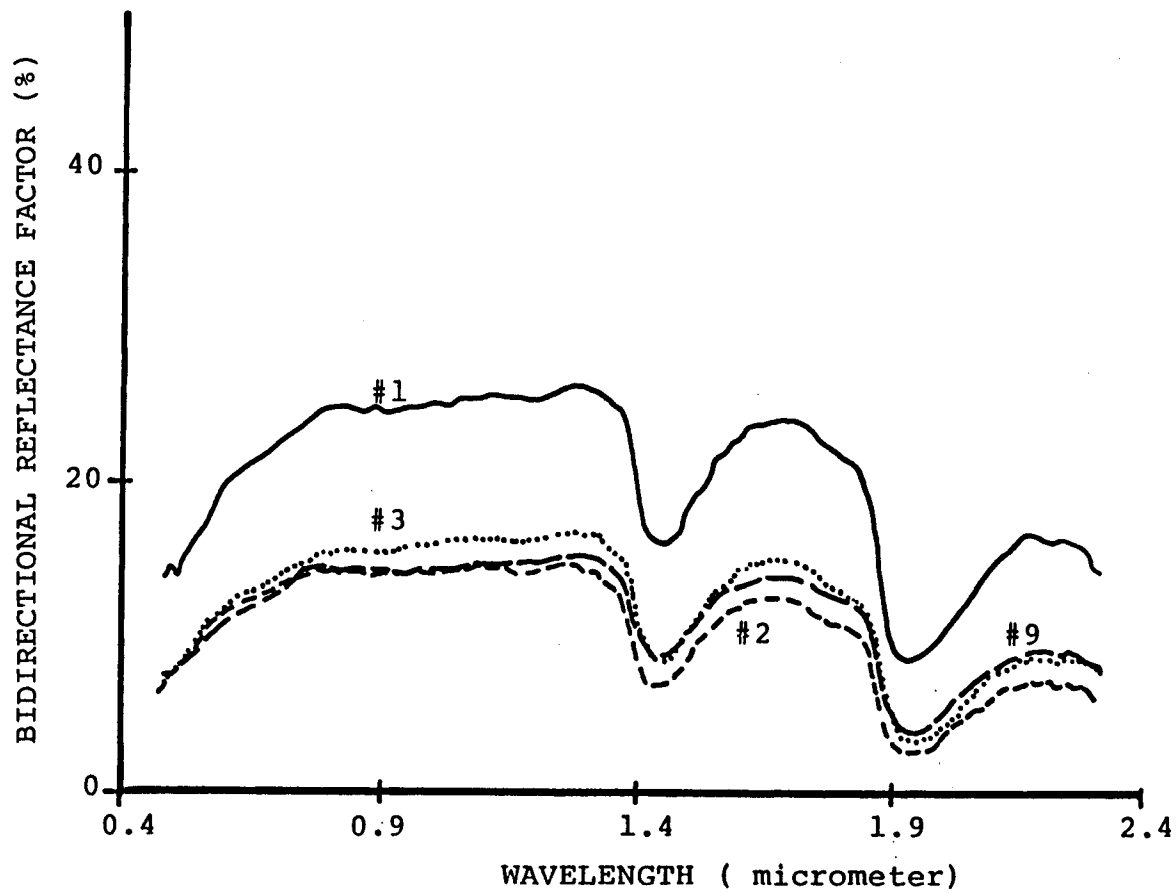
Figure 30. Selected soil samples 1,2,3,9 at the second water content level (2-day air dry) before leaching.

Table 5. The band means (three replicates) for soil sample #1.**

Bands (micrometers)	Band means (BRF, %)				
	Before leaching at			After leaching at	
	(1)*	(2)	(3)	(4)	(5)
Simulated Landsat MSS Bands					
0.50–0.60	16.5	13.4	29.7	17.1	30.4
0.60–0.70	26.5	20.0	37.1	21.9	37.8
0.70–0.80	23.4	18.9	40.6	24.1	41.2
0.80–1.10	24.8	20.8	42.3	25.0	43.0
Simulated Thematic Mapper Bands					
0.45–0.52	13.5	8.2	24.0	14.1	24.9
0.52–0.60	17.3	11.9	30.8	17.8	31.5
0.63–0.69	21.3	16.3	37.4	22.1	38.1
0.76–0.90	24.5	20.1	41.7	24.7	42.5
1.15–1.30	25.8	22.7	44.2	25.9	44.7
1.55–1.75	23.3	23.3	45.5	23.7	45.4
2.08–2.35	15.6	17.8	38.9	16.3	38.6
Water Absorption Bands					
1.42–1.52	17.0	18.6	43.1	18.0	43.0
1.92–2.02	9.3	10.2	34.6	9.4	34.0

*(1) saturation for 24 hrs
 (2) 2–day air dry
 (3) 6–day air dry
 (4) saturation for 48 hrs
 (5) oven dry; for 5 hrs/50°C

**For the band means of soil samples 4,5,6,7,8,10,11 and 12
  see Appendix.

Table 6. The band means (three replicates) for soil sample #2.

Bands (micrometers)	Band means (BRF, %)				
	Before leaching at			After leaching at	
	(1)*	(2)	(3)	(4)	(5)
Simulated Landsat MSS Bands					
0.50-0.60	8.9	8.4	22.9	11.9	22.0
0.60-0.70	11.9	11.5	28.4	15.4	25.4
0.70-0.80	13.3	13.0	31.2	17.1	29.9
0.80-1.10	13.9	13.8	32.9	17.8	31.6
Simulated Thematic Mapper Bands					
0.45-0.52	6.7	6.3	18.3	9.8	17.7
0.52-0.60	9.4	8.9	23.8	12.4	22.8
0.63-0.69	12.0	11.6	28.6	15.5	27.6
0.76-0.90	13.8	13.6	32.4	17.6	30.9
1.15-1.30	14.2	14.7	34.3	18.3	33.0
1.55-1.75	11.9	14.3	35.2	15.8	33.1
2.08-2.35	6.7	9.8	29.4	10.0	27.0
Water Absorption Bands					
1.42-1.52	7.3	10.6	32.5	10.6	29.4
1.92-2.02	2.9	4.9	23.7	4.7	19.9

*(1) saturation for 24 hrs
 (2) 2-day air dry
 (3) 6-day air dry
 (4) saturation for 48 hrs
 (5) oven dry; for 5 hrs/50°C

Table 7. The band means (three replicates) for soil sample #3.

Bands (micrometers)	Band means (BRF, %)				
	Before leaching at			After leaching at	
	(1)*	(2)	(3)	(4)	(5)
Simulated Landsat MSS Bands					
0.50-0.60	9.5	8.5	13.2	11.1	10.6
0.60-0.70	12.6	11.4	13.0	14.8	14.2
0.70-0.80	14.5	13.2	15.0	16.8	17.2
0.80-1.10	15.8	14.5	16.5	18.3	18.7
Simulated Thematic Mapper Bands					
0.45-0.52	7.4	7.2	8.1	9.0	8.5
0.52-0.60	9.9	8.8	10.3	11.6	11.7
0.63-0.69	12.7	11.5	13.1	14.9	15.1
0.76-0.90	10.1	14.1	16.0	17.7	18.0
1.15-1.30	16.4	15.4	17.7	10.3	19.9
1.55-1.75	14.4	14.6	18.0	16.7	18.9
2.08-2.35	8.2	9.7	13.9	17.0	13.5
Water Absorption Bands					
1.42-1.52	9.3	11.0	15.2	19.2	14.9
1.92-2.02	3.7	4.7	9.0	4.3	7.7

*(1) saturation for 24 hrs
 (2) 2-day air dry
 (3) 6-day air dry
 (4) saturation for 48 hrs
 (5) oven dry; for 5 hrs/50°C

Table 8. The band means (three replicates) for soil sample #9.

Bands (micrometers)	Band means (BRF, %)				
	Before leaching at			After leaching at	
	(1)*	(2)	(3)	(4)	(5)
Simulated Landsat MSS Bands					
0.50–0.60	8.7	7.4	15.8	10.7	19.8
0.60–0.70	11.4	10.3	21.3	14.2	26.9
0.70–0.80	13.1	12.1	24.6	16.4	30.8
0.80–1.10	14.0	13.1	26.9	17.8	33.7
Simulated Thematic Mapper Bands					
0.45–0.52	7.5	6.2	25.3	8.8	14.5
0.52–0.60	9.0	7.7	16.6	11.1	20.9
0.63–0.69	11.5	10.3	21.5	14.3	27.1
0.76–0.90	13.1	12.9	29.7	17.0	37.6
1.15–1.30	14.6	10.6	29.1	18.8	36.3
1.55–1.30	13.1	12.9	29.7	17.0	37.6
2.08–2.35	8.3	14.2	25.0	11.2	31.8
Water Absorption Bands					
1.42–1.52	9.1	14.1	27.4	11.8	34.6
1.92–2.02	4.1	5.8	19.2	5.2	25.6

*(1) saturation for 24 hrs
 (2) 2-day air dry
 (3) 6-day air dry
 (4) saturation for 48 hrs
 (5) oven dry; for 5 hrs/50°C

Figure 31. Comparison among   different soil surface conditions of
     soil samples after 6-days of air drying. Notice the non-saline,
     non-cracked and the homogenization in color of sample 1 (far right)
     compared with the salt-accumulated, cracked and heterogeneous
     colors of samples 2,3,4,5,6. (Photograph: Al-Mahawili, 1981)
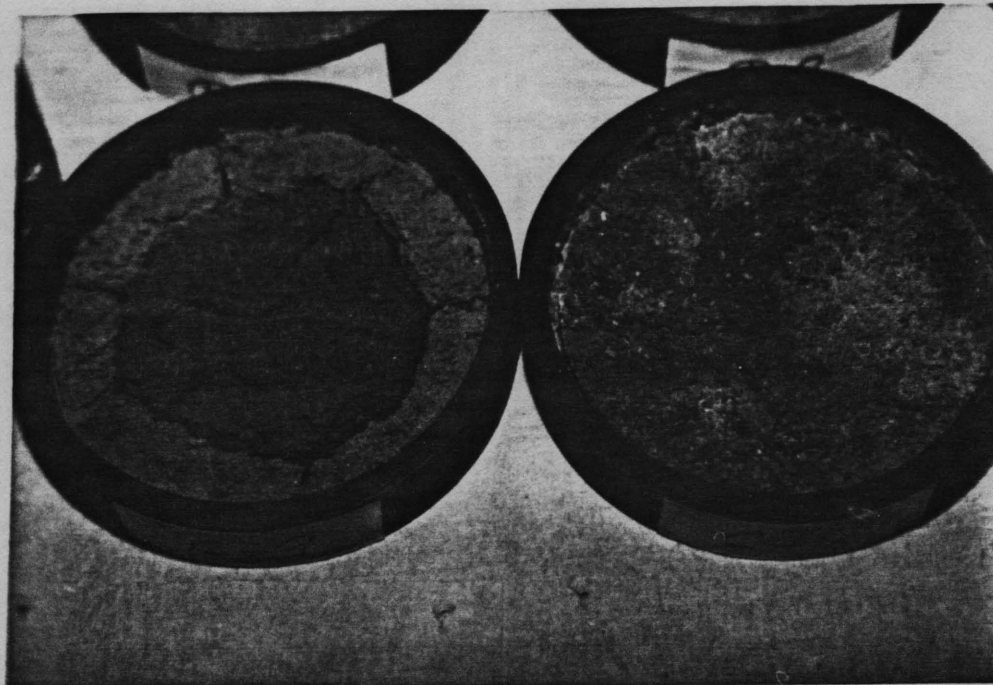
(a)
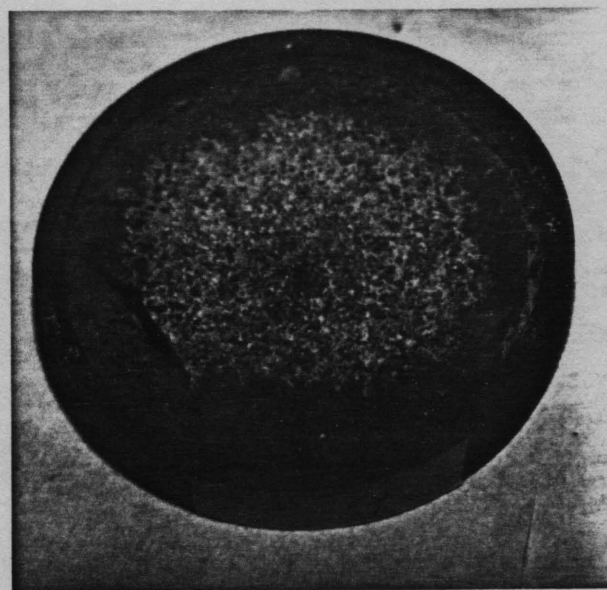
(b)

Figure 32. Comparison between different salt accumulations on soil surfaces after 6-days of air drying (before leaching). (a) Sample (NaCl) and sample 9 (MgCl$_2$) salts; (b) sample 4 (NaCl). Notice different soil colors and shape, width and depth of cracks. (Photograph: Al-Mahawili, 1981)
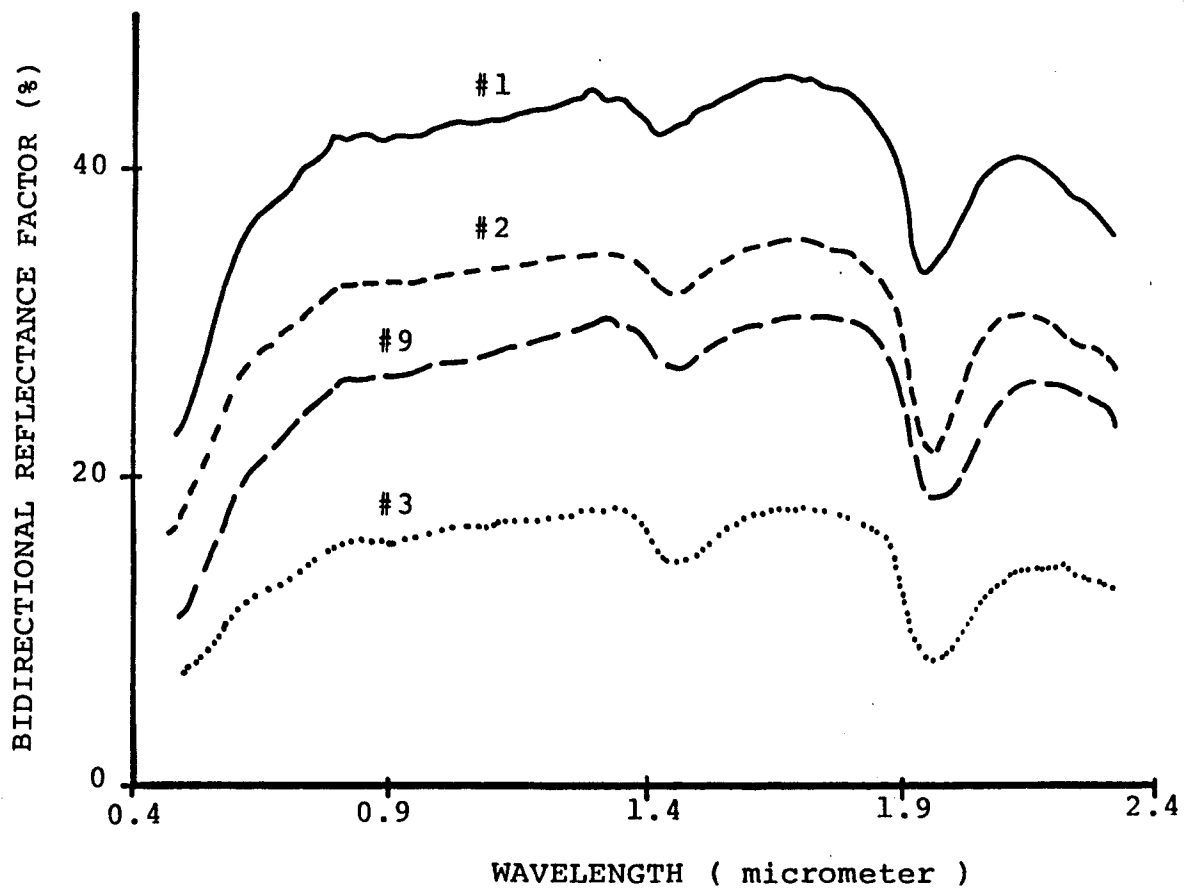
Figure 33. Selected soil samples 1,2,3,9 at third water content level (6-day air dry) before leaching.

wider and deeper. The non-saline gypsiferous samples (Samples 1 and 2) had no such surface features (Figure 31). With the drop of water content to an average of 15% compared to 21% of the previous stage, almost all the samples showed the highest spectral reflectance values (Figure 33). On the other hand, BRF values did vary from one soil sample to another depending on the type and total concentration of salts (EC: mmhos/cm), soil color and water content per sample. Due to the difference in day-night average temperatures, which exceeds 20°C at summer time in the research area, an enormous different salt-water interaction occurs. At mid-day when the duration and intensity of temperature increases the evaporation rate at soil surface, the activity of capillary movement increases and becomes more influential in transporting dissolved salts on the soil solution to the surface. During the night when the temperature is much less, evaporation rate is lower and humidity is higher, salts usually attract moisture from the atmosphere. This attraction of atmospheric moisture by salts varies with different cations (Mg^{++}, Na^+, Ca^{++}) where the interaction of these cations with a water molecule (H^+OH^-) can be thought of as a simple ion-dipole attraction. Both the charge and the radius of the cation determine the strength of such an interaction; the higher the charge and the smaller the ionic radius, the greater the ion-dipole interaction. Hence, soils with $MgCl_2$ and $CaCl_2$ because of the strong ion-dipole interactions remain moist in the dry, hot summer, even during the day. Furthermore, these soils (as is the case in the research area) with such highly deliquescent salts appear moist and almost dark brown in color and may be mistaken for black alkali (11).

Spectral reflectance characteristic curves* of the selected soil samples have indicated different spectral characteristics in relation to water content, soil texture and electrical conductivity at each single stage of the experiment (Figures 28,30 and 33).

---

*Four representative curves were selected from the total twelve curves. The selected curves represent soil samples 1,2,3,9. The selection was based on the type of salt, EC, texture, ESP, SAR, O.M.%. For the other sample BRF curves, see Appendix.

The spectral reflectance curves of sample 1 through all three levels of water content maintained the highest BRF% values. Because of its low electrical conductivity and coarse texture sample 1 released water upon drying faster than the others. This is in addition to the other chemical-physical properties which characterized the sample as a non-saline, gypsiferous soil. In the simulated Landsat 0.5-1.1 μm range the near infrared bands (0.7-0.8 μm and 0.8-1.1 μm) showed higher BRF values than the visible in all the three water content levels (Appendix: Figures A,C,G). This is related to the coarse soil texture, low water content and the fast rate of water release upon drying.

A comparison of data for samples 1,2,3 and 9 reveals that the lower reflectance values for samples 2,3 and 9 are related to their high EC, medium-fine texture, and slow release of water upon drying. The water retention in the representative samples of 2,3, and 9 is much higher than that of sample 1 because of the extreme differences in salt concentration.

Reflectance values greatly increased with the decrease of water content in the second and third stages of the experiment. The effect of the drying process in these samples was striking, especially for the six-day drying period, but it was rather more influential in soil sample (Table 5). The infrared bands were more reflective than the visible.

The reflectance curves of the four representative soil samples indicate that there is an association between water content and infrared bands; the higher the water content at saturation, the less effective are the infrared bands, near and middle, in separating differences in quantity and quality of salt. This is related to the characteristic of water in reflecting more energy in the visible and absorbing more energy in the infrared bands. Most of the saline soil samples represented by 2,3 and 9, because of their darker colors and higher electrical conductivity values (EC) maintained lower reflectance throughout the drying cycle.

The effect of organic matter in decreasing the spectral reflectance in these saline soils was not apparent. Instead, the results

were more related to the EC, water content and quantity and quality of salts. These chemical properties and characteristics, in addition to the other existing differences, have masked the role of organic matter in decreasing spectral reflectance within the three water content levels or stages of the experiment (see Appendix).

The same phenomenon occurred and repeated itself with the gypsum content. Most of the data were scattered and unrelated to the quantity of gypsum present. In the highly saline soil samples where the EC value has exceeded the salinity limit of 4 mmhos/cm, the effect of gypsum on reflectance has been masked. The high reflectance of sample 1 is related to both gypsum content (4.6%) and the EC (2.4 mmhos/cm). This relationship held throughout the drying cycle.

The water absorption bands (1.42-1.52 μm and 1.92-2.02 μm) maintained the lowest BRF values throughout the drying cycle. The 1.92-2.02 μm band was more water absorbant than was the 1.42-1.52 μm. Both bands gave extremely low reflectance values for saline samples having a moisture content in the range of 25 to 40%.

After Leaching

An analysis of the leached samples revealed that the following changes in soil characteristics occurred: (1) a sharp decrease in the electrical conductivity values, especially in the samples whose EC was above the 4 mmhos/cm salinity limit, and (2) the soil color of the saline soil samples changed from lower to higher chroma and value (Table 9). These major changes caused the liberation of the soils' total pore space from the dissolved salts in the soil solution, creating better aeration within the soil. As a direct effect of leaching upon the soil porosity, most of the samples had a higher water content at saturation after leaching than they had before leaching (Table 10). The leaching process did not have a significant effect on soil sample 1, the gypsiferous soil, in lowering its EC or changing its color (Table 9).

Table 9. Comparison between electrical conductivity and soil colors for soil samples before and after leaching.

SOIL SAMPLE No.	BEFORE LEACHING			AFTER LEACHING		
	MUNSELL COLOR (d r y)	(MOIST)	E.C. (mmhos/cm)	MUNSELL COLOR (d r y)	(moist)	E.C. (mmhos/cm)
1	10YR6/4	10YR4/3	2.49	10YR6/4	10YR4/3	2.45
2	10YR3/3	10YR3/2	379.50	10YR6/3	10YR4/4	3.00
3	10YR6/3	10YR3/3	372.00	10YR6/3	10YR4/4	5.7
4	10YR6/3	10YR3/3	326.00	10YR6/4	10YR4/3	3.90
5	10YR6/3	10YR4/2	428.00	10YR6/4	10YR4/3	6.40
6	10YR4/3	10YR3/3	269.00	10YR5/3	10YR4/3	5.50
7	10YR3/2	10YR3/1	276.00	10YR6/3	10YR4/4	3.30
8	10YR6/3	10YR4/3	224.00	10YR6/3	10YR4/3	2.60
9	10YR3/3	10YR3/2	281.00	10YR5/3	10YR4/3	4.90
10	10YR6/3	10YR5/3	7.30	10YR6/3	10YR4/3	2.60
11	10YR6/3	10YR5/3	37.20	10YR6/3	10YR4/4	2.50
12	10YR5/2	10YR4/3	4.27	10YR5/3	10YR4/3	1.10

Table 10. Comparison between the average water content
for all stages of the experiment.*

STAGE OF EXPERIMENT	AVERAGE WATER CONTENT
At saturation: 24 hrs. (before leaching)	29.5 %
At 2-day air dry (before leaching)	21.0 %
At 6-day air dry (before leaching)	15.0 %
At saturation: 48 hrs. (after leaching)	35.0 %
At oven dry: 5 hrs./50°C. (after leaching)	28.0 %

* The average water content is calculated for all
the twelve soil samples per each stage.

Specular reflection did occur within the 48 hrs of saturation and most of the leached soil samples showed higher BRF values than at saturation before leaching (Figures 34 and 35). In the second water content level (at oven dry), all the samples showed even higher reflectance because of the rapid release of moisture related to the decreased electrical conductivity by leaching (Figures 36,37 and 38).

Soil samples 2,3, and 9 gave higher reflectance after leaching than before leaching in all bands, at both water content levels. Soil sample 1 maintained the highest BRF values in all water content levels, before and after leaching. Although the electrical conductivity was greatly decreased upon leaching, many samples remained saline regardless of the time of leaching*. This suggests that more leaching time was required to decrease the electrical conductivity below 4 mmhos/cm** (Table 9).

Computer Analysis and Interpretation
of Landsat Satellite Multispectral Scanner Data

Laboratory studies of spectral reflectance characteristics of the saline and gypsiferous soil samples were initially conducted as part of the experiment to support the computer analysis of Landsat MSS data with specific reflectance characteristics of these soils under different water content levels.

The primary results of the laboratory measurements of spectral reflectance indicate that saline soils, when compared with non-saline (leached) and gypsiferous soils, give lower reflectance in both the visible and infrared bands. Upon drying, these saline soils gave higher reflectance values in both the visible and infrared bands.

Although the laboratory studies of soil reflectance do not represent field conditions of soils, these studies provide a better understanding of relationships among reflectance and other physical/chemical

---

*The average time of leaching was 30-45 minutes.

**In actual field conditions, more time is usually given to the extremely saline soils. Such additional time varies between one to several months (Author's note).
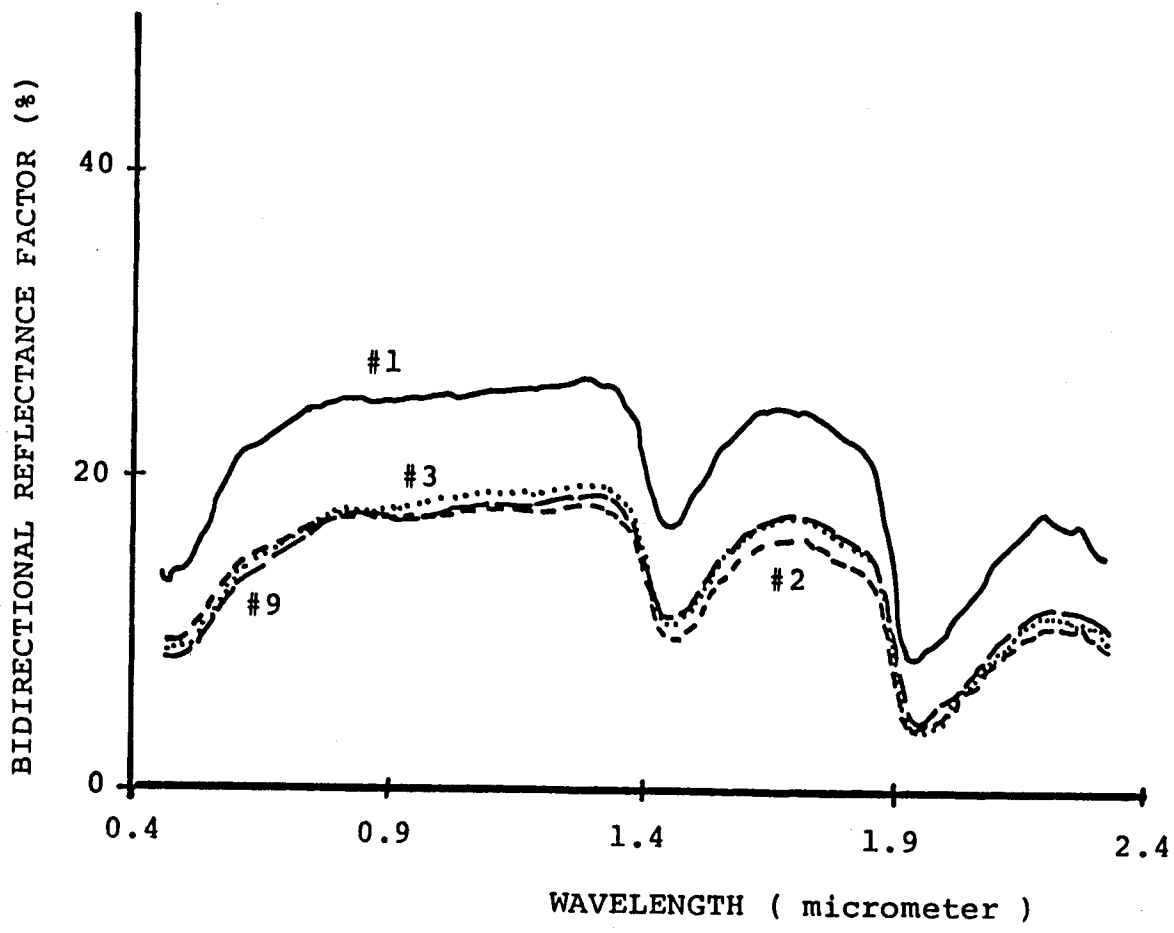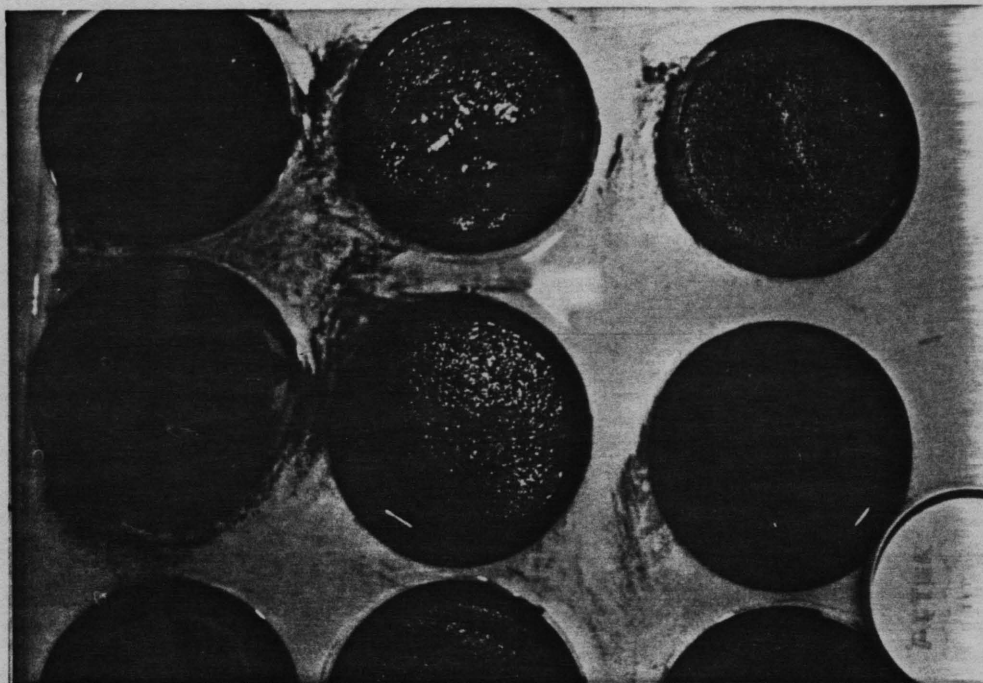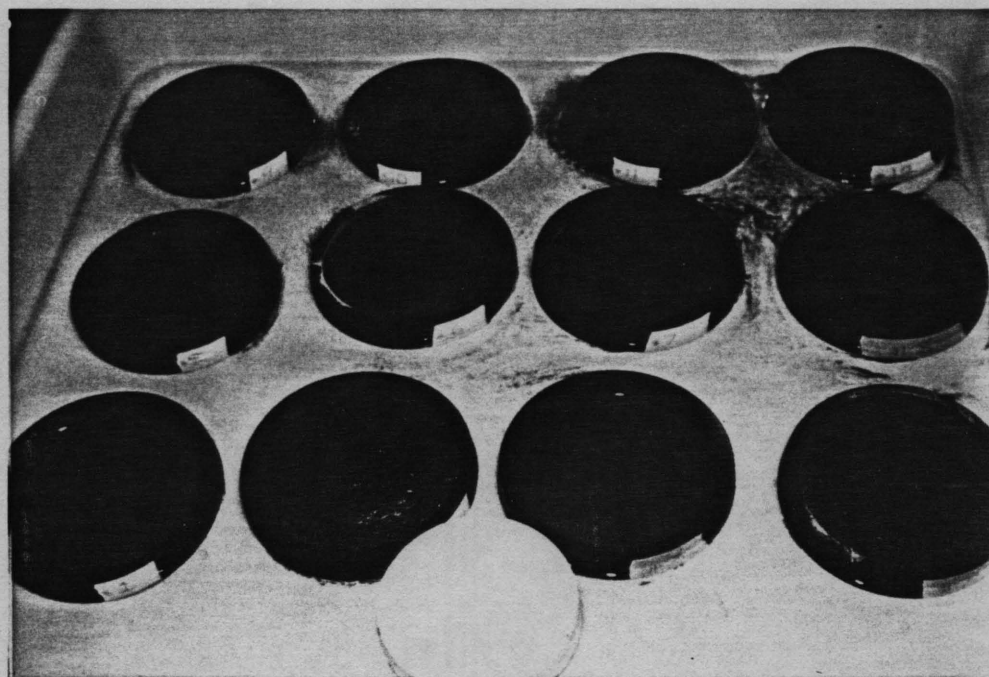
Figure 34. Selected soil samples 1,2,3,9 at first water content level (saturation) after leaching.

(a)

(b)

Figure 35. Soil samples after 48 hours of saturation (after leaching).
(a) top view; (b) side view   (Photograph: Al-Mahawili, 1981)

Order of samples in both photos (top to bottom; left to right):
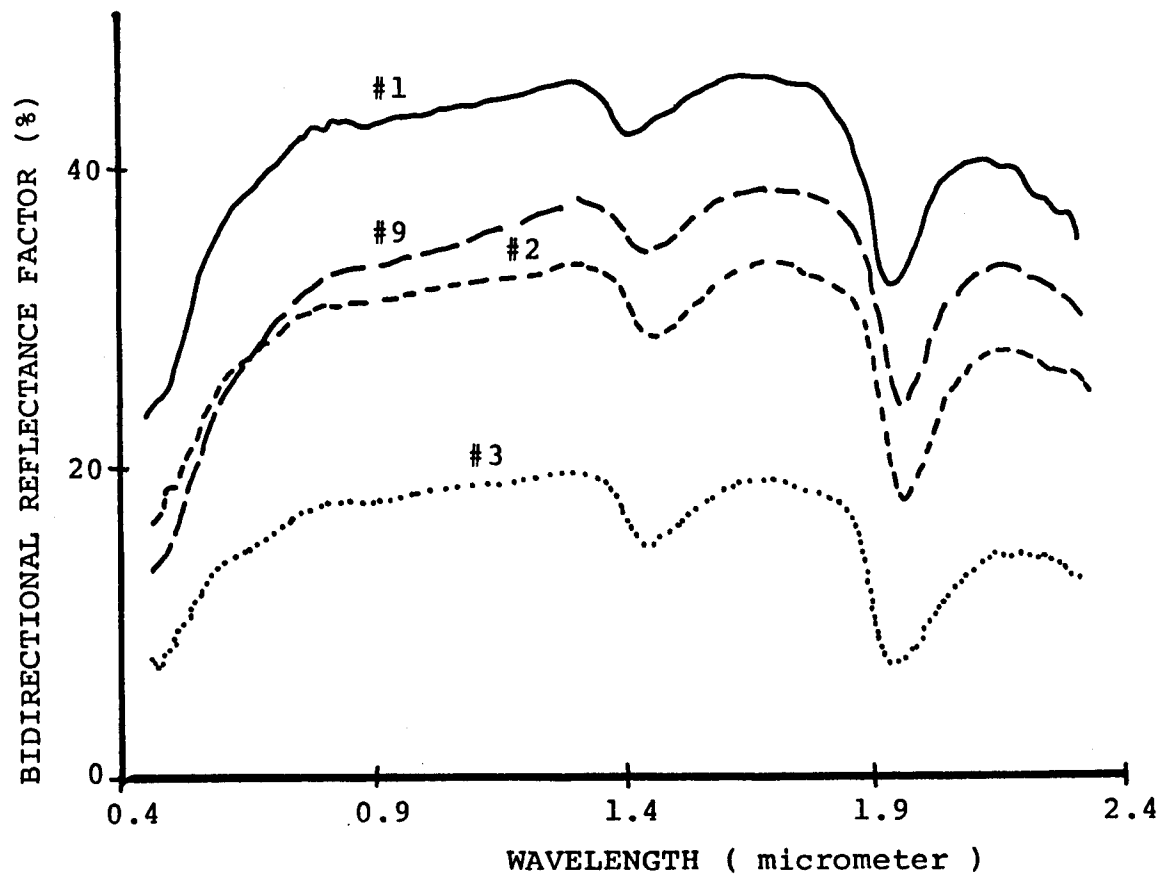Row 1: 9-10-11-12; Row 2: 5-6-7-8; Row 3: 1-2-3-4

Figure 36. Selected soil samples 1,2,3,9 at second water content level (oven-dry for 5 hrs at 50°C) after leaching.
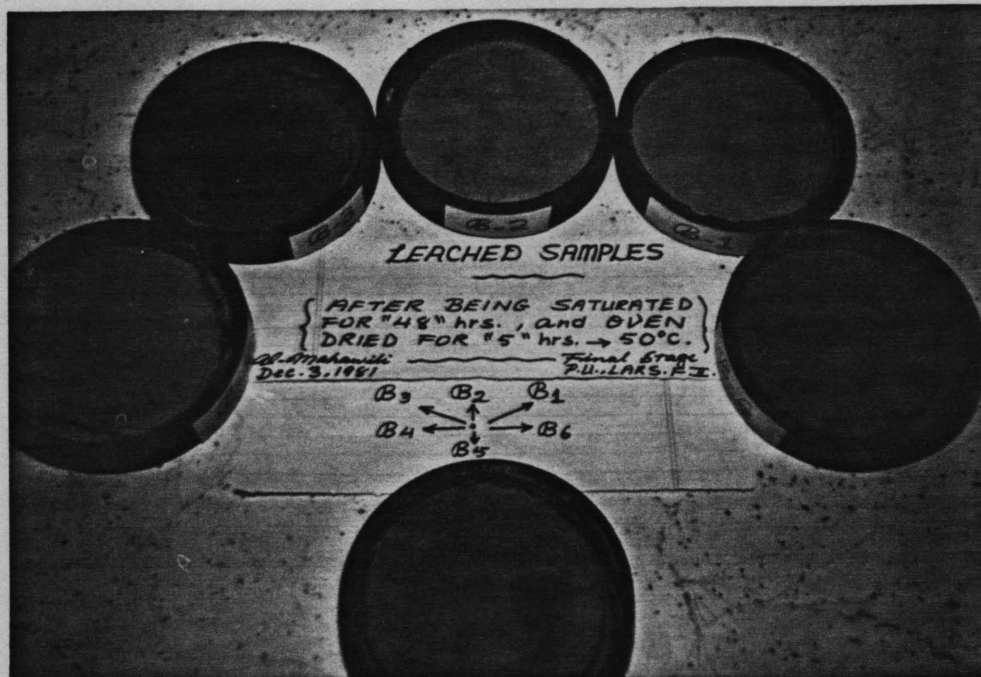
Figure 37.   Soil samples 1,2,3,4,5,6 after being leached and oven
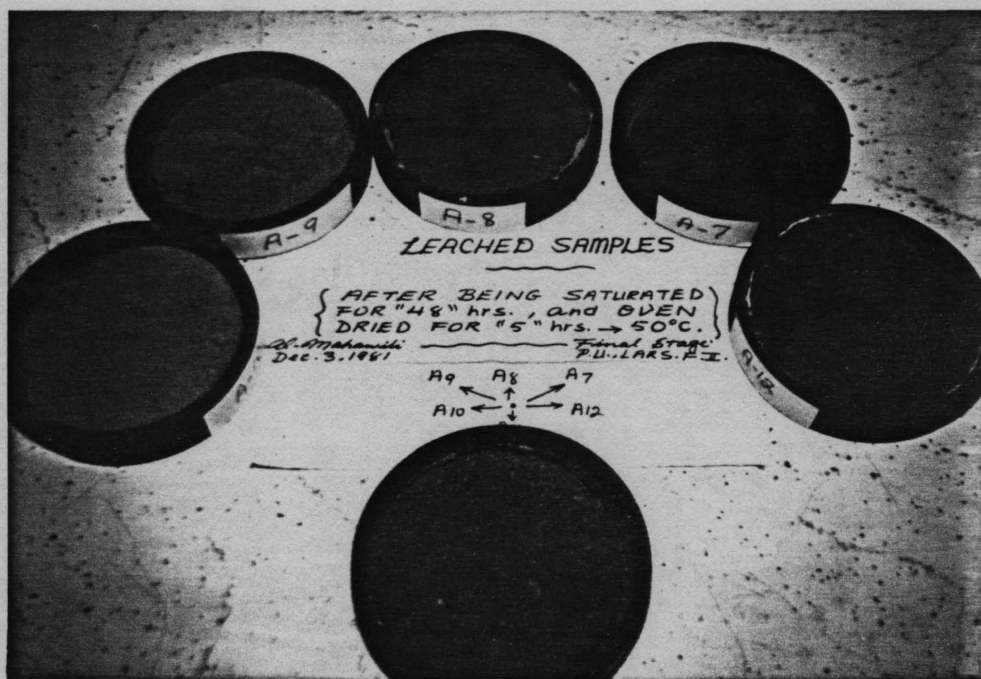dried.   (Photograph: Al-Mahawili, 1981)

Figure 38.   Soil samples 7,8,9,10,11,12 after being leached and
oven dried.   (Photograph: Al-Mahawili, 1981)

properties of soils. The body of knowledge attained from such studies is essential if optimum benefit is to be derived from the analysis and interpretation of spectral measurements obtained from air and space platforms. Our understanding of these relationships will enhance our ability to use computer-digital analysis of Landsat multispectral scanner data for inventorying and monitoring land resources.

Data Acquisition

Landsat multispectral scanner data, whose specific characteristics are listed below, were used for the digital analysis. The data tape was obtained from the EROS Data Center at Sioux Falls in South Dakota.

DATA STORAGE TAPE FILE

```
FLIGHT LINE ID...................................20603-06530 IRAQ
DATE DATA TAKEN..................................16/9/1976
TIME DATA TAKEN..................................0853 HOURS
PLATFORM ALTITUDE...............................3062000 FEET
GROUND HEADING...................................180 DEGREES
FIELD OF VIEW....................................0.036 RADIANS
DATA SAMPLES PER CHANNEL PER LINE...............480
SAMPLE RATE......................................0.09 MILLIRADIANS
FRAME CENTER LONGITUDE...........................316.86
```

SPECTRAL BANDWIDTH IN MICROMETERS

CHANNEL	LOWER	UPPER	CHANNEL	LOWER	UPPER
(1)	0.50	0.60	(2)	0.60	0.70
(3)	0.70	0.80	(4)	0.80	1.10

The date of Landsat data selected for analysis was 16 October 1976. It was selected for the following reasons: (1) no trace of clouds, dust or vapor has occurred on the scene which might present an interference with the clarity of reflected energy from the different targets, i.e., soils, vegetation, water bodies, man-made features, etc. and (2) no change in the soil-atmosphere interactions is expected because of rainfall, evapotranspiration and ground water fluctuation within this month; thus, the rapid accumulation of salts on the soil surface during the previous months is at its maximum level.

Correlating Remotely Sensed Data with Ground Truth

Ground truth data were collected during the summer of 1981 for the entire research area. The ground truth data (see Methods and Materials) included the collection of (a) soil surface samples, (b) surface descriptions related to accumulation of salts, vegetation and sample locations, (c) chemical and physical analyses of the soil samples, (d) acquisition of a soil salinity map as a reference, and (e) laboratory reflectance measurements of soil samples collected in the field according to specific experimental design.

Geometrical Correction

Due to the Earth's rotation which normally causes an image distortion for Landsat data, a geometrical correction of the MSS data was carried out by rotating and rescaling it to an approximate scale of 1:24,000 (see Appendix). The geometrical correction process was conducted and produced by GEMCOR with a ratio from LARSYS run number 76023800, lines 601-939, and columns 2567-3155, thus covering the whole scene in which the research area is located.

Computer Training Area

In order to train the computer for the upcoming digital analysis, certain training areas were chosen for this purpose. The concept behind this choice was based on the fact that single or combined land cover types and/or features will have various or similar responses to the solar energy in the forms of reflection, absorption and emittance. Thus, these land cover types will vary according to the electromagnetic spectrum in their spectral characteristics within the visible and infrared wavelengths.

The selection of the training areas was a process based upon the actual field observations which included, among other things, a representation of the existing soil surface features. Nine training areas were selected and covered the following soil conditions:

(1) bare, nonsaline, desert-gypsiferous soils;

(2) bare, extremely saline soils with dark-brown accumulation of salts;

(3) bare, extremely saline soils with white to light brown accumulation of salts;

(4) extremely saline soils with scattered growth of weeds;

(5) extremely saline soils with dense growth of weeds;

(6) saline soils with moist surfaces;

(7) free water (Euphrates River, irrigation and drainage canals, waterlogged soils and ponded water;

(8) date palms, fruit shrubs and field crops; and

(9) roads and other man-made features.

As a result of clustering*, sixteen spectral classes were obtained for the entire research area (Table 11; Figures 39 through 43).

Landsat and Exotech Model 20C Data

The result of spectral reflectance measurements in the 0.8-1.1 μm band from both Landsat and the indoor spectroradiometer was as follows: The relative reflectance values for the Landsat MSS band 4 (0.8-1.1 μm) were much lower than the BRF values for the same band simulated on the Exotech 20C.

This difference is related to the fact that the dynamic range of this band (0.8-1.1 μm) is approximately half (0-128) of the other three bands (0.256). This difference was eliminated by the Exotech Model 20C by the horizontal one level setup for all the bands involved. Thus, a comparison is possible if this fact is considered, i.e., increasing or doubling the dynamic range in the spectral class curves will normalize somewhat the existing difference.

---

*Clustering is "a process which groups individual spectrally similar data points into a predefined number of groups (clusters) specified by the analyst."

Table 11. Classification data of the final groups of land cover types.

CLASS ORDER	LAND COVER TYPES	MAGNITUDE	VISIBLE/INFRARED (RATIO)	INFRARED (%)
1	WATER BODIES	113	1.47	40
2, 4, 7.	VEGETATION -I-	139	0.70	59
		148	0.80	54
		163	0.90	52
3,9,13,5.*	VEGETATION -II-	136	1.00	49
		173	1.00	50
		190	1.09	48
		154	1.00	50
6,8,10,11, 12,14.	SALINE, IRRIGATED SOILS	146	1.17	46
		162	1.13	47
		202	1.20	45.2
		176	1.15	46.4
		188	1.20	45.3
		214	1.21	45
15, 16.	GYPSIFEROUS SOILS	225	1.22	45
		241	1.22	45

* Class Order 5 was a representative for both man-made features
   and Vegetation -II-.

RELATIVE REFLECTANCE VALUES

80
70
60
50
40
30
20
10

(A)

W A T E R   B O D I E S

RIVERS; IRRIGATION AND DRAINAGE CANALS; WATER-LOGGED SOILS; AND FLOODED AREAS DUE TO NATURAL AND/OR UNCONTROLLED IRRI- GATION PRACTICES.

0   1   2   3   4

L A N D A S T   C H A N N E L S

74
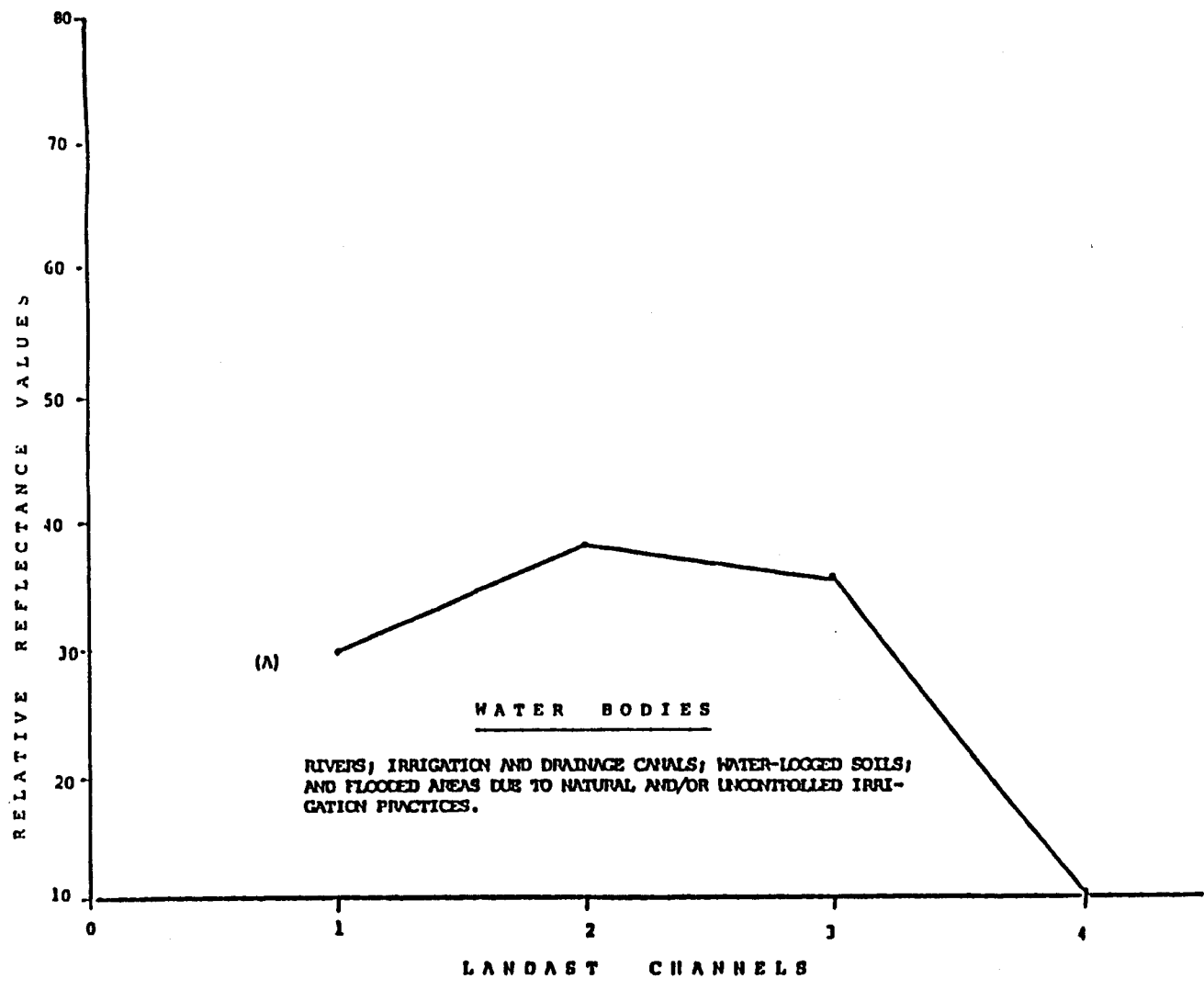
Figure 39. Spectral group A.

VEGETATION (I)

VEGETATION COVER IS APPROXIMATELY (50-75 %). IT IS
A COMBINATION OF DENSE IN-SITU WEEDS, DATE PALMS, AND
ISOLATED FIELD CROPS-CULTIVATED AREAS.

(B_1)

LANDSAT CHANNELS

RELATIVE REFLECTANCE VALUES
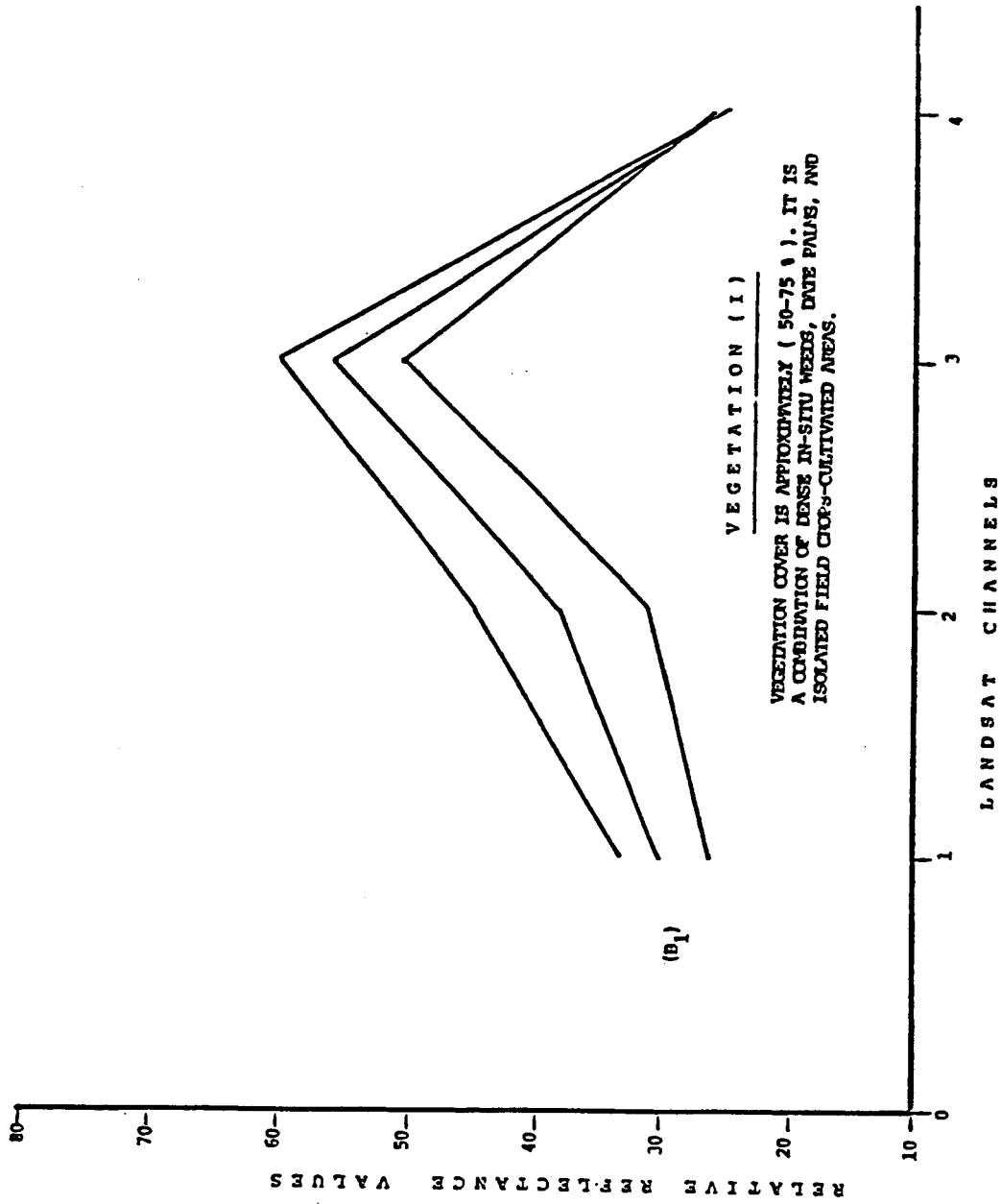
Figure 40. Spectral group B_1.

VEGETATION (II)

VEGETATION COVER IS APPROXIMATELY (30-50 %). IT IS
A COMBINATION OF SCATTERED WEEDS, DATE PALMS AND SHRUBS.

(B₂)

LANDSAT CHANNELS

RELATIVE REFLECTANCE VALUES
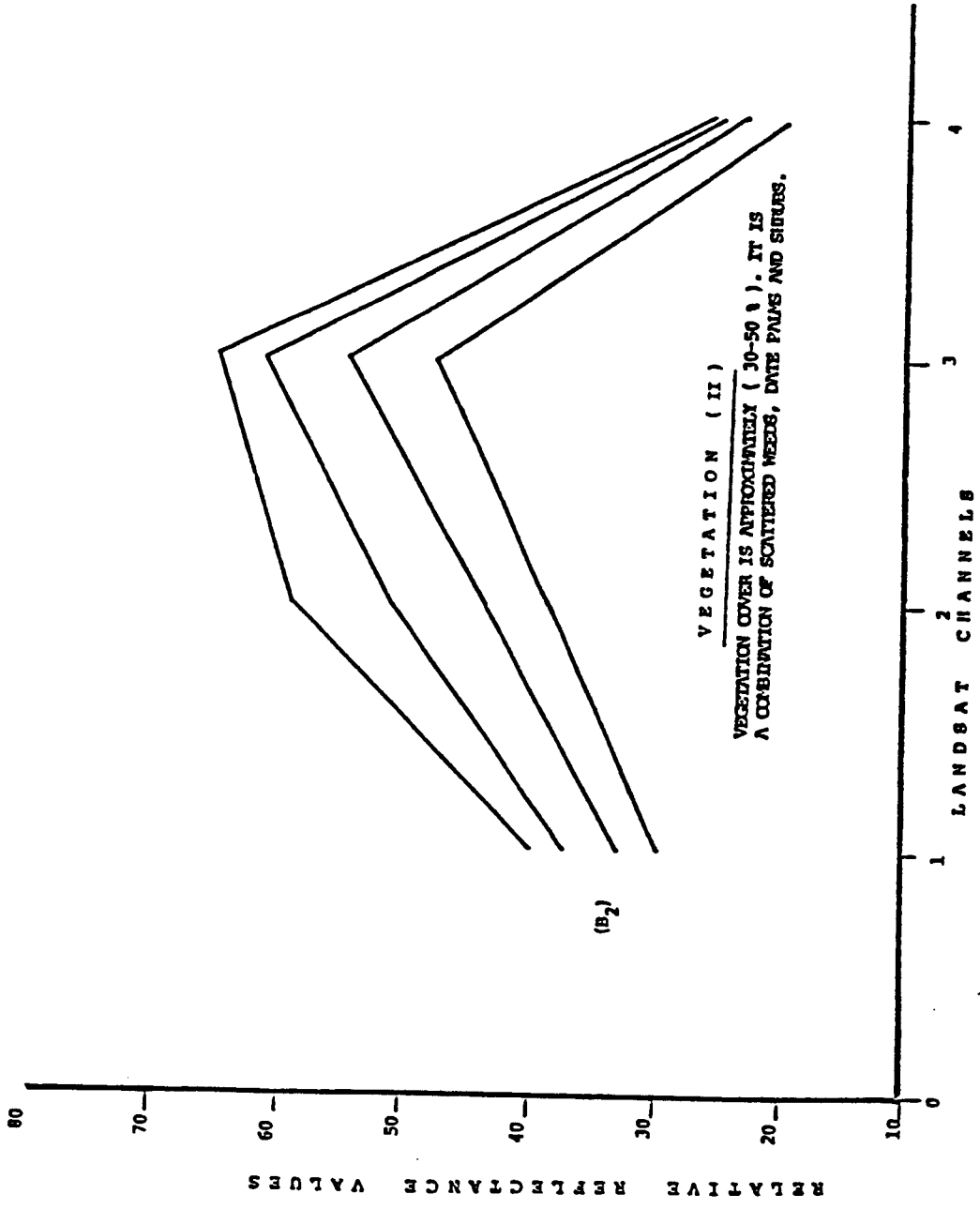
Figure 41. Spectral group B₂.
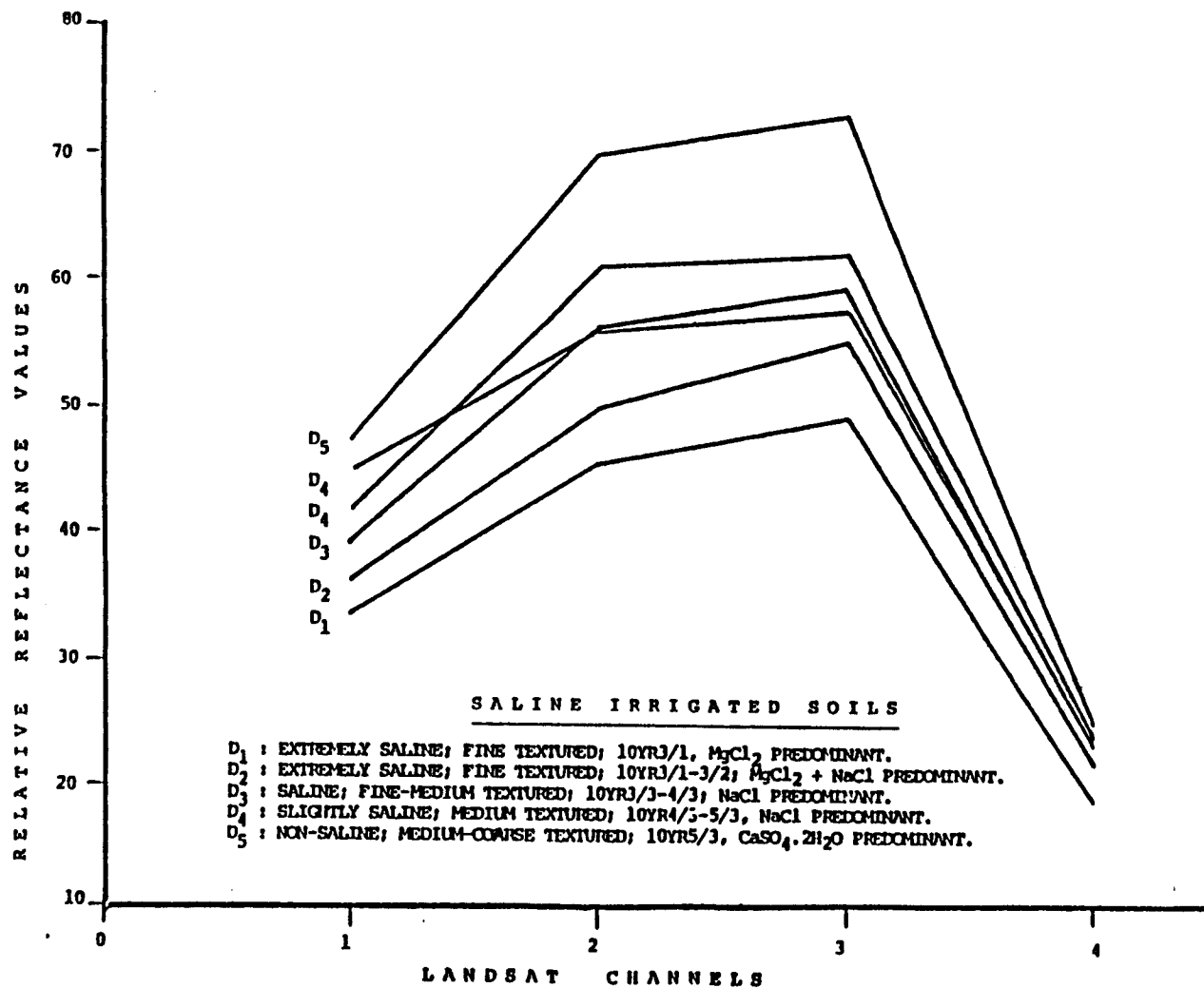
Figure 42. Spectral group D.

The chart shows RELATIVE REFLECTANCE VALUES (y-axis, 10 to 80) plotted against LANDSAT CHANNELS (x-axis, 0 to 4), labeled (E).

GYPSIFEROUS " DESERT " SOILS

NON - SALINE; GYPSIFEROUS (DESERT) SOILS; 10YR6/4; COARSE TEXTURED; PEBBLES AND CRUSTED GYPSUM ACCUMULATIONS ARE EXPOSED ON THE SURFACE; WEEDS ARE RARE TO NIL; SEVERE WIND EROSION; CULTIVATION IS ENTIRELY RESTRICTED TO RAINFALL-COLLECTING BASINS (VERY FEW).

Figure 43. Spectral group E.

78

Table 12. Final grouping and interpretation of 16 clustered
spectral classes in research area.
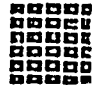
CLASS ORDER	FINAL NUMBER OF GROUPS	INTERPRETATION	S Y M B O L S
1	A	<u>WATER BODIES</u> : river, drainage and irrigation canals, water-logged soils, and ponded water due to topography and/or uncontrolled irrigation practices.	
2+4+7	B₁	<u>VEGETATION</u> : dense and scattered weeds, date palms, and field crops. Approximate vegetation percent(50-75%); with (25%) bare soil.	
3+9+13	B₂	scattered weeds, isolated fruit shrubs and date palms. Approximate vegetation percent (25-50 %).	
5	C	<u>PAVED ROAD</u> : Baghdad-Rutba high-way and other man-made features and activities, i.e., i.e., villages, houses,etc.	
6	D₁	<u>SALINE IRRIGATED SOILS</u> : Extremely saline, fine textured soils, 10YR3/1, MgCl₂ is predominant, fallow, very shallow-saline ground water, very slow permeability and infiltration rates.	
8	D₂	Extremely saline, fine textured soils, 10YR3/1-3/2, MgCl₂ and NaCl are predominant, less moist soil surfaces than the upper class, very shallow and saline ground water, very slow permeability and infiltration rates.	

Table 12. (Continued)

| CLASS ORDER	FINAL NUMBER OF GROUPS	INTERPRETATION	S Y M B O L S
12	D_3	Saline, fine-medium textured soils, 10YR3/3-4/3, NaCl is predominant, less moist surfaces, scattered growth of weeds, shallow-saline ground water, slow-moderately slow permeability and infiltration rates.	
10+11	D_4	Saline-slightly saline, medium textured soils, 10YR4/3 - 5/3, NaCl is predominant, crusted surfaces due to salinity, cultivated in some parts but no significant production, moderate-saline ground water, permeability, and infiltration.	
14	D_5	non-saline, medium-coarse textured soils, 10YR5/3, deep and ineffective ground water on capillary movement, although saline, moderate-moderately fast permeability and infiltration.	
15+16	E	GYPSIFEROUS " DESERT " SOILS : non-saline, gypsiferous, coarse textured soils, 10YR6/4, gravel, pebbles and gypsum are often exposed on the surface, crusted soil surfaces, fallow, very deep and usable ground water in certain parts for livestock and irrigation; in certain locations only.	
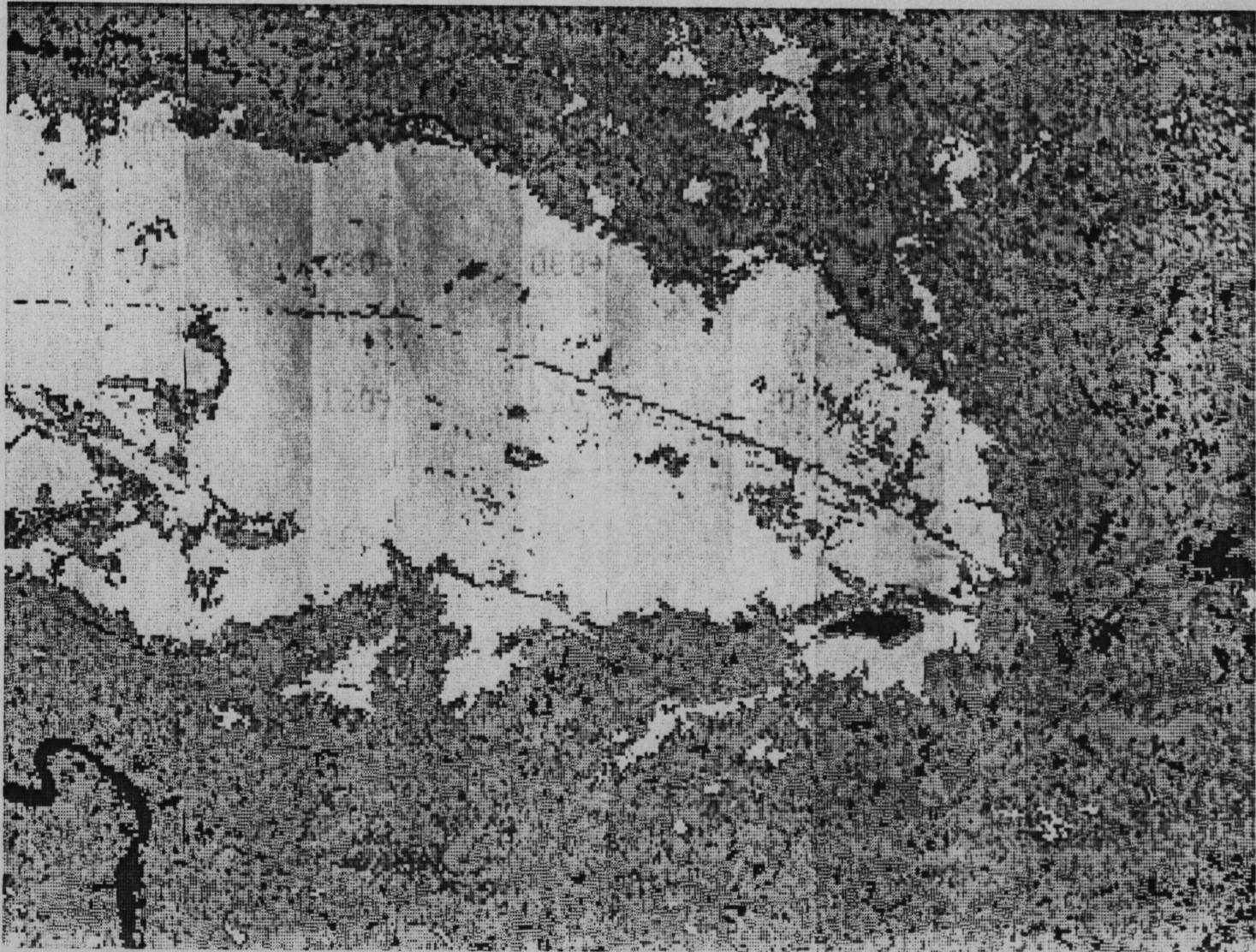
Figure 44. Digital map of research area.

Figure 45. Landsat color composite image of research area (bands 4,5,7)
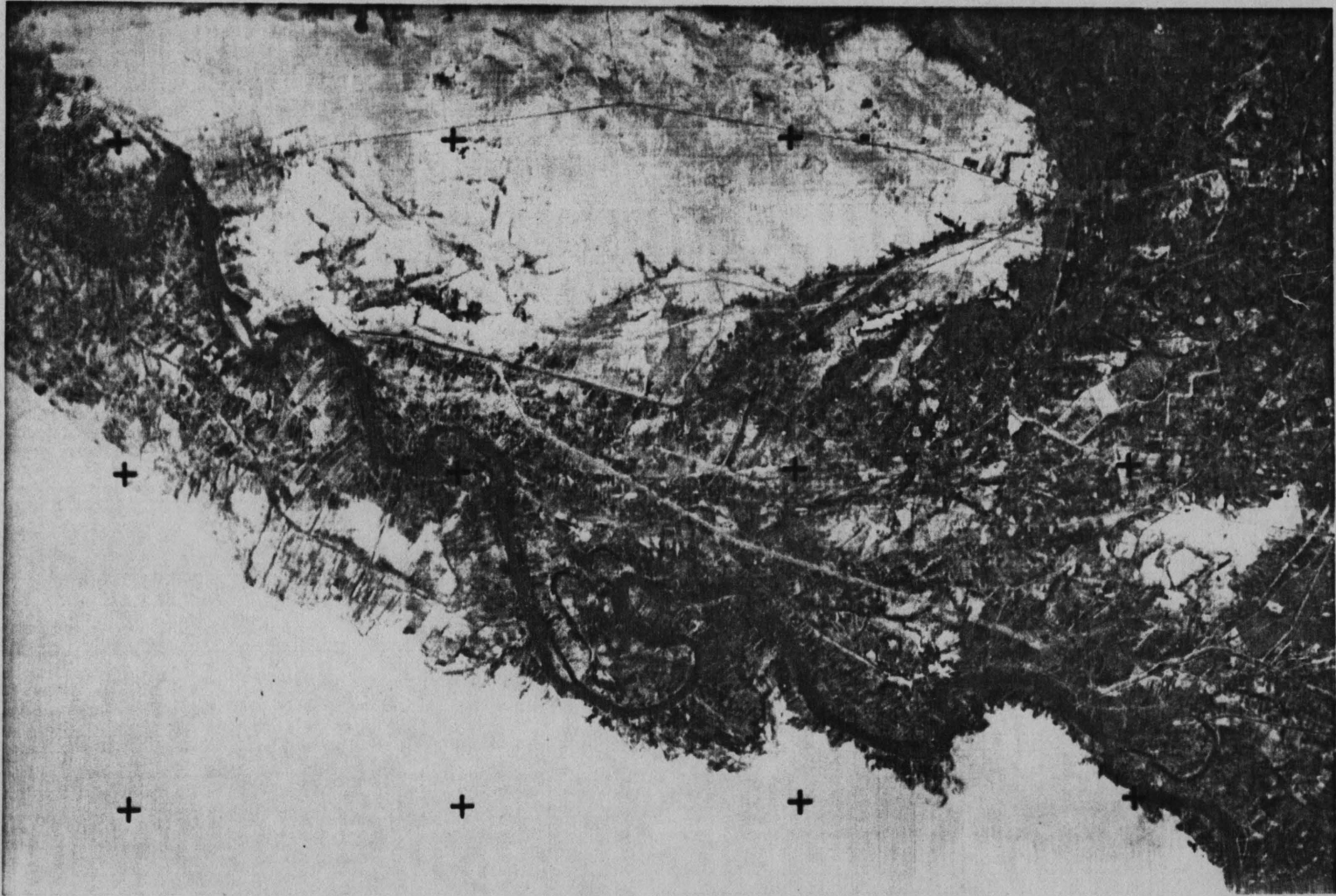16 September 1976.

Figure 46. Landsat Return Beam Vidicon (RBV) image of research area (9 October 1980).
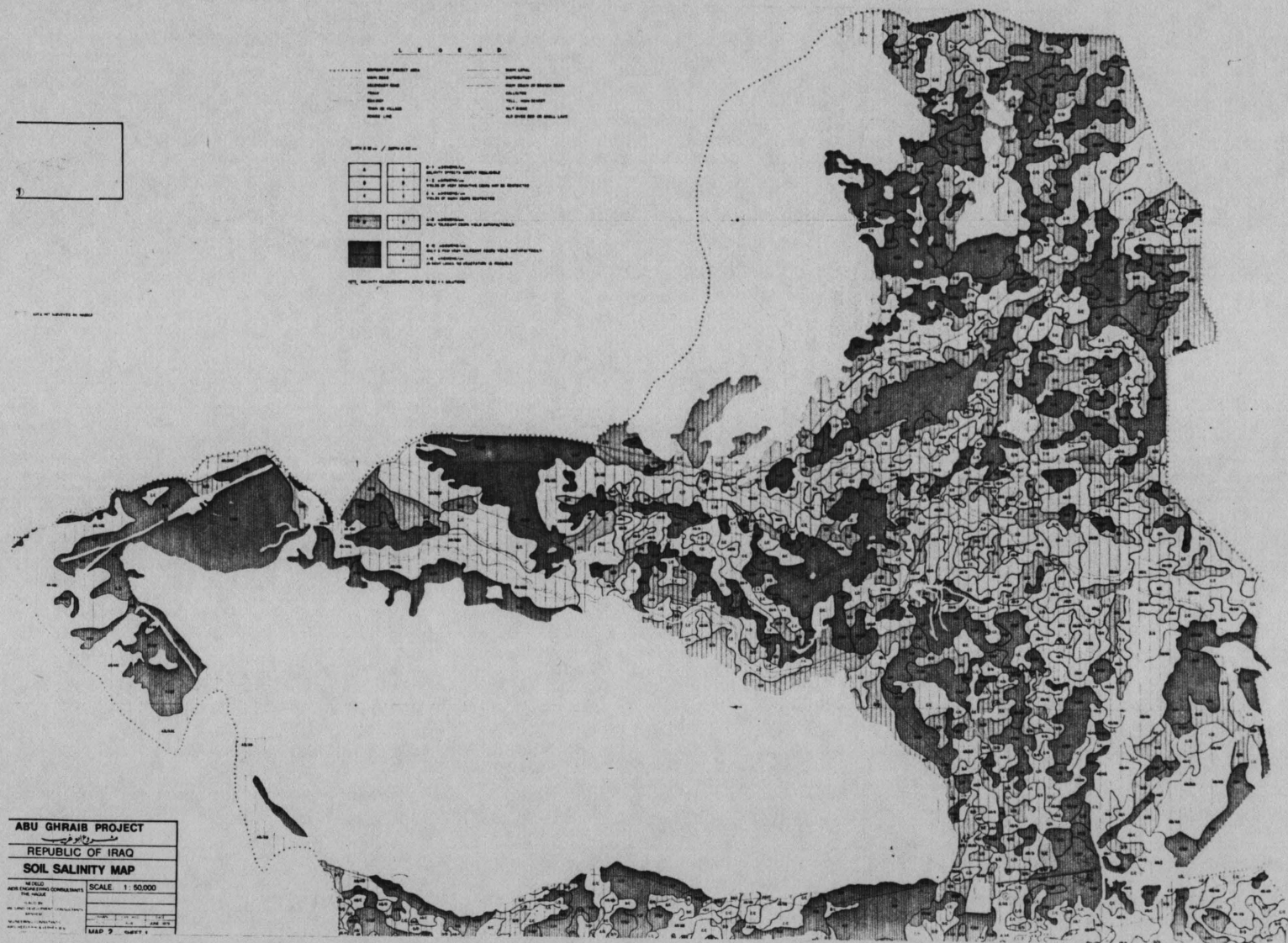
Figure 47. Soil salinity map of research area (38). June 1978.

CONCLUSIONS

1) The laboratory measurements of spectral reflectance and the digital analysis of Landsat multispectral scanner data have indicated that saline soils, whose Electrical Conductivity values exceeded the salinity limit of 4 mmhos/cm, were associated with lower spectral reflectance values than those obtained by the non-saline, gypsiferous soils in the visible, near and middle infrared portions of the spectrum (0.45-2.35 μm).

2) In general, saline soils reflect less energy than do non-saline soils. The variation in reflectance from saline soils is related to solubility of salts and the resulting water retantion characteristics.

3) Leaching decreased the Electrical Conductivity and increased the value and chroma of the saline soils. As a result, the leached soils had an increase in reflectance values. The non-saline, gypsiferous soils were not affected by leaching.

4) The laboratory measurements indicated that in the water content range of 25% to 40%, saline soils exhibit relatively low reflectance. With the continuous decrease in water content, reflectance generally increased. This increase was related to the water retention characteristics of the individual salts.

5) The laboratory measurements also indicated that it is inappropriate to measure reflectance of the soils (saline, non-saline and gypsiferous before and/or after leaching) under saturation conditions because of the specular effect on the sensor's spectral detection. It is advised, based on this conclusion, that spectral measurements of saturated soils either be avoided or the angle of view of the spectroradiometer be changed to eliminate specular effect.

6) Digital analysis of Landsat multispectral scanner (MSS) was used successfully to delineate and map different soil salinity levels in the irrigated-saline soils. This capability, which was based on the specific spectral reflectance charactristics of each salinity level, was greatly enhanced by the laboratory results of the same soils under different water content levels.

7) Gypsiferous soils exhibited the highest relative reflectance values in the results from the analysis of Landsat MSS data.

8) Landsat MSS data were used successfully to separate different land cover types within the research area.

9) In this research, the infrared bands in both the laboratory and Landsat MSS measurements were superior to the visible bands in spectral differentiating of quantity and quality of soil salinity.

RECOMMENDATIONS

To expand the application capabilities of this study in the area of salt affected soils, the following recommendations should be considered :

1) A grid sampling system must be applied for a complete coverage of the area to be spectrally studied. A detailed sampling procedure, depending on the spatial variation of salinity differences, is recommended.

2) The analysis of the soil samples which are to be collected must include, in addition to the standard chemical and physical analysis, a detailed clay mineralogy study. This may help to define some of the spectral variability among soils.

3) Similar study should be carried out of salt affected soils under different climatic environment and relate their reflectance characteristics to the ones in this research. Such positive or negative comparisons may help further and advance application of spectral reflectance characteristics of saline soils.

4) If laboratory spectral measurements are to be carried out, an experimental network should include a close-interval of wetting/ drying cycles and their effects on spectral variations among saline soils.

5) It is recommended that studies be pursued to develop a feasible methodology to use sequential Landsat coverage to detect changes in the salinity status of irrigated areas.

BIBLIOGRAPHY

1. Alphen, J. G. van and F. de los R. Romero. 1971. Gypsiferous soils. Bulletin #12. International Institute for Land Reclamation and Improvement, Wageningen, The Netherlands.

2. Angstrom, A. 1925. The albedo of various surfaces of grounds. Geografiska Ann. 7:323.

3. Baumgardner, M. F., S. J. Kristof, C. J. Johannsen and A. L. Zachary. 1970. Effects of organic matter on the multispectral properties of soils. Proc. Ind. Acad. Sci. 79:413-422.

4. Bear, F. E. 1960. Chemistry of the Soil. 3rd print., Reinhold Pub. Co., New York.

5. Beck, R. H. et al. 1976. Spectral characteristics of soil related to the interaction of soil moisture, organic carbon and clay content. LARS Information Note 081176, Laboratory for Applications of Remote Sensing, Purdue University, West Lafayette, Ind.

6. Bernstein, L. 1962. Salt-affected soils and plants. UNESCO-The Problems of Arid Zones. Proc. Paris Symp. France.

7. Black, C. A. et al. 1965. Methods of soil analysis, Part 1: Physical and mineralogical properties. Amer. Soc. Agron. Wisconsin.

8. Black, C. A. et al. 1965. Methods of soil analysis, Part 2: Chemical and microbiological properties. Amer. Soc. Agron. Wisconson.

9. Blanchard, J. R., R. Greely and R. Goettelman. 1974. Use of visible, near infrared and thermal infrared remote sensing to study soil moisture. NASA TMX-62,343.

10. Buol, S. W., E. D. Hole and R. J. McCracken. 1980. Soil genesis and classification. Iowa State University, Ames.

11. Buringh, P. 1960. Soils and soil conditions in Iraq. Iraqi Ministry of Agriculture, Baghdad, Iraq.

12. Fuchs and Tanner. 1968. Surface temperature measurements of bare soil. J. Appl. Meteorology 7(2):303-305.

13. Hillel, D. 1971. Soil and Water. Academic Press, New York.

14. Hillel, D. 1980. Fundamentals of Soil Physics. Academic Press, New York.

15. Hoffer, R. M. and C. J. Johannsen. 1969. Ecological potential in spectral signature analysis. In Remote Sensing in Ecology, University of Georgia Press, Athens, Georgia. pp. 1-16.

16. Hunt, G. R., J. W. Salisbury and C. J. Lenhoff. 1971. Visible and near infrared spectra of minerals and rocks: IV. Sulphides and sulphates. Modern Geology. 3:1-14.

17. Hunt, G. R., J. W. Salisbury and C. J. Lenhoff. 1974. Visible and near infrared spectra of minerals and rocks: IX. Basic and ultra basic igneous rocks. Modern Geology. 5:15-22.

18. Hunt, G. R., J. W. Salisbury and C. J. Lenhoff. 1970. Visible and near infrared spectra of minerals and rocks: I. Silicate minerals. Modern Geology. 2:287-289.

19. International Institute for Land Reclamation and Improvement. 1972. Drainage principles and applications. Pub. #16, Vol. 1. Wageningen, The Netherlands.

20. Kaminsky, S. A. and R. A. Weismiller. 1979. An investigation of analysis techniques of Landsat MSS data designed to aid soil survey. LARS Technical Report 080879. Laboratory for Applications of Remote Sensing, Purdue University, West Lafayette, Ind.

21. Kirschner, F. R., S. A. Kaminsky, R. A. Weismiller, H. R. Sinclair and E. J. Hinzel. 1978. Map unit composition assessment using drainage classes defined by Landsat data. Soil Sci. Soc. Am. J. 42:768-771.

22. Kling, E. G. 1954. The Physiology of Plants on Saline Soils. Moscow, USSR.

23. Kohnke, H. 1968. Soil Physics. McGraw-Hill, New York.

24. Kozlowski, T. T. 1968. Water Deficits and Plant Growth, Vol. 1. Academic Press, New York.

25. Kristof, S. J. 1971. Preliminary multispectral studies of soils. J. Soil Water Conserv. 26:15-18.

26. Kristof, S. J. and M. F. Baumgardner. 1975. Changes of multispectral soils patterns with increasing crop canopy. Agron. J. 67:317-321.

27. Kristof, S. J. and A. L. Zachary. 1974. Mapping soil types from multispectral scanner data. Photogramm. Eng. 40:1427-1434.

28. Leamer, R., V. J. Meyers and L. F. Silva. 1973. A spectro-radiometer for field use. Rev. of Scientific Instr. 44(5):611-614.

29. Lindberg, J. D. and D. G. Snyder. 1972. Diffuse reflectance spectra of several clay minerals. Am. Mineral. 57:485-493.

30. Luthin, J. 1957. Drainage of Agricultural Lands. Amer. Soc. of Agronomy, Wisconsin.

31. Lyon, T. L., H. O. Buckman and N. C. Brady. 1952. The Nature and Properties of Soils. Macmillan Co., New York.

32. Marlatt, W. E. 1967. Remote sensing and in situ temperature measurements of land and water surfaces. J. Appl. Meteorol. 6:272-279.

33. Meyer, M. P. 1967. Infrared color photography in plant science. Part V. Proc. of Winter Haven, Florida workshop. pp. 5-7.

34. Meyer, M. P. and L. Calpouzos. 1968. Detection of crop diseases identifications. Photog. Eng. Rem. Sens. J. 36:1116-1125.

35. Meyers, V. E. et al. 1965. Remote sensing for estimating soil salinity. J. Irrig. and Drain. ASCE 92(IR4).

36. Montgomery, O. L. and M. F. Baumgardner. 1974. The effect of the physical and chemical properties of soil on the spectral reflectance of soils. LARS Information Note 112674. Laboratory for Applications of Remote Sensing, Purdue University, West Lafayette, Ind.

37. National Academy of Science. 1970. Remote Sensing: with special reference to agriculture and forestry. Washington, D.C.

38. NEDECO. 1978. Abu-Ghraib Project. Vol. I. Soil Survey Report. Iraqi Ministry of Agriculture and Ag. Reform. Baghdad, Iraq.

39. Peterson, J. B. and M. F. Baumgardner. 1981. Use of spectral data to estimate the relationship between soil moisture tensions and their corresponding reflectance. Tech. Report 143, Water Research Center, Purdue University, West Lafayette, Ind.

40. Planet, W. G. 1970. Some comments on reflectance measurements of wet soils. Rem. Sens. Environ. 1:127-129.

41. Reeves, R. G. (ed.). 1975. Manual of Remote Sensing. Vol. I. Am. Soc. Photog., Virginia.

42. Reeves, R. G. (ed.). 1975. *Manual of Remote Sensing*. Vol. II. Am. Soc. Photogramm., Virginia.

43. Rudd, R. D. 1974. *Remote Sensing: A Better View*. Dux Press, Massachusetts.

44. Russell, R. S. and D. A. Barber. 1960. The relationship between salt uptake and the absorption of water by intake plants. Annual Rev. of Plant Physiology. 11:127.

45. Schilfgaarde, J. van. (ed.). 1974. *Drainage for Agriculture*. Am. Soc. Agron., Wisconsin.

46. Shaw, D. E. 1968. Determination of surface moisture by visible polarization measurements. General Electric Co., Space Science Laboratory.

47. Shockley, W. G., S. J. Knight and E. B. Lipscomb. 1962. Identifying soil parameters with an infrared spectrometer. Proc. 2nd Intl. Symp. on Remote Sensing of Environ. Ann Arbor, Mich.

48. Silva, L. F., J. E. Cipra and R. M. Hoffer. 1971. Extended field wavelength spectroradiometry. Proc. 7th Intl. Symp. on Remote Sensing of Environ. Ann Arbor, Mich. pp. 1509-1518.

49. Singh, A. N. et al. 1977. Delineating salt affected soils in the Ganges plain (India) by digital analysis of Landsat data. LARS Technical Report 111477. Laboratory for Applications of Remote Sensing, Purdue University, West Lafayette, Ind.

50. Soil Survey Staff. 1975. Soil Taxonomy Handbook #436. U.S. Dept. of Agriculture, Washington, D.C.

51. Stoner, E. R. and M. F. Baumgardner. 1980. Physiochemical, site and bidirectional reflectance factor characteristics of uniformly moist soils. LARS Technical Report 111679. Laboratory for Applications of Remote Sensing, Purdue University, West Lafayette, Ind.

52. Stoner, E. R. and E. H. Horvath. 1971. The effect of cultural practices on multispectral responses from surface soils. Proc. 7th Intl. Symp. on Remote Sensing of Environ. Ann Arbor, Mich. pp. 2109-2113.

53. Strogonov, B. P. 1964. *The Physiological Basis of Salt Tolerance*. D. Davy and Co., Inc., New York.

54. Swain, P. H. and S. M. Davis. (eds.). 1978. *Remote Sensing: The Quantitative Approach*. McGraw-Hill Co., New York

55. U.S. Salinity Laboratory Staff. 1954. *Diagnosis and Improvement of Saline and Alkali Soils*. Handbook #60. U.S. Dept. of Agriculture, Washington, D.C.

56. Vanderbilt, V. C., L. L. Biehl, B. F. Robinson, M. E. Bauer and A. S. Vanderbilt. 1980. Linear polarization of light by two wheat canopies measured at many view angles. LARS Technical Report 090981. Laboratory for Applications of Remote Sensing, Purdue University, West Lafayette, Ind.

57. Weast, R. C. (ed.). 1981. Handbook of chemistry and physics. 61st edition. CRC Press, Florida.

58. Weismiller, R. A. and S. A. Kaminsky. 1978. Application of remote sensing technology to soil survey research. J. Soil Water Conserv. 33:287-289.

59. Weismiller, R. A., F. R. Kirschner, S. A. Kaminsky and E. J. Hinzel. 1979. Spectral classification of soil characteristics to aid the soil survey of Jasper County, Indiana. LARS Technical Report 040179. Laboratory for Applications of Remote Sensing, Purdue University, West Lafayette, Ind.
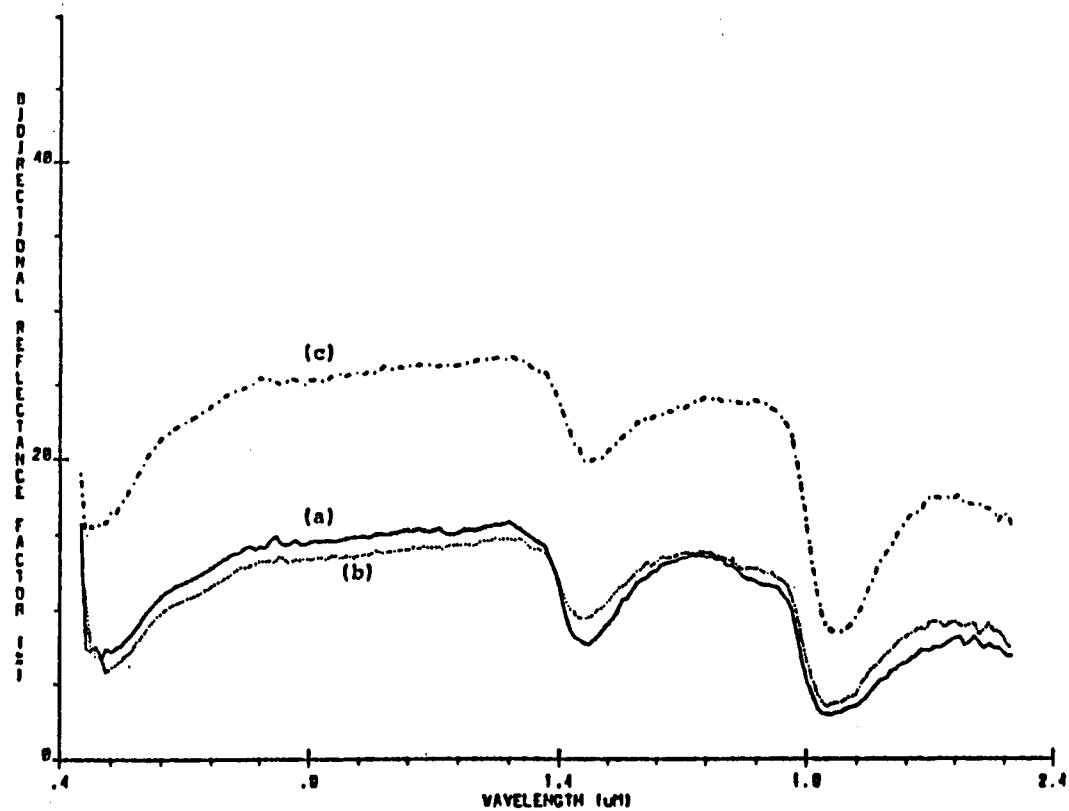
Figure A. The spectral reflectance characteristics for sample Four (BEFORE LEACHING) at (a) saturation, (b) 2-day air dry, and (c) 6-day air dry.
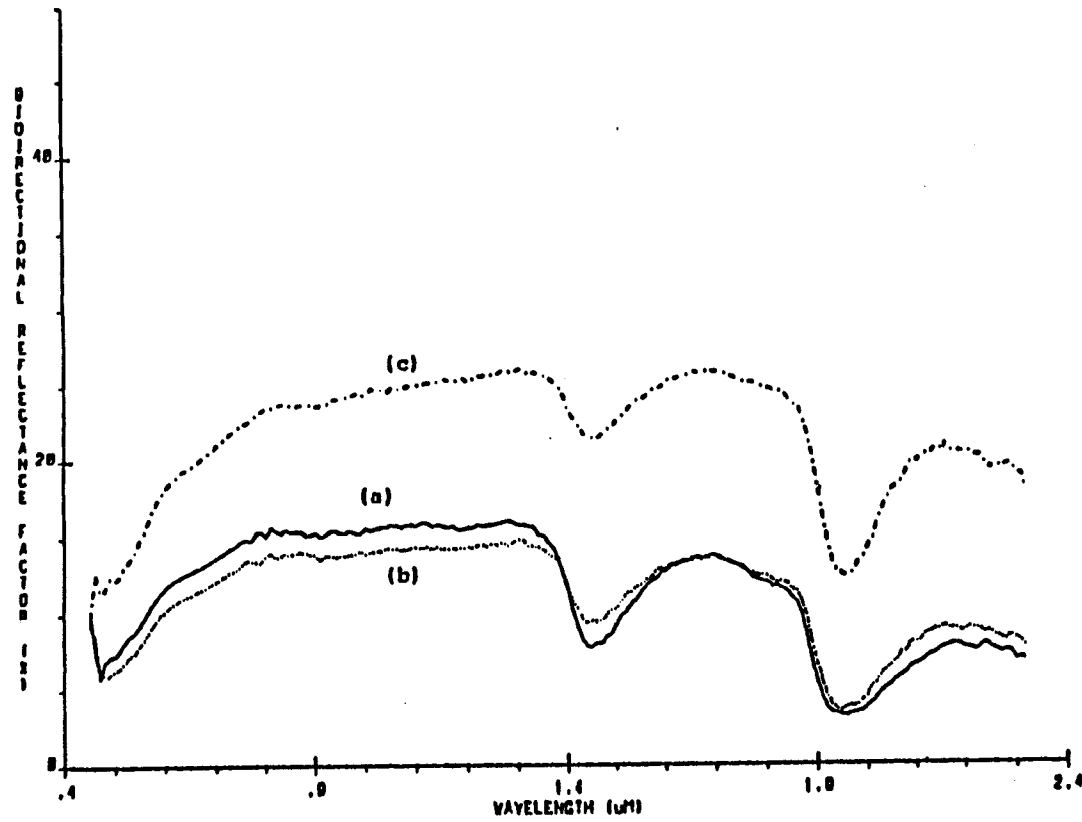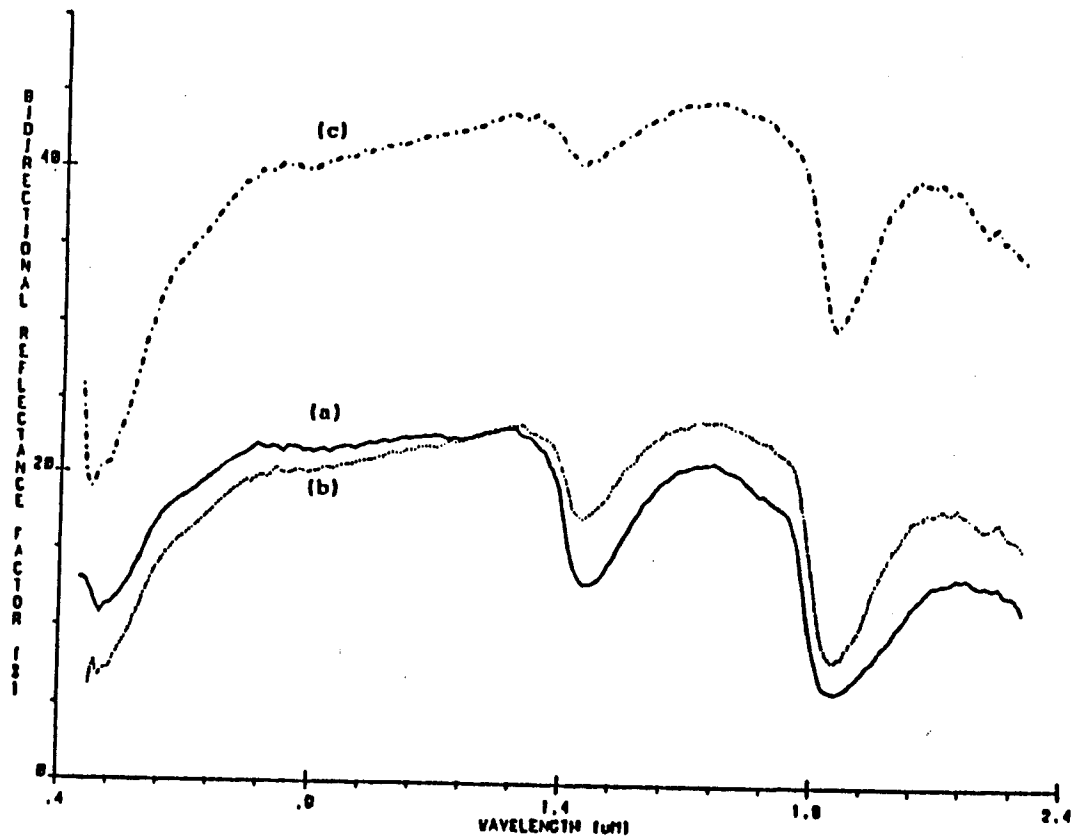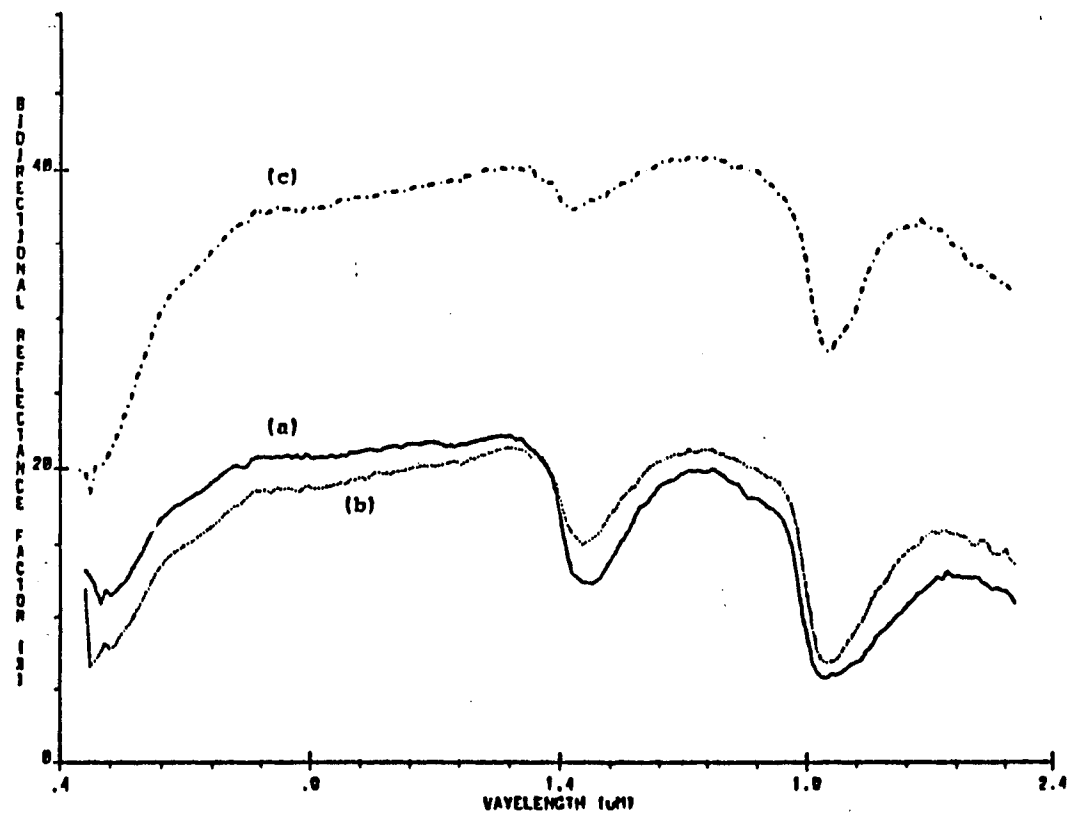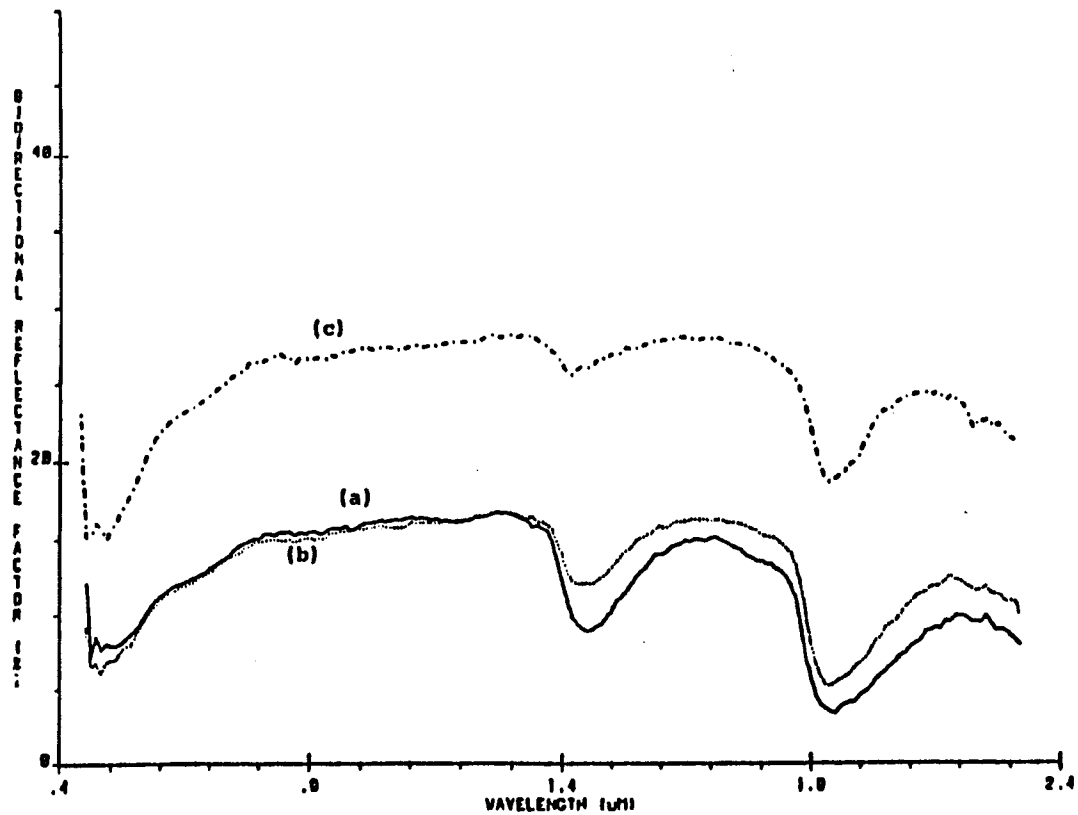
Figure B. The spectral reflectance characteristics for sample Five (BEFORE LEACHING) at (a) saturation, (b) 2-day air dry, and (c) 6-day air dry.
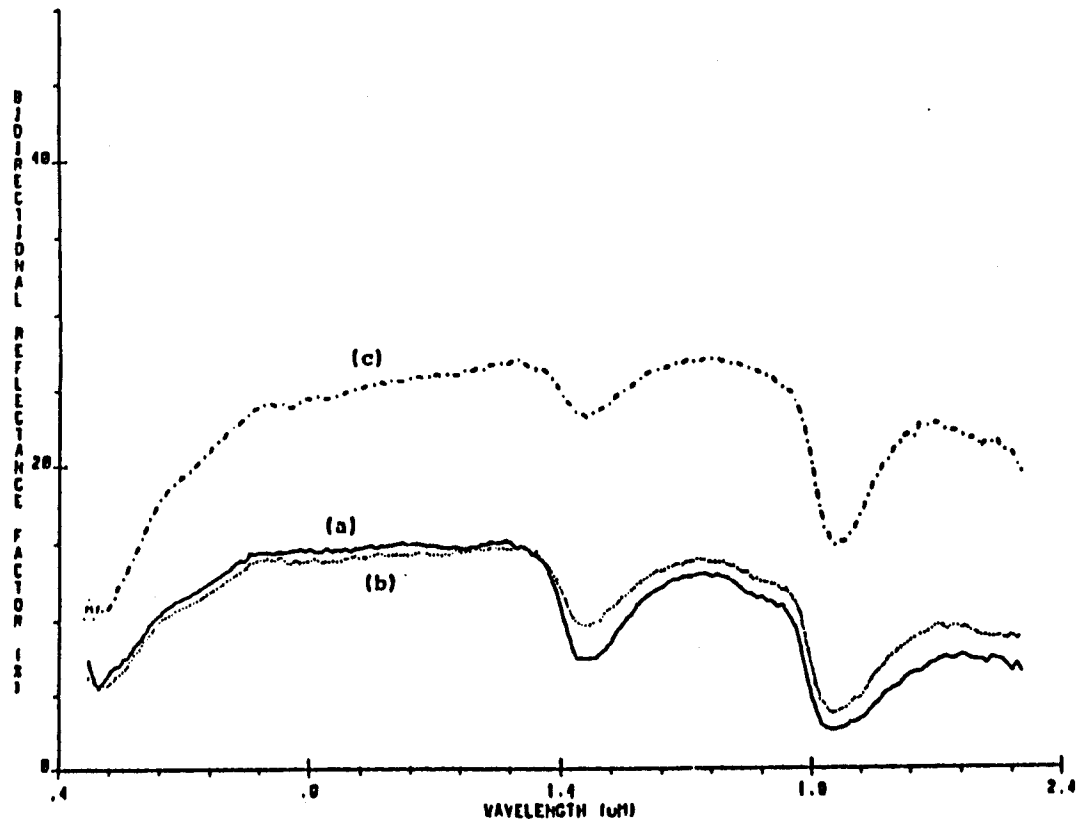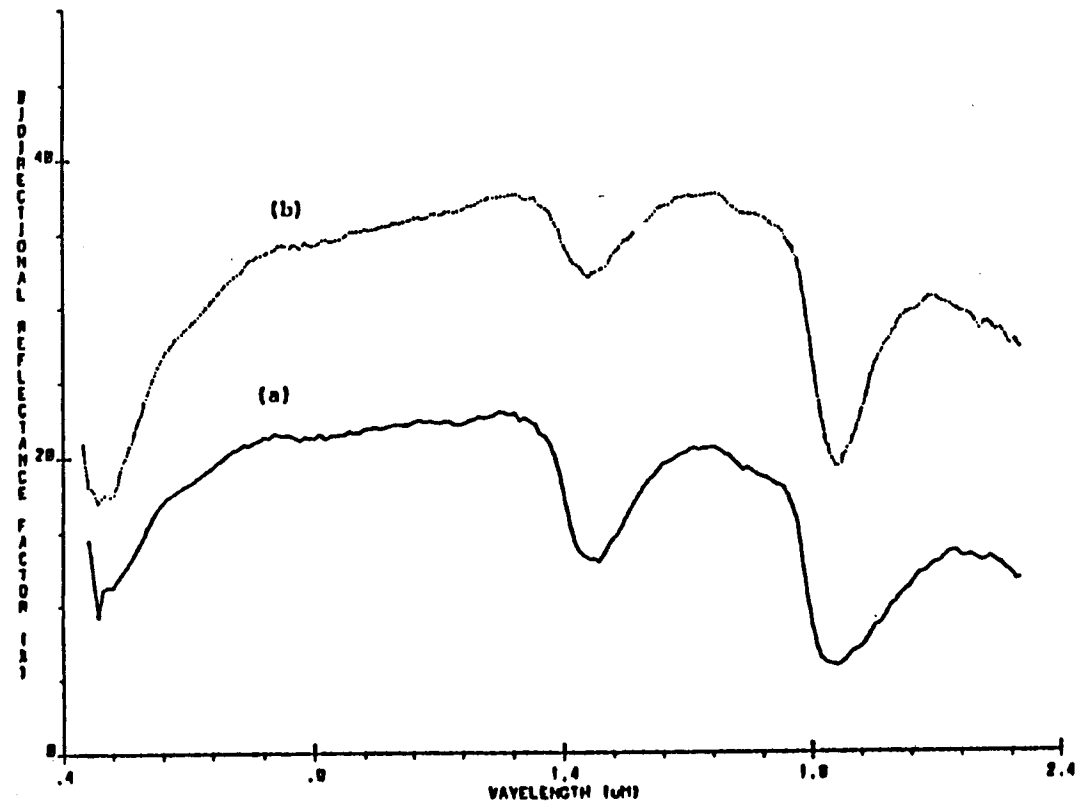
Figure C.   The spectral reflectance characteristics for sample Six
             (BEFORE LEACHING) at (a) saturation, (b) 2-day air dry,
             and (c) 6-day air dry.
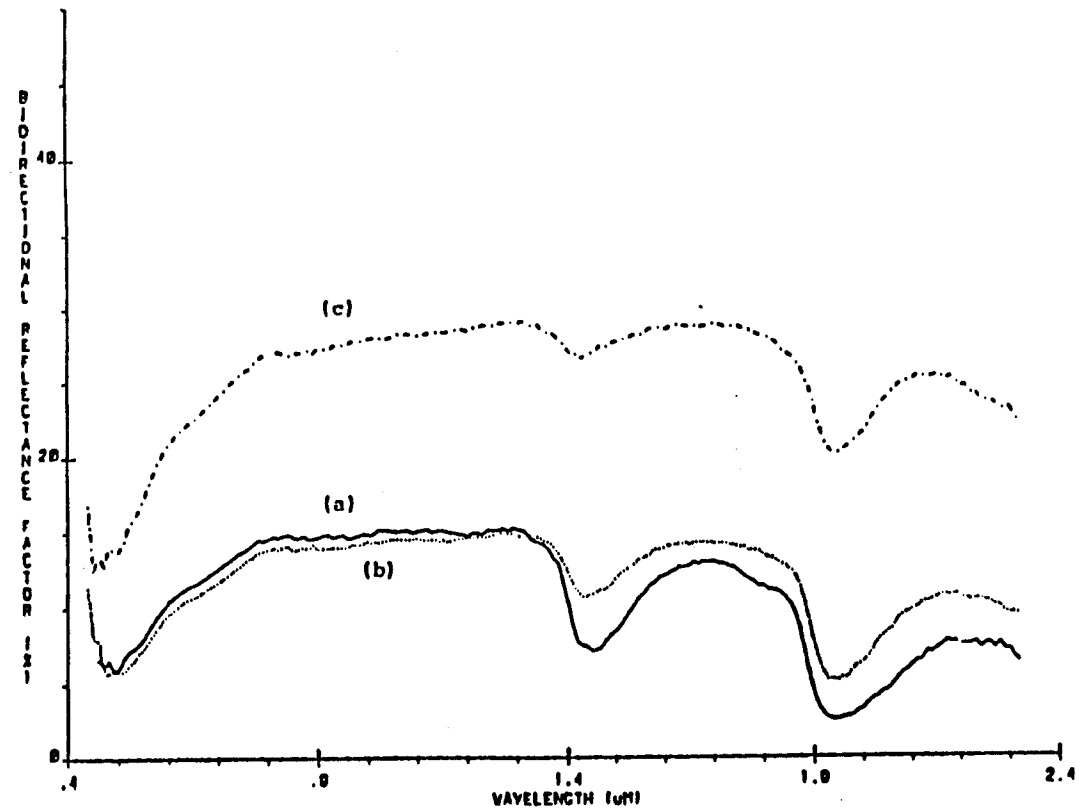
Figure D. The spectral reflectance characteristics for sample Seven
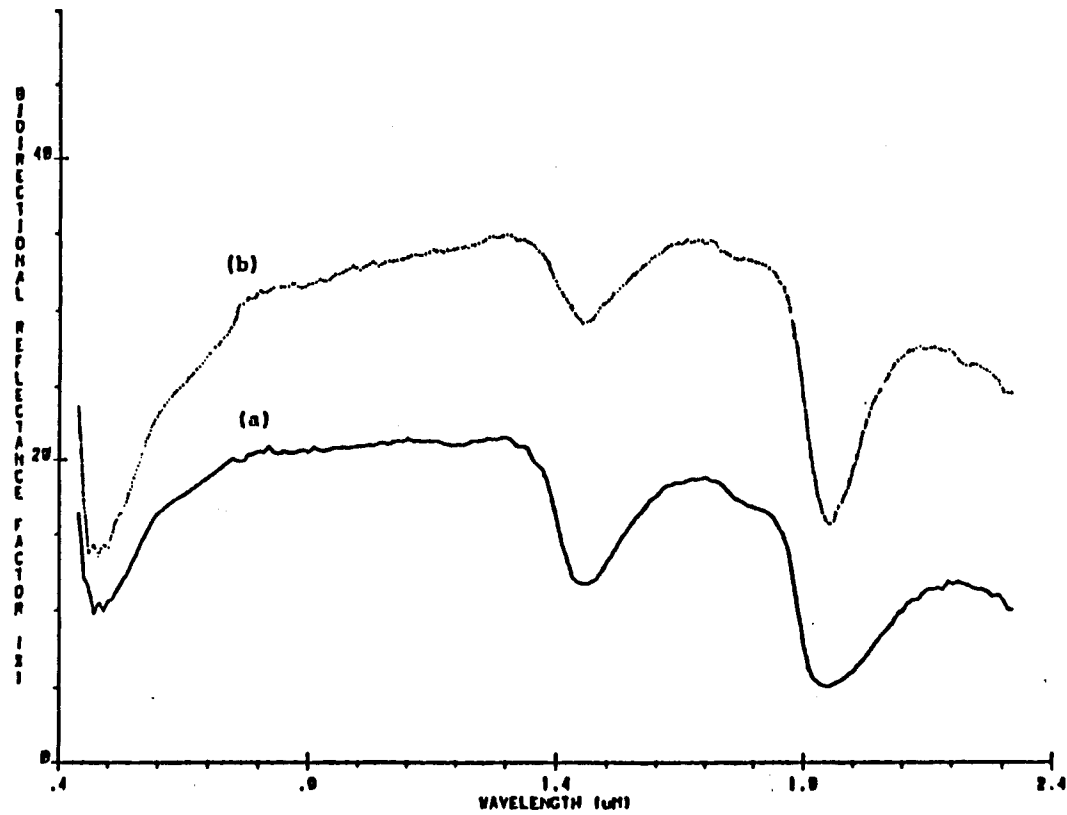(BEFORE LEACHING) at (a) saturation, (b) 2-day air dry,
and (c) 6-day air dry.
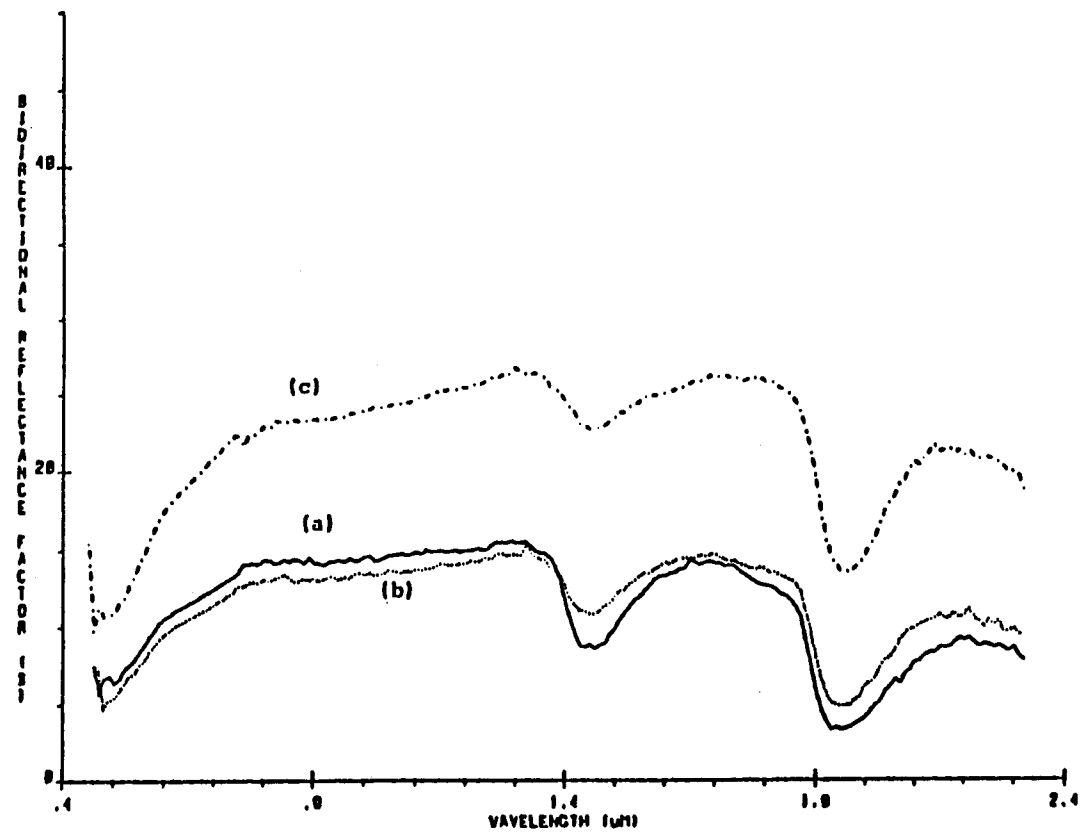
Figure E. The spectral reflectance characteristics for sample Eight (BEFORE LEACHING) at (a) saturation, (b) 2-day air dry, and (c) 6-day air dry.

Figure F. The spectral reflectance characteristics for sample Ten
(BEFORE LEACHING) at (a) saturation, (b) 2-day air dry,
and (c) 6-day air dry.

Figure   G. The spectral reflectance characteristics for sample Eleven
(BEFORE LEACHING) at (a) saturation, (b) 2-day air dry,
and (c) 6-day air dry.

Figure H. The spectral reflectance characteristics for sample Twelve (BEFORE LEACHING) at (a) saturation, (b) 2-day air dry, and (c) 6-day air dry.
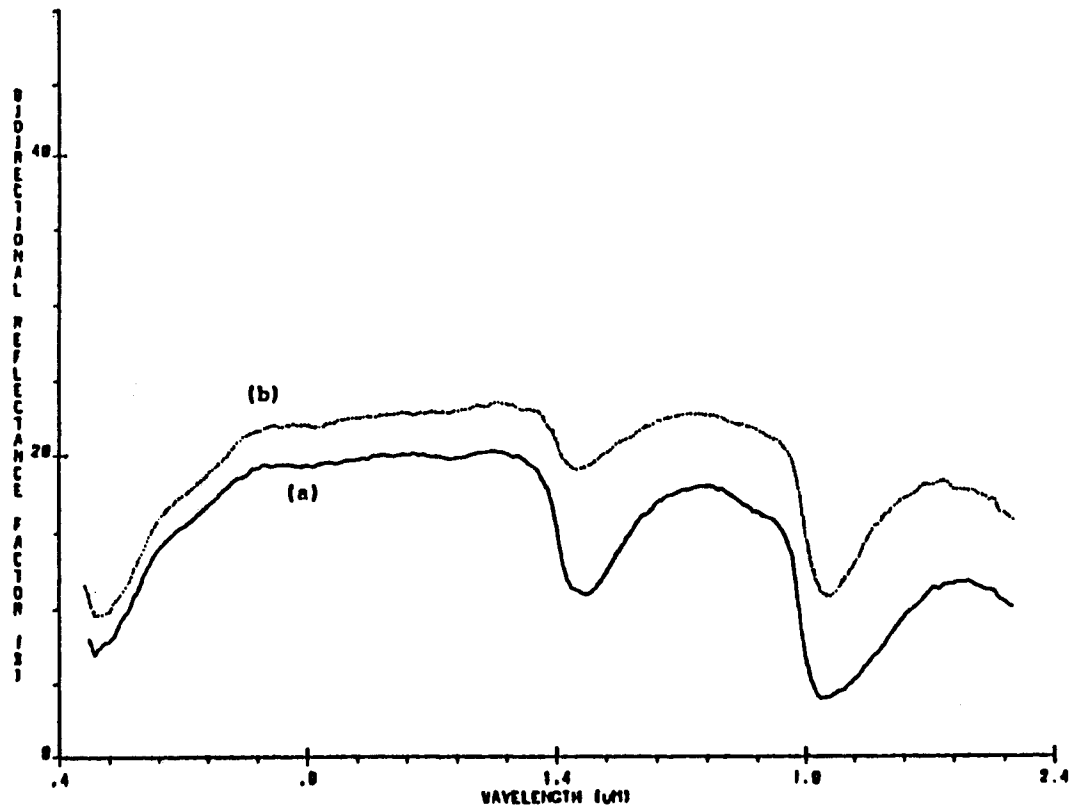
Figure I. The spectral reflectance characteristics for sample Four
(AFTER LEACHING) at (a) saturation and (b) oven dry.

Figure J. The spectral reflectance characteristics for sample Five
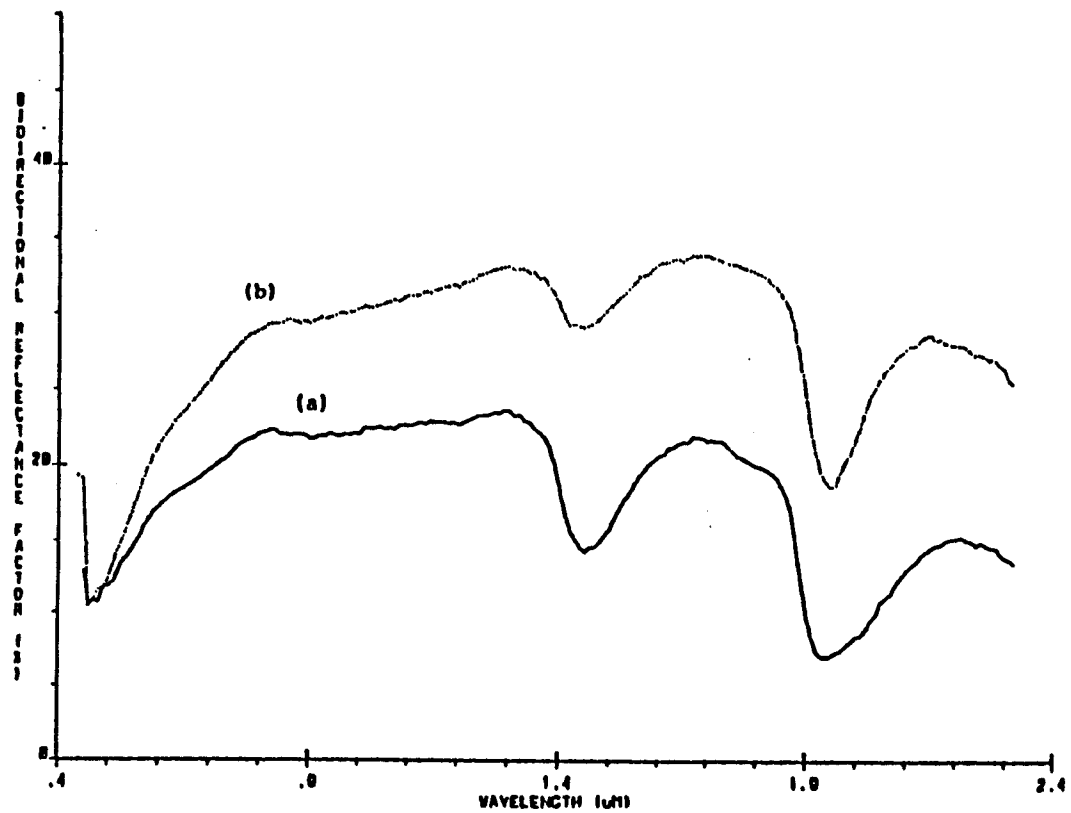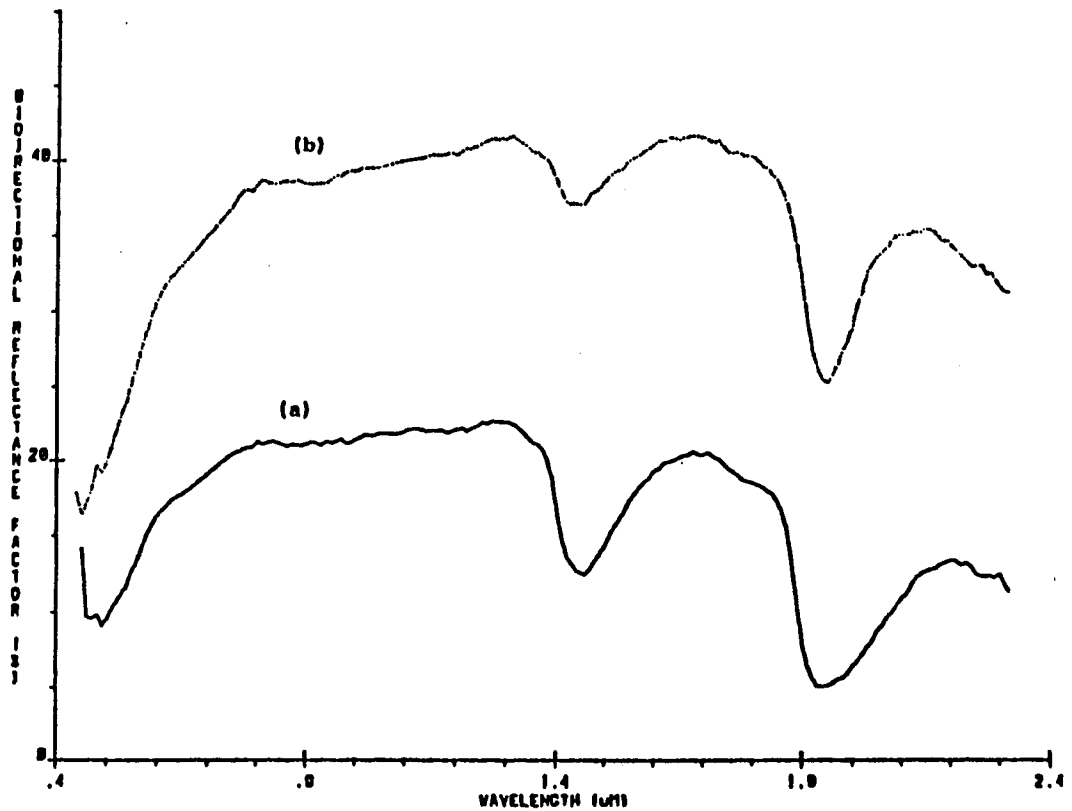(AFTER LEACHING) at (a) saturation and (b) oven dry.
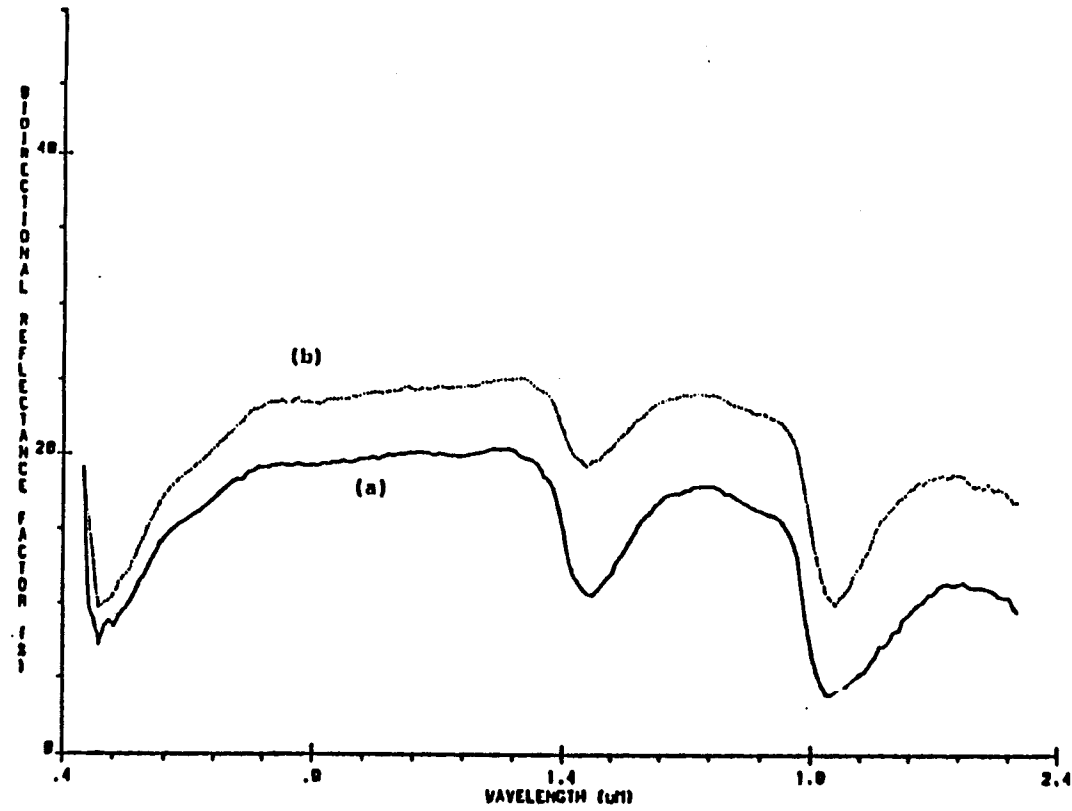
Figure K. The spectral reflectance characteristics for sample Six (AFTER LEACHING) at (a) saturation and (b) oven dry.

Figure L. The spectral reflectance characteristics for sample Seven
(AFTER LEACHING) at (a) saturation and (b) oven dry.

Figure M. The spectral reflectance characteristics for sample Eight (AFTER LEACHING) at (a) saturation and (b) oven dry.

Figure N. The spectral reflectance characteristics for sample Ten
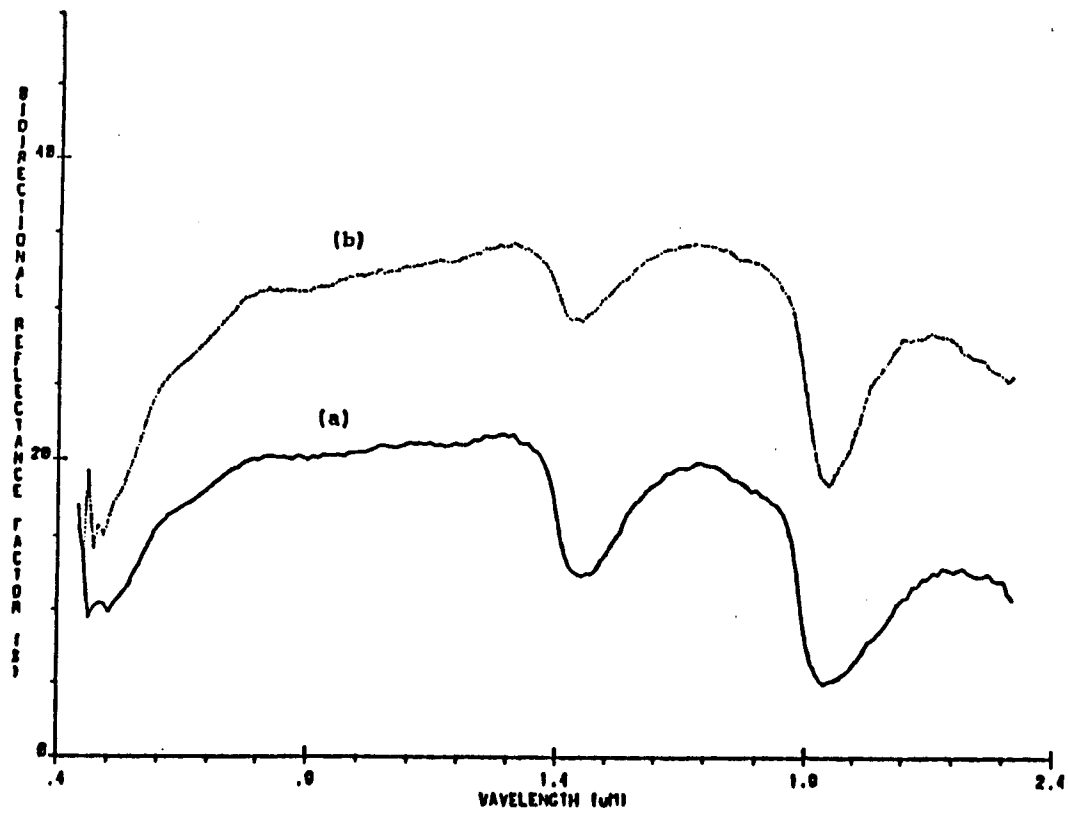(AFTER LEACHING) at (a) saturation and (b) oven dry.

Figure 0. The spectral reflectance characteristics for sample Eleven (AFTER LEACHING) at (a) saturation and (b) oven dry.
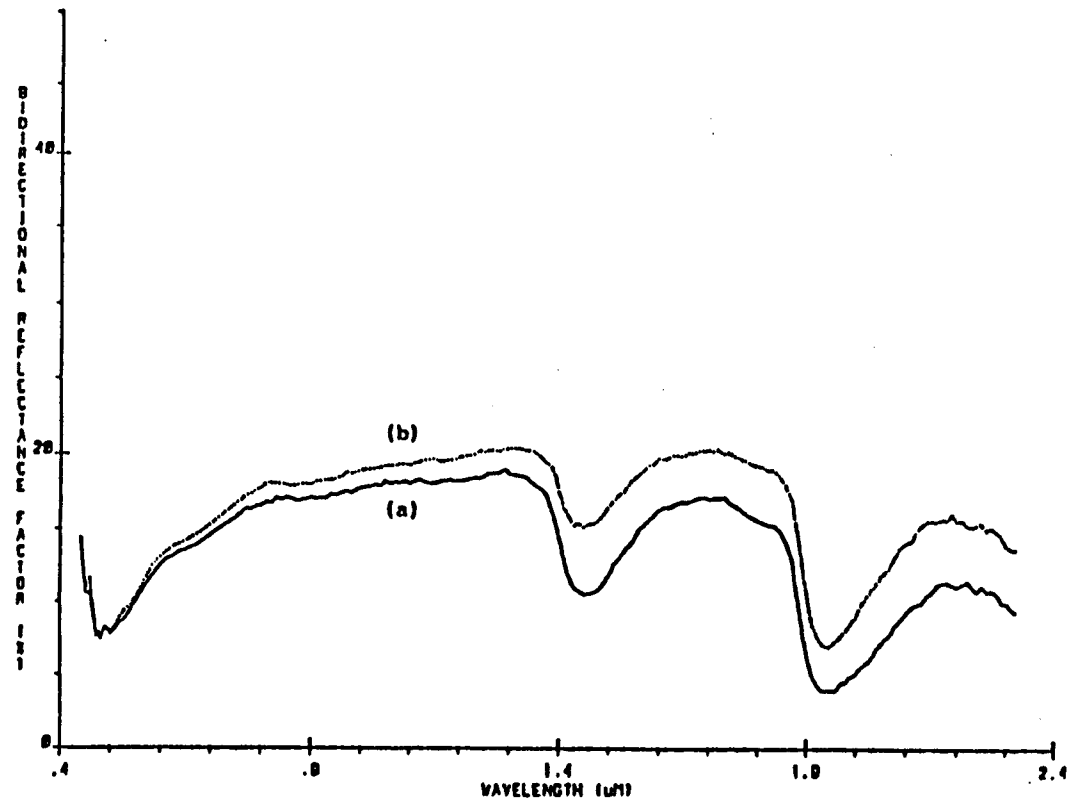
Figure. P . The spectral reflectance characteristics for sample Twelve
(AFTER LEACHING) at (a) saturation and (b) oven dry.